ผลของไบโอดีเซลเบลนด์ต่อสมบัติของอิลาสโตเมอร์

นาย สุริยะ พรตั้งจิตลิขิต

วิทยานิพนธ์นี้เป็นส่วนหนึ่งของการศึกษาตามหลักสูตรปริญญาวิทยาศาสตรมหาบัณฑิต
สาขาวิชาปิโตรเคมีและวิทยาศาสตร์พอลิเมอร์
คณะวิทยาศาสตร์ จุฬาลงกรณ์มหาวิทยาลัย
ปีการศึกษา 2549

ISBN : 974-14-2989-4

EFFECTS OF BIODIESEL BLEND ON PROPERTIES OF ELASTOMERS

Mr. Suriya Porntangjitlikit

A Thesis Submitted in Partial Fulfillment of the Requirements
for the Degree of Master of Science Program in Petrochemistry and Polymer Science
Faculty of Science
Chulalongkorn University
Academic Year 2006

ISBN : 974-14-2989-4

Thesis Title	EFFECTS OF BIODIESEL BLEND ON PROPERTIES OF ELASTOMERS
By	Mr. Suriya Porntangjitlikit
Field of Study	Petrochemistry and Polymer Science
Thesis Advisor	Associate Professor Wimonrat Trakarnpruk, Ph.D.

Accepted by the Faculty of Science, Chulalongkorn University in Partial Fulfillment of the Requirements for the Master's Degree

……………………………………………Dean of the Faculty of Science

(Professor Piamsak Menasveta, Ph.D.)

Thesis Committee

……………………………………………Chairman

(Professor Pattarapan Prasassarakich, Ph.D.)

W. Trakarnpruk

…………………………………………… Thesis Advisor

(Associate Professor Wimonrat Trakarnpruk, Ph.D.)

Warinthorn Chavasiri

……………………………………………Member

(Assistant Professor Warinthorn Chavasiri, Ph.D.)

……………………………………………Member

(Associate Professor Mongkol Sukwattanasinitt, Ph.D.)

สุริยะ พรตั้งจิตลิขิต : ผลของไบโอดีเซลเบลนด์ต่อสมบัติของอิลาสโตเมอร์ (EFFECTS OF BIODIESEL BLEND ON PROPERTIES OF ELASTOMERS)
อาจารย์ที่ปรึกษา: รศ. ดร.วิมลรัตน์ ตระการพฤกษ์; 116 หน้า. ISBN 974-14-2989-4

ไบโอดีเซลที่ผลิตจากน้ำมันปาล์มกลั่น และน้ำมันพืชใช้แล้ว ผสมกับน้ำมันดีเซลในอัตราส่วน 5 และ 10 เปอร์เซ็นต์โดยปริมาตรของไบโอดีเซล นำมาศึกษาผลของไบโอดีเซลผสมที่มีต่อการเปลี่ยนแปลงคุณสมบัติของยางหกชนิดคือ เอ็นบีอาร์ เอชเอ็นบีอาร์ เอ็นบีอาร์พีวีซี อะครีลิครับเบอร์ โคพอลิเมอร์เอฟเคเอ็ม และเทอร์พอลิเมอร์เอฟเคเอ็ม เปรียบเทียบกับไบโอดีเซลและน้ำมันดีเซล โดยการแช่ในยางในน้ำมันตัวอย่างที่เวลา 22 670 และ 1008 ชั่วโมง ศึกษาคุณสมบัติด้าน น้ำหนัก ปริมาตร ความแข็ง ความสามารถทนต่อแรงดึง และระยะยืดมากที่สุดที่เปลี่ยนแปลงไปของยางที่อุณหภูมิ 50 องศาเซลเซียส ผลการทดลองพบว่า คุณสมบัติเชิงกลของยาง เอ็นบีอาร์ เอ็นบีอาร์พีวีซี และอะคริลิครับเบอร์ หลังจากแช่ในน้ำมัน โดยพบการเปลี่ยนแปลงมากขึ้นเมื่อปริมาณไบโอดีเซลในน้ำมันเพิ่มขึ้น และพบการเปลี่ยนแปลงเพียงเล็กน้อยในยาง เอชเอ็นบีอาร์ โคพอลิเมอร์เอฟเคเอ็ม และเทอร์พอลิเมอร์เอฟเคเอ็ม และพบการเปลี่ยนแปลงมากขึ้นในยางเอ็นบีอาร์ เอ็นบีอาร์พีวีซี และอะครีลิครับเบอร์ หลังจากแช่ในน้ำมันที่อุณหภูมิ 100 องศาเซลเซียส เนื่องจากการดูดซึมไบโอดีเซลของยางที่แช่ในน้ำมัน และพบว่าอุณหภูมิกลาสทรานซิชั่นของยางอะคริลิครับเบอร์ลดลงเมื่อผ่านการแช่ในไบโอดีเซล

สาขาวิชา ปิโตรเคมีและวิทยาศาสตร์พอลิเมอร์ ลายมือชื่อนิสิต Suriya P.
ปีการศึกษา 2549 ลายมือชื่ออาจารย์ที่ปรึกษา W. Trakarnpruk

#4773417923 : PETROCHEMISTRY AND POLYMER SCIENCE
KEYWORD: BIODIESEL, ELASTOMER, PROPERTIES, DIESEL, NBR, HNBR,NBR PVC, COPOLYMER FKM, TERPOLYMER FKM

SURIYA PORNTANGJITLIKIT: EFFECTS OF BIODIESEL BLEND ON PROPERTIES OF ELASTOMERS.
THESIS ADVISOR: ASSOC. PROF. WIMONRAT TRAKARNPRUK, Ph.D.
116 pp. ISBN 974-14-2989

Biodiesels produced from refining and used cooking oil were blended with diesel in 5% and 10% by volume. The effects of biodiesel blends on property change of six types of elastomers; NBR, HNBR, NBR PVC, acrylic rubber copolymer FKM and Terpolymer FKM, were compared with those of pure biodiesel and diesel. The immersion time is varied to 22, 670 and 1008 hours. Properties measured in this work include mass change, volume change, hardness change, tensile and elongation changes. At immersion temperature of 50°C, the experimental results showed that the properties of NBR, NBR PVC and acrylic rubber immersed in biodiesel were affected. The mechanical properties were deteriated. The extent of property changes were proportional to biodiesel concentration. For copolymer FKM, terpolymer FKM and HNBR, the properties changed slightly. At high temperature, 100°C, more significant change was observed in acrylic rubber, NBR and NBR/PVC. This is due to the absorption of biodiesel by rubber in those samples. From the glass transition temperature measurement of acrylic rubber, the value decreased after immersed in biodiesel.

Field of study Petrochemistry and Polymer science Student's signature....Suriya P....
Academic year...............2006........................ Advisor's signature...W. Trakarnpruk...

ACKNOWLEDGEMENTS

First, I would like to express my greatest gratitude and sincere to my advisor, Associate Professor Dr. Wimonrat Trakarnpruk for her continuous attention and guidance through the years of my study. In addition, I also wish to express deep appreciation to Professor Dr. Pattarapan Prasassarakich, Assistant Professor Dr. Warinthorn Chavasiri and Associate Professor Dr. Mongkol Sukwattanasinitt for serving as the chairman and members of my thesis committee, respectively, for their valuable suggestions and comments. Moreover, I greatly appreciated the Program of Petrochemistry and Polymer Science and Graduate School, Chulalongkorn University for research grant.

Appreciation is also extended to PTT Research and Technology Institute for biodiesel and instrument for experiment. I would like to express deep appreciation to Mr. Prachid Saramolee, IRC (Thailand) Co., Ltd. for his assistance for elastomer support and information.

Special thanks to Mr. Boonchai Seentrakoon and Ms. Chonlada Komin for helping in coordinative, valuable suggestions and encouragement.

Finally, I would like to affectionately give all my gratitude to my parents and Ms.Wilawan Porntangjitlikit for their love, understanding, encouragement and support throughout my entire study. Without them, I would never be able to achieve this goal.

CONTENTS

Page

LIST OF TABLES

LIST OF FIGURES

Page

Page

Page

LIST OF ABBREVIATIONS

^oC	Degree Celsius
^oC/min	Degree Celsius per minutes
^oF	Degree Fahrenheit
%	Percentages
% vol	Percentages of volume
% wt	Percentages of weight
% w/w	Percentages of weight by weight
cSt	Centistoke
g	Gram(s)
h	Hour(s)
kg/L	Kilogram per liter
lb/in^2	Pound per square inches
m	Meter
mg	Milligram
mg KOH/g	Miligram potassium hydroxide per gram
ml	Milliliter
ml/min	Milliliter per minute
µl	Microliter
mm	Millimeter
mm/min	Millimeter per minute
mm Hg	Millimeter
µm	Micrometer
mm^2/s	Square millimeter per second
mol	Molar
ppm	Part per million
ASTM	The American Society for Testing and Materials
CH_4	Methane
CO_2	Carbon dioxide
DAHs	Dicyclic aromatic hydrocarbons
DIN	German Industry Standard
EPDM	Ethylene propylene diene terpolymer

H_2S	Hydrogen sulfide
H_2SO_4	Sulfuric acid
Hz	Hertz
IP	Institute of Petroleum Standard
$K.min^{-1}$	Kelvin per minutes
MAHs	Monocyclic aromatic hydrocarbons
MPa	Mega Pascal
MW	Molecular weight
$N.cm^{-2}$	Newton per square centimeter
NO_X	Oxide of nitrogen
PAHs	Polycyclic aromatic hydrocarbons
S.D.	Standard Deviation
Tg	Glass transition temperature
Tm	Crystalline melting temperature

CHAPTER I

INTRODUCTION

Today, fossil fuel is running out. In 1970s, over 17 billion barrels of oil were extracted each year. As of 1997, 807 billion barrels of crude oil had been extracted from the Earth's crust. If the worldwide rate of consumption of oil remained constant at the current amount of 24 billion barrels of oil per year, we would run out of oil in 2040. Fossil fuel prices will increase sharply due to the decrease in world oil supply as shown in Figure 1.1.

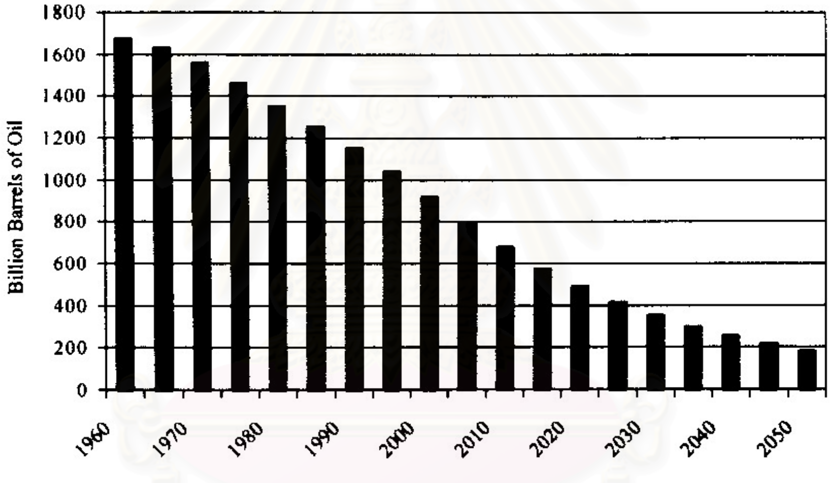

Figure 1.1 World oil supply.

At the same time, air pollution is one of the most serious environmental problems all over the world. Our planet is currently undergoing a period of global warming. Average worldwide temperature is increasing. Scientific evidence shows that we are increasing atmospheric carbon dioxide, and thereby contributing to global warming, by burning fossil fuels [1].

Besides carbon dioxide, diesel engines of buses and trucks exhaust have polycyclic aromatic and sulfur compound that makes diesel particulate matter. It is almost totally respirable and has a significant health impact on humans. It has been classified by several government agencies as either "human carcinogen" or "probable human carcinogen". It is also known to increase the risk of heart and respiratory diseases [2].

In 1895, the first diesel engine was developed by Dr. Rudolf Diesel. He tested his engine with vegetable oil. After that, with the advent of cheap petroleum, appropriate crude oil fractions were refined to be used as fuel, and diesel fuels and diesel engines were evolved together. Most of these engines are designed to run on less viscous fuels than vegetable oil which powered the original engine. In the 1930s and 1940s, vegetable oil was used as diesel fuels from time to time, but usually only in emergency situations. But it has some problem because the viscosity of vegetable oil is higher than diesel viscosity leading to operational problem such as engine deposits. In the 1970s, scientists discovered that the viscosity of vegetable oil could be decreased through a simple chemical process. The process yields a vegetable oil base fuel that works as well as diesel fuel in modern diesel engines. This fuel is called "biodiesel" [1, 3].

1.1 Advantages of biodiesel [4]

- Renewable

Diesel comes from petroleum, a non-renewable resource whose supplies are dwindling. Biodiesel is produced from oilseed crops, animal fats and waste cooking oils.

- Cleaner

Emissions from using biodiesel are far cleaner than diesel. Because it produces fewer particulate matter, carbon monoxide, total hydrocarbon, sulfate and polycyclic aromatic hydrocarbon as shown in Table 1.1. Pure biodiesel is nontoxic and spills biodegrade easily in soil and water. So, biodiesel reduces greenhouse gases contributing to global warming.

Table 1.1 Emission of biodiesel

Emission	**Change from Regular Diesel**	
	B20	B100
Particulates	-12%	-47%
Total unburned hydrocarbons	-20%	-67%
Carbon monoxide	-12%	-48%
Nitrogen oxides	+2 - +4%	+10%
Greenhouse gases/ global warming		-80%
Sulfates	-20%	-100%
Polycyclic aromatic hydrocarbons	-13%	-80%

- Locally produced

Biodiesel can be grown and produced in domestic, supporting local farmers and local economies and reducing the country's dependence on imported oil.

- Energy efficient

Petroleum diesel use results in a net energy loss of 19.5%. Biodiesel produces 3.2 units of fuel for every unit of energy consumed throughout its life cycle, creating a net energy gain of 220%.

- Easy to use

Biodiesel can be used with current fueling infrastructure and in all diesel vehicles with few or no engine modifications.

- Safe to handling

Biodiesel offers safety benefits over petroleum diesel because it is mush less combustible, with a flash point greater than 150 ^{o}C. For petroleum diesel is 77 ^{o}C. It is safe to handle, store, and transport.

1.2 Material compatibility of biodiesel

Material compatibility is concerned whenever the fuel composition is changed in the fuel system based on the historical data available. Biodiesel is oxygenated methyl esters of vegetable oil cause have surprising strong solvent properties respect to natural rubber soft plastic and metallic component. Thus changes in fuel composition and the introduction of alternative fuels often create many unforeseen problems in rubber soft plastic and metallic components in the fuel system presence biodiesel. In case of rubber it may be slowly deteriorated in the following part: the rubber filler hose which goes from the filler opening to the fuel tank, the rubber fuel lines which run from the fuel tank to the fuel filter, and the fuel line which runs from the fuel filter to the injection pump. When fuel lines or gaskets are affected, they usually get stick and soften or swell, causing fuel to leak and spill from connections [5].

1.3 The objectives of research

1.3.1 To investigate the effects of biodiesel, made from palm oil and used vegetable oil, on properties of elastomers used in diesel engine.

1.3.2 To compare the change in elastomer properties between diesel, biodiesel and biodiesel blends (5% and 10% biodiesel).

1.4 The scope of research

Six types of elastomer commonly found in fuels systems (NBR, HNBR, NBR PVC, Acrylic rubber, Copolymer FKM and Terpolymer FKM) were chosen for the study. Diesel, biodiesel and diesel blended with biodiesel in 5% and 10% were compared the effect on properties change of the elastomers. The physical properties were measured according to American Society of Testing and Materials (ASTM) D471, “Standard Test Method for Rubber Property-Effect of Liquids,” These evaluations were performed at 50°C and 100°C for 0, 22, 670 and 1006 hours. Tensile strength, hardness, mass, volume and elongation were determined for all specimens. Dynamic mechanical properties of the most deteriorate specimen were investigated.

CHAPTER II

THEORY AND LITERATURE REVIEWS

2.1 Vegetable oil

2.1.1 Palm oil [6]

The oil palm *(Elaeis guineensis)* is native to West Africa but is also cultivated in southeast Asia, especially Malaysia. The fruit consists of mesocarp or outer pulp, endocarp or shell and the palm kernel itself. The mesocarp contains 25-55% of palm oil, whilst the kernel contains 45-55% plam kernel oil. Although both oils are derived from the same fruit, they differ markedly in composition as shown in Table 2.1 and the palm kernels are therefore carefully separated from the pulp during processing. Palm oil must be extracted at the point of harvesting, as enzymes present in the fruit would otherwise cause hydrolysis and deterioration of the oil. The extraction units are therefore located in the centre of plantations. As the trees bear fruit all year round, and as transportation to the processing plant is so short, the palm oil plantation and processing plant is the most productive source of vegetable oil in the world.

Palm oil is a semi-solid fat and as such it needs no hydrogenation prior to use in food applications. It is often used as a component in margarine, biscuit for blends, etc. Palm oil may be fractionated into several components. In Malaysia, it is often fractionated by dry or detergent fractionation processes into a hard stearin fraction and an almost liquid olein. Palm oil may also be solvent fractionated to give a more liquid olein.

2.1.2 Used cooking oil [7]

Fats and oils are heated during commercial processing and during frying. Heating during processing mainly involves hydrogenation, physical refining, and deodorization. Temperature used in these processes may range from 120 ^{o}C to 270 ^{o}C.

The oil is not in contact with air, which eliminates the possibility of oxidation. At the high temperatures used in physical refining and deodorization, several chemical changes may take place. These include randomization of the glyceride structure, dimer formation, *cis-trans* isomerization, and formation of conjugated fatty acids of polyunsaturated fatty acids. For deep frying, the temperatures used are in the range of 160 ^{o}C to 195 ^{o}C. Deep frying is a complex process involving both the oil and the food to be fried. The reactions taking place are schematically presented in Figure 2.1. Steam is given off during the frying, which removes volatile antioxidants, free fatty acids, and other volatiles. Contact with the air leads to autoxidation and the formation of a large number of degradation products. The presence of steam results in hydrolysis, with the production of free fatty acids and partial glycerides.

As shown in Figure 2.1, oil breakdown during frying can be caused by oxidation and thermal alteration. Oxidation can result in the formation of oxidized monomeric, dimeric, and oligomeric triglycerides as well as volatile compounds including aldehydes, ketones, alcohols, and hydrocarbons. In addition, oxidized sterols may be formed. Thermal degradation can result in cyclic monomeric triglycerides and nonpolar dimeric and oligomeric triglycerides. The polymerization reaction may take place by conversion of part of the cw-cw-1,4 diene system of linoleates to the *trans-trans* conjugated diene. The 1,4 and 1,3 dienes can combine in a Diels-Alder type addition reaction to produce a dimer as shown in Figure 2.2. Other possible routes for dimer formation are through free radical reactions. As shown in Figure 2.3, this may involve combination of radicals, intermolecular addition, and intramolecular addition. From dimers, higher oligomers can be produced; the structure of these is still relatively unknown. Another class of compounds formed during frying is cyclic monomers of fatty acids.

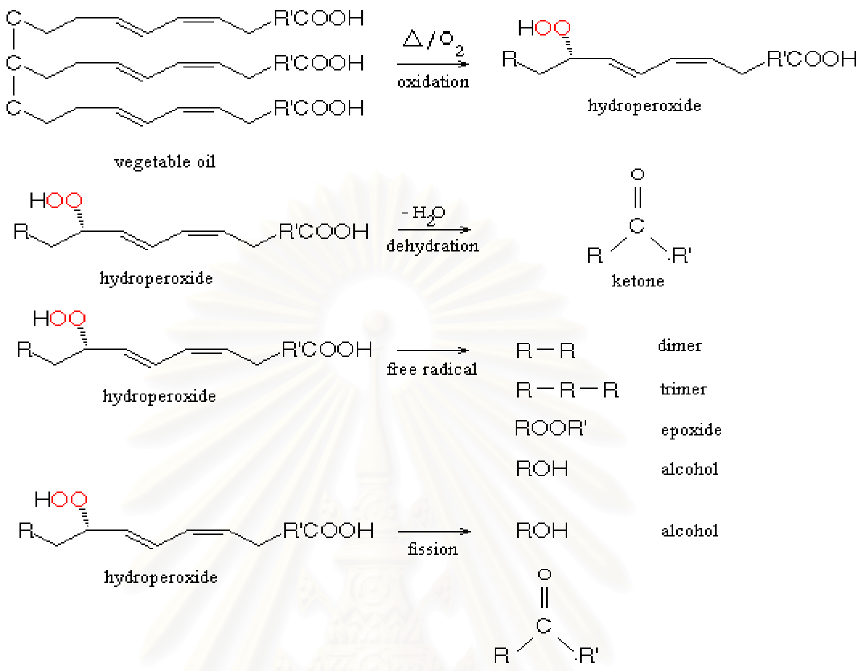

Figure 2.1 Chemical reactions occurring during deep frying.

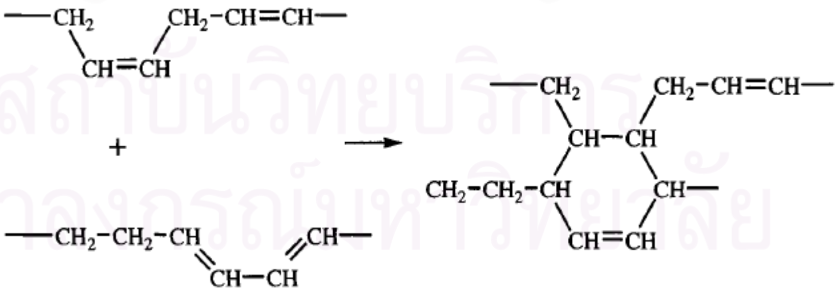

Figure 2.2 Polymerization of diene systems to form dimmer.

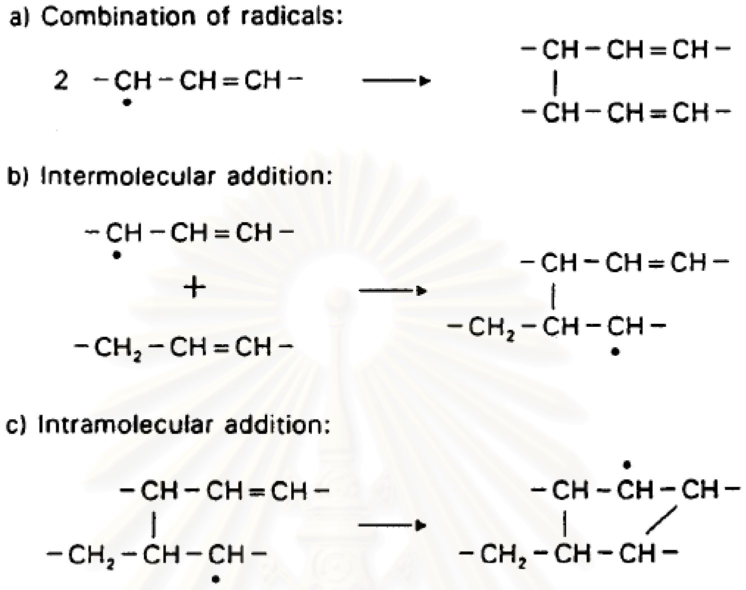

Figure 2.3 Nonpolar dimmer formation through free radical reactions.

2.2 Biodiesel [8]

Biodiesel is defined as mono-alkyl esters of long chain fatty acids derived from vegetable oils or animal fats which conform to ASTM D6751 specifications for use in diesel engines with little or no modifications. Biodiesel blends are denoted as, "BXX" with "XX" representing the percentage of biodiesel contained in the blend (ie: B20 is 20% biodiesel, 80% petroleum diesel).

2.3 Transesterification

Transesterification is an organic reaction where an ester is transformed into another through interchange of the alkoxy moiety. When the original ester is reacted with an alcohol, the transesterification process is called alcoholysis (Equation 2.1). The transesterification is an equilibrium reaction and the transformation occurs essentially by mixing the reactants. However, the presence of a catalyst (typically a strong acid or base) accelerates considerably the adjustment of the equilibrium. In order to achieve a high yield of the ester, the alcohol has to be used in excess.

$$\mathrm{RCOOR' + R''OH \xrightleftharpoons{\textit{catalyst}} RCOOR'' + R'OH} \qquad (2.1)$$

2.3.1 Transesterification of vegetable oils

In the transesterification of vegetable oils, a triglyceride reacts with an alcohol in the presence of a strong acid or base, producing a mixture of fatty acids alkyl esters and glycerol (Equation 2.2). The overall process is a sequence of three consecutive and reversible reactions, in which di- and monoglycerides are formed as intermediates. The stoichiometric reaction requires 1 mol of a triglyceride and 3 mol of the alcohol. However, an excess of the alcohol is used to increase the yields of the alkyl esters and to allow its phase separation from the glycerol formed.

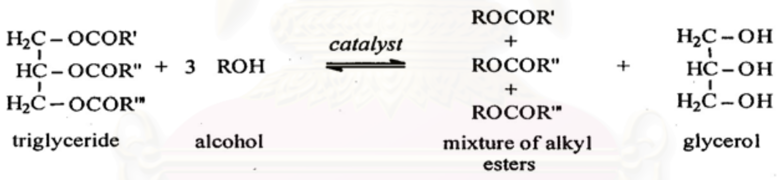

$$\underset{\text{triglyceride}}{\begin{array}{l}\mathrm{H_2C-OCOR'}\\ \mathrm{HC-OCOR''}\\ \mathrm{H_2C-OCOR'''}\end{array}} + \underset{\text{alcohol}}{3\ \mathrm{ROH}} \xrightleftharpoons{\textit{catalyst}} \underset{\text{mixture of alkyl esters}}{\begin{array}{c}\mathrm{ROCOR'}\\ +\\ \mathrm{ROCOR''}\\ +\\ \mathrm{ROCOR'''}\end{array}} + \underset{\text{glycerol}}{\begin{array}{l}\mathrm{H_2C-OH}\\ \mathrm{HC-OH}\\ \mathrm{H_2C-OH}\end{array}} \qquad (2.2)$$

2.3.2 Acid-catalyzed process

The transesterification process is catalyzed by Bronsted acids, preferably by sulfonic and sulfuric acids. These catalysts give very high yields in alkyl esters, but the reactions are slow, requiring, typically, temperatures above 100 ^{o}C and more than 3 hours to reach complete of soybean oil, in the presence of 1 mol% of H_2SO_4, with an alcohol/oil molar ratio of 30:1 at 65 ^{o}C, takes 50 hours to reach complete conversion of the vegetable oil (>99%), while the butanolysis (at 117 ^{o}C) and ethanolysis (at 78 ^{o}C), using the same quantities of catalyst and alcohol, take 3 and 18 hours, respectively.

The alcohol/vegetable oil molar ratio is one of the main factors that influence the transesterification. An excess of the alcohol favors the formation of the products. On the other hand, an excessive amount of alcohol makes the recovery of the glycerol difficult, so that ideal alcohol/oil ratio has to be established empirically, considering each individual process.

The mechanism of the acid-catalyzed transesterification of vegetable oils is shown in Figure 2.4, for a monoglycerides. The protonation of the carbonyl group of the ester leads to the carbocation II which, after a nucleophilic attack of the alcohol, produces the tetrahedral intermediate III, which eliminates glycerol to form the new ester IV, and to regenerate the catalyst H^+.

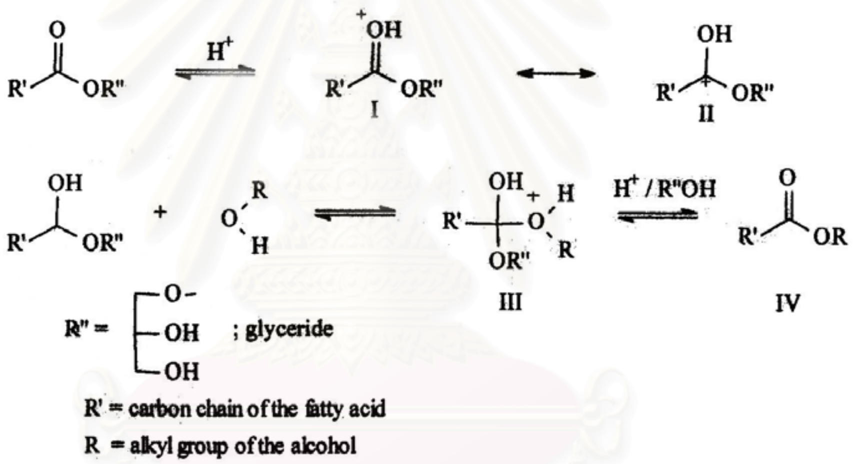

Figure 2.4 Mechanism of the acid-catalyzed transesterification of vegetable oils.

According to this mechanism, carboxylic acids can be formed by reaction of the carbocation II with water present in the reaction mixture. This suggests that an acid-catalyzed transesterification should be carried out in the absence of water, in order to avoid the competitive formation of carboxylic acids which reduce the yields of alkyl esters.

2.3.3 Base-Catalyzed Process

The base-catalyzed transesterification of vegetable oils proceeds faster than the acid-catalyzed reaction. Due to this reason, together with the fact that the alkaline catalysts are less corrosive than acidic compounds, industrial processes usually favor base catalysts, such as alkaline metal alkoxides and hydroxides as well as sodium or potassium carbonates.

The mechanism of the base-catalyzed transesterification of vegetable oils is shown in Figure 2.5. The first step (Equation 2.3) is the reaction of the base (B) with the alcohol, producing an alkoxide and the protonated catalyst. The nucleophilic attack of the alkoxide at the carbonyl group of the triglyceride generates a tetrahedral intermediate (Equation 2.4), from which the alkyl ester and the corresponding anion of the diglyceride are formed (Equation 2.5). The latter deprotonates the catalyst, thus regenerating the active species (Equation 2.6), which is now able to react with a second molecule of the alcohol, starting another catalytic cycle. Diglycerides and monoglycerides are converted by the same mechanism to a mixture of alkyl esters and glycerol.

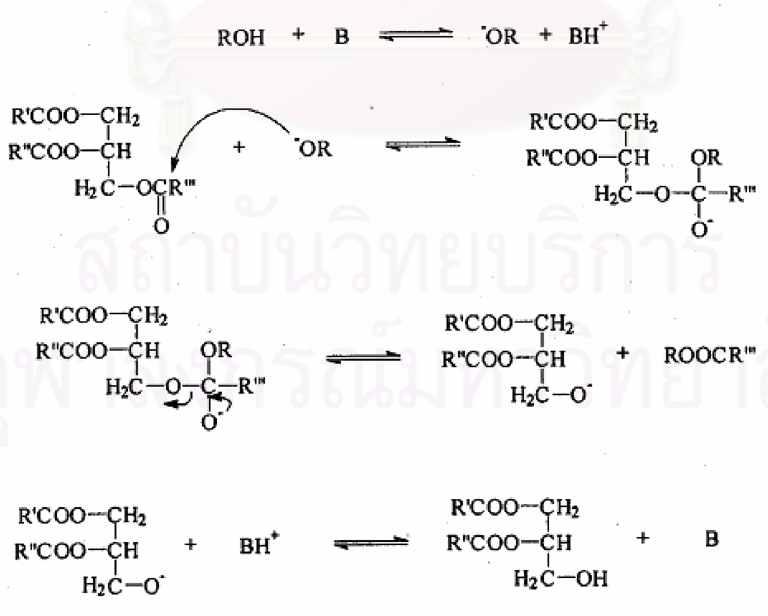

(2.3)

(2.4)

(2.5)

(2.6)

Figure 2.5 Mechanism of the base-catalyzed transesterification of vegetable oils.

2.3.4 Chemical composition [8]

The chemical composition of fat and oil esters is dependent upon the length and degree of unsaturation of the fatty acid alkyl chains. Table 2.1 presents elemental analysis data for methylesters of soybean oil and conventional diesel fuel. The carbon/hydrogen ratio of biodiesel from other sources will be slightly different, depending upon the degree of unsaturation. The most important compositional difference between D-2 and biodiesels is oxygen content. Biodiesel contains 10-12 wt% oxygen, which lowers energy density and, and as will be shown, lowers the particulate emission. In the United States, on road commercial Number 2 diesel can contain up to 500 ppm sulfur by ASTM D-2622. Biodiesel is essentially sulfur free. Sulfur is converted to sulfur oxide in the tailpipe and a fraction of the sulfur oxide is converted to sulfuric acid, which is counted as particulate, a regulated pollutant. Sulfur oxides are also regarded as air pollutants although they are not regulated as such from diesel engines. Petroleum derived diesel also contains from 20 to 40 vol% aromatic compounds. Aromatics are known to increase emissions of particulate and NOx. Biodiesel is essentially non-aromatic. Petroleum diesel contains essentially no olefinic bonds. Biodiesels can contain a significant number of these reactive, unsaturated sites.

Table 2.1 Typical elemental composition of soybean oil methyl esters and conventional Number 2 diesel fuel

%wt	Number 2 diesel	Methyl soyester
C	87	77.2
H	13	11.9
O	0	10.8
S	< 0.05	-

Table 2.2 shows the chemical structure of the fatty acid chains found in the most common biodiesel source materials. Except for C3 and C5 compounds, only acids with an even number of carbons occur naturally. Acids may be saturated (contain only single bonds) or unsaturated (contain one or more double bonds). Table

2.2 also shows the melting and boiling points of various fatty acids. The saturated acids exhibit higher freezing points than the unsaturated acids. Stearic acid, for example, is solid to 70 °C, while oleic acid melts at 6 °C. The only difference is the presence of a single double bond in the structure of oleic acid. For freezing point, chemical structure is very important. The boiling points of the acids, on the other hand, are dependent on the length of the carbon chain but nearly independent of the degree of unsaturation of the fatty acid.

Table 2.2 Structural formula, melting, and boiling points for fatty acids and methyl esters in the diesel boiling range

			Fatty acids		Methyl esters	
Acid chain	No. of carbons	Structure	Melting point (°C)	Boiling point (°C)	Melting point (°C)	Boiling point (°C)
Caprylic	8	$CH_3(CH_2)_6COOH$	16.5	239	-40	193
Capric	10	$CH_3(CH_2)_8COOH$	31.3	269	-18	224
Lauric	12	$CH_3(CH_2)_{10}COOH$	43.6	304	5.2	262
Myristic	14	$CH_3(CH_2)_{12}COOH$	58.0	332	19	295
Palmitic	16	$CH_3(CH_2)_{14}COOH$	62.9	349	30	338
Palmitoleic	16	$CH_3(CH_2)_5CH=CH(CH_2)_7COOH$	33	-	0	-
Stearic	18	$CH_3(CH_2)_{16}COOH$	69.9	371	39.1	352
Oleic	18	$CH_3(CH_2)_7CH=CH(CH_2)_7COOH$	16.3	-	19.9	349
Linoleic	18	$CH_3(CH_2)_4CH=CHCH_2CH=CH(CH_2)_7COOH$	-5	-	35	366
Linolenic	18	$CH_3CH_2CH=CHCH_2CH=CHCH_2CH=CH(CH_2)_7COOH$	-11	-	-	-
Arachidic	20	$CH_3(CH_2)_{18}COOH$	75.2	-	50	-
Eicosenoic	20	$CH_3(CH_2)_7CH=CH(CH_2)_9COOH$	23	-	15	-
Behenic	22	$CH_3(CH_2)_{20}COOH$	80	-	54	-
Erucic	22	$CH_3(CH_2)_7CH=CH(CH_2)_{11}COOH$	34	-	-	-

Table 2.3 summarizes typical fatty acid composition data for various triglycerides. For most fats and oils of interest the majority of the fatty acids have 16 and 18 carbon length chains. Animal tallow is composed of about 60% saturated, paimitic and stearic acids. The remainder is singly unsaturated oleic acid. Soybean oil, corn oil, peanut oil etc. contain predominantly unsaturated acids, the majority containing oleic and linoleic acids (doubly unsaturated). Rapeseed oil from some sources contains a high percentage of the monounsaturated, C22 erucic acid.

Table 2.3 Weight percent of fatty acids in various fat and oils feedstocks

Carbon number	Saturated acids							Mono unsaturated acids				Di	Tri
	8	10	12	14	16	18	> 18	< 16	16	18	> 18		
Beef tallow	—	—	0.2	2–3	25–30	21–26	0.4–1	0.5	2–3	39–42	0.3	2	
Butter	1–2	2–3	1–4	8–13	25–32	8–13	0.4–2	1–2	2–5	22–29	0.2–1.5	3	
Coconut	5–9	4–10	44–51	13–18	7–10	1–4	—	—	—	5–8		1–3	
Cod liver	—	—	—	2–6	7–14	0–1		0–2	10–20	25–31	35–52		
Corn	—	—	—	0–2	8–10	1–4			1–2	30–50	0–2	34–56	
Cottonseed	—	—	—	0–3	17–23	1–3				23–41	2–3	34–55	
Lard	—	—	—	1	25–30	12–16		0.2	2–5	41–51	2–3	4–22	
Linseed	—	—	—	0.2	5–9	0–1	—	—	—	9–29		8–29	45–67
Palm	—	—	—	1–6	32–47	1–6	—	—	—	40–52		2–11	
Palm kernal	2–4	3–7	45–52	14–19	6–9	1–3	1–2		0–1	10–18		1–2	
Peanut	—	—	—	0.5	6–11	3–6	5–10		1–2	39–66		17–38	
Rapeseed	—	—	—	—	2–5	1–2	0.9		0.2	10–15	50–60	10–20	5–10
Safflower	—	—	—	—	5.2	2.2				76.3		16.2	
Soybean	—	—	—	0.3	7–11	3–6	5–10		0–1	22–34		50–60	2–10
Sunflower					6.0	4.2	1.4			18.7		69.3	0.3
Tung	—	—	—	—	—	—	—	—	—	4–13		8–15	bulk

2.3.5 Cetane number[9]

The cetane number of the fuel, specified by ASTM D-613, is a measure of its ignition delay with higher cetane numbers indicating shorter time between the initiation of fuel injection and ignition, a desirable property in diesel engine fuel. The cetane index is defined by ASTM D-976. The cetane index is a calculated property that correlates well with cetane number for natural petroleum stocks. Cetane index is also a measure of fuel aromaticity and is therefore not relevant to biodiesel, which contains no aromatic compounds.

The cetane number of biodiesels depends on the parent oil source but in general is at the high end of the range typical of Number 2 diesel, cetane numbers range from 45.8 to 56.9 for soy and from 48 to 61.8 for rapeseed methylesters. This broad range of values is probably caused by differences in the fractional conversion of triglycerides to esters and by the presence of residual methanol and glycerol in the fuel. Highly saturated esters such as those prepared from tallow and used frying oil have the highest cetane numbers. The effect of blending biodiesel on cetane number is near linear for mixtures of esters with either Number 1 or Number 2 fuels. As shown in Figure 2.6 where the high correlation coefficients support a linear relationship between cetane number of the neat fuels and blends, in spite of the apparent curvature of the trend for soybean oil methylesters. Cetane number increases with chain length, decreases with number of double bonds, and decreases as double bonds and carbonyl groups move toward the center of the chain. For pure esters of stearic acid, cetane number was approximately 75, but for esters of linolenic acid with three double bonds, cetane number had dropped to the mid-twenties.

Cetane number increased from 47.9 to 75.6 for saturated C10 through C18 esters. At and above C12, the cetane numbers were above 60. Preparation of esters with longer chain alcohols, such as ethanol or butanol, had little effect on cetane number. Emission testing has shown that above 55-60, increased cetane has little or no impact on further emissions reductions. Increasing cetane number has been shown to reduce nitrogen oxide (NO_x) emissions. Cetane number can be enhanced using ignition improvers which suggest a strategy for eliminating the increased NO, emission usually observed with biodiesels and blends. Neat biodiesel does not respond to treatment with ethylhexylnitrate which is widely used as a cetane improver for low quality diesel fuels.

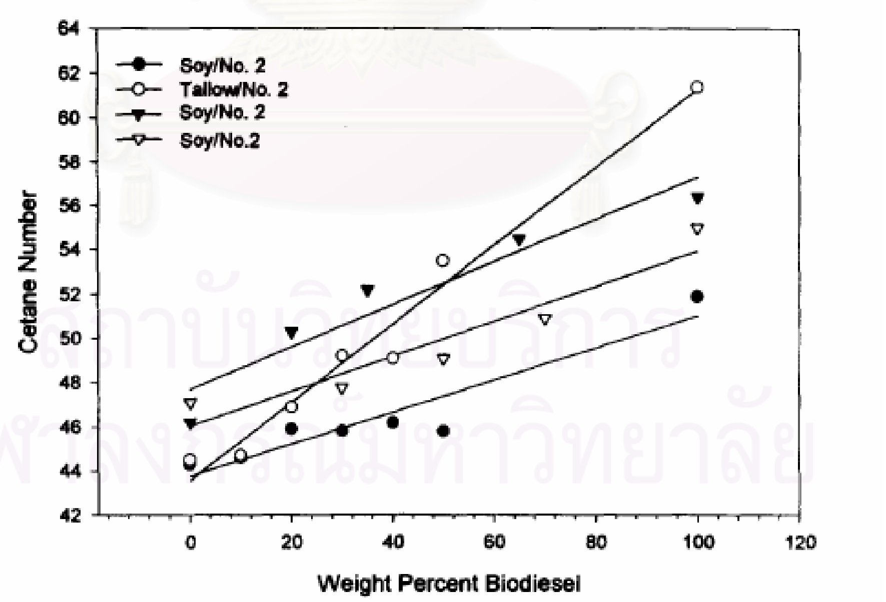

Figure 2.6 Cetane number for blends of soy and tallow methylesters with Number2 diesel.

2.3.6 Flash point

Flash point (ASTM D-93) is a measure of the temperature to which a fuel must be heated such that the mixture of vapor and air above the fuel can be ignited. All Number 2 diesel fuels have relatively high flash points (54° (2 minimum, 71° (2 typical). The flash point of neat biodiesel is even higher, typically greater than 90 °C. Low flash points may be caused by residual methanol in the ester. A material with about 90 °C or greater flash point is considered as non-hazardous from a storage and fire-hazard point of view under U.S. Department of Transportation regulations. Neat biodiesel is thus much safer than diesel in this regard. In blends, the diesel flash point will prevail up to the 50% blend level and then the flash point will begin to rise.

2.3.7 Distillation temperatures

As mixtures of a few relatively similar compounds, fat and oil ester fuels have a narrow boiling range relative to Number 2 diesel and exhibit average boiling points ranging between about 325 and 350 °C, this temperature range is near the high end of the range reported for diesel. In B-20 blends, fuels meeting the ASTM T-90 distillation specification (as measured by ASTM D-86) can be produced. However, EMA have reported that intake valve deposit formation is a problem with soy based B-20 at light load and this may be related to the large percentage of olefinic, high boiling molecules in soyesters. If biodiesel have low initial boiling points suggesting the presence of methanol or glycerol, which was not removed after ester synthesis. These fuels might also be expected to have low cetane numbers and flash points.

2.3.8 Specific gravity

Number 2 diesel exhibits a specific gravity of 0.85 (ASTM D-287). Biodiesel specific gravity varies between 0.86 and 0.90 and is typically 0.88. Therefore volumetric metering of biodiesel (as in the unit injectors used in modern diesel engines) results in the delivery of a slightly greater mass of fuel. Biodiesels have a lower energy content on both a volumetric and a mass basis.

2.3.9 Viscosity

The ASTM D-445 specification of maximum 4.1 cSt viscosity at 40°C is barely met by soybean oil methylesters. Viscosity values for esters of rapeseed oil and tallow exceed this value significantly. In any case, the viscosity of neat biodiesels is higher than for typical Number 2 diesel. High viscosity leads to poorer atomization of the fuel spray and less accurate operation of the fuel injectors. Additionally, the average viscosity of biodiesel and biodiesel blends increases more rapidly as temperature is decreased than that of Number 2 diesel. Monoglyceride impurities have also been shown to significantly increase the viscosity of methyl soyesters. The effect of biodiesel content on the viscosity of blends is shown in Figure 2.7. The blend viscosity is lower than would be predicted from a linear combination model, probably because dissolution of biodiesel in D-2 minimizes intramolecular interactions responsible for this property. The viscosity of blends containing up to 30 wt% of soy or rape methylesters will most likely meet standards for Number 2 diesel.

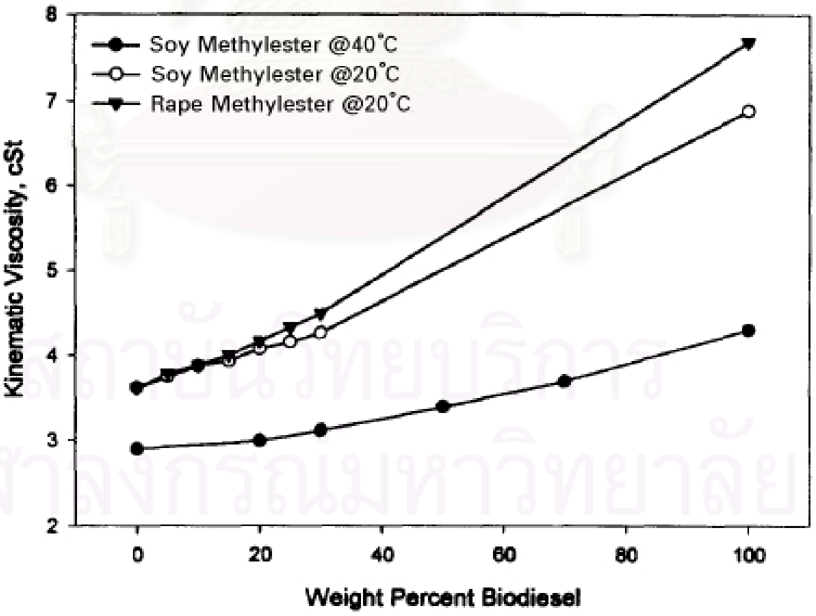

Figure 2.7 Effect of blending soybean and rapeseed esters on diesel fuel viscosity.

2.3.10 Storage and stability

Stability encompasses thermal stability under both hot and cold conditions, resistance to oxidation, polymerization, and microbial activity during storage, and absorption of water. The main source of instability in biodiesel fuels is unsaturation in the fatty acid chain. If two or more double bonds are present, they have a mutually activating effect. In oxidative instability, the methylene carbons between the olefinic carbons are the sites of first attack. After hydrogen is removed from such carbons oxygen rapidly attacks and a hydroperoxide is ultimately formed where the polyunsaturation has been isomerized to include a conjugated diene. This reaction is a chain mechanism that can proceed rapidly once an initial induction period has occurred. The greater the level of unsaturation in a fatty oil or ester, the more susceptible it will be to oxidation. Once the hydroperoxides have formed, they decompose and inter-react to form numerous secondary oxidation products including aldehydes, alcohols, shorter chain carboxylic acids, and higher molecular weight oligomers often called polymers. Another polymerization mechanism, vinyl polymerization, has been proposed as being part of the degradation process of fatty oils and esters. However, conventional understanding of oxidation chemistry would imply that such processes would not be significant when oxygen was abundant, so its precise level of importance has not been determined. The metals and elastomers in contact with biodiesel during storage can also impact stability. Oxidation leads to the formation of hydroperoxides, which can attack elastomers or polymerize to form insoluble gums. These problems are characterized by increased deposits on injectors and pump parts, increased pressure drops across filters, and a few failed injectors and pumps. The interesting thing is that these problems only occur in the fuels that contain biodiesel. The comparison petroleum diesel fuels that have been used in these limited programs never exhibited any of these problems.

2.3.11 Iodine number

Iodine number (DIN 53241/IP 84/81) is a measure of the degree of unsaturation of the fuel. Unsaturation can lead to deposit formation and storage stability problems with fuels. Soy and rapeseed methylester have iodine values of approximately 133 and 97. Lower value is expected based on the greater degree of saturation of this material. Fuel with iodine number greater than 115 is not acceptable because of excessive carbon deposits. Many biodiesel fuels are produced from feed stocks that are naturally highly unsaturated. Removal of the unsaturation by, for example, hydrogenation leads to a worsening of cold flow properties.

2.3.12 Oxidative stability and gum number

Oxidation stability is measured by ASTM D2274. Oxidation stability of number 2 diesel compared to, methylesters of tallow and soy were far more prone to oxidation. Number 2 diesel consumed 5% of the available oxygen, tallow methylesters consumed 60%, and soybean oil methylesters consumed 90%. Certain minor components of biodiesel, such as tocopherol, are natural antioxidants and that these are removed if the biodiesel is purified by distillation. In comparative oxidation tests, the peroxide value (a measure of the amount of hydroperoxides present) increased roughly four times faster for a distilled soy methylester than for undistilled. Interestingly, formation of hydroperoxides resulted in a significant increase in cetane number over the course of these relatively short-term tests (up to 24 days). Clearly an understanding of the maximum acceptable hydroperoxide level in biodiesel is needed. This information must include the impact of hydroperoxides on elastomers and metals, fuel combustion properties, microbial activity, and gum formation.

Oxidation products formed in biodiesel will affect fuel storage life and contribute to deposit formation in tanks, fuel systems and filters. Gum number is a measure of deposit formation. Fuels with high iodine numbers may possess high gum numbers. Gum numbers for methyl- and ethylesters of soybean oil and found 16,400 and 19,200, respectively. Gum deposits were most significant for metals containing copper while acid numbers were highest for samples in contact with steel and aluminum. Clearly soy based biodiesel fuels exhibit poor stability relative to conventional diesel. This is also true for rapeseed based biodiesel, as demonstrated during a 2-year storage stability study where peroxide and acid values increased by more than one order of magnitude.

2.3.13 Water absorption

Water present in fuel can cause the formation of rust and, in the presence of acids and hydroperoxides formed by fuel oxidation, lead to corrosion. Water is also a necessary ingredient for microbial growth, which can occur at the interface between the fuel and any free water phase. ASTM standard D-975 allows up to 500 ppm water in D-2. As the solubility of water in D-2 is only about 60 ppm (at 25 °C), any water above this level will be present as a separate phase either at the bottom of the tank or suspended as an emulsion. Water solubility data are available for methyl soyester and for a 20% blend with D-2. The solubility of water in pure methyl soyester was found to be ≈1500ppm while only 40 ppm dissolved in the B-20.

2.4 Elastomer [10]

Elastomers are the group of polymers that can easily undergo very large reversible elongations ($\leq$ 500 – 1000%) at relatively low stresses. This requires that the polymer be completely (or almost completely) amorphous with a low glass transition temperature and low secondary forces so as to obtain high polymer chain mobility. Some degree of crosslinking is needed so that the deformation is rapidly and completely reversible (elastic). The initial modulus of an elastomer should be very low (<100 N cm^{-2}), but this should increase fairly rapidly with increasing elongation; otherwise, it would have no overall strength and resistance to rupture at low strains. Most elastomers obtain the needed strength via crosslinking and the incorporation of reinforcing inorganic fillers (e.g., carbon black, silica). Some elastomers undergo a small amount of crystallization during elongation, especially at very high elongations, and this acts as an additional strengthening mechanism. The T_m of the crystalline regions must be below or not significantly above the temperature of the elastomer in order that the crystals melt and deformation are reversible when the stress is removed. The extent of crosslinking and the resulting strength and elongation characteristics of an elastomer cover a considerable range depending on the specific end use.

2.4.1 Acryonitrile–butadiene rubber (NBR) [11]

Nitrile Rubber (NBR) is commonly considered the workhorse of the industrial and automotive rubber products industries. NBR is actually a complex family of unsaturated copolymers of acrylonitrile and butadiene. By selecting an elastomer with the appropriate acrylonitrile content in balance with other properties, the rubber compounder can use NBR in a wide variety of application areas requiring oil, fuel, and chemical resistance. In the automotive area, NBR is used in fuel and oil handling hose, seals and grommets, and water handling applications. With a temperature range of –40 °C to +125 °C, NBR materials can withstand all but the most severe automotive applications. On the industrial side NBR finds uses in roll covers, hydraulic hoses, conveyor belting, graphic arts, oil field packers, and seals for all kinds of plumbing and appliance applications. Worldwide consumption of NBR is about 368,000 metric tons annually. Figure 2.8 shows the chemical structure of NBR, indicating the three possible isomeric structures for the butadiene segments.

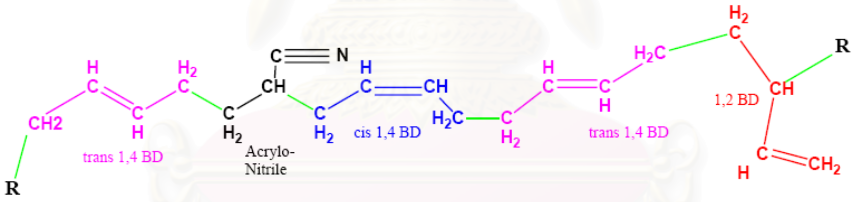

Figure 2.8 NBR structure.

2.4.2 Hydrogenated nitrile butadiene rubber (HNBR) [12]

HNBR is widely known for its physical strength and retention of properties after long-term exposure to heat, oil, and chemicals. Depending on filler selection and loading, HNBR compounds typically have tensile strengths of 20–31 MPa when measured at 23 °C. Compounding techniques allow for HNBR to be used over a broad temperature range, -40 °C to 165 °C, with minimal degradation over long periods of time. For low-temperature performance, low acryonitrile grades should be used; high-temperature performance can be obtained by using highly saturated HNBR grades with white fillers. As a group, HNBR elastomers have excellent resistance to common automotive fluids (e.g., engine oil, coolant, fuel, etc.) and many industrial chemicals. Like NBR, fluid and chemical resistance improves as the acryonitrile content is increased.

The unique properties attributed to HNBR have resulted in wide adoption of HNBR in automotive, industrial, and assorted, performance-demanding applications. On a volume basis, the automotive market is the largest consumer, using HNBR for a host of dynamic and static seals, hoses, and belts.

2.4.3 Nitrile/PVC resin blends (NBR/PVC) [13]

PVC resin are blended with nitrile polymer to provide increased resistance to ozone and abration. The PVC also provide a significant improvement in solvent resistant, yet maintains similar chemical and physical properties, commonly noted among nitrile elastomers. The addition of the PVC resin also provide a greater pigment carrying capacity which allow better retention of pastel and bright colors.

2.4.4 Acrylic rubber [14]

Acrylic rubber can be emulsion- and suspension-polymerized from acrylic esters such as ethyl, butyl, and/or methoxyethyl acetate to produce polymers of ethyl acetate and copolymers of ethyl, butyl, and methoxyl acetate. Polyacrylate rubber, such as Acron® from Cancarb Ltd., Alberta, Canada, possesses heat resistance and oil resistance between nitrile and silicone rubbers. Acrylic rubbers retain properties in the presence of hot oils and other automotive fluids, and they resist softening or cracking when exposed to air up to 392 °F (200 °C). The copolymers retain flexibility down to 40 °F (–40 °C). Automotive seals and gaskets constitute a major market. These properties and inherent ozone resistance are largely due to the polymer’s saturated “backbone”. Polyacrylates are vulcanized with sulfur or metal carboxylate, with a reactive chlorine-containing monomer to create a cross-linking site. Copolymers of ethylene and methyl acrylate, and ethylene acrylics, have a fully saturated “backbone,” providing heat-aging resistance and inherent ozone resistance. They are compounded in a Banbury mixer and fabricated by injection molding, compression molding, resin transfer molding, extrusion, and calendaring.

2.4.5 Fluoroelastomers (FKM)

Fluoroelastomers can be polymerized with copolymers and terpolymers of tetrafluoroethylene, hexafluoroethylene, and vinylidene fluoride. The fluorine content largely determines chemical resistance and *Tg,* which increases with increasing fluorine content. Low-temperature flexibility decreases with increasing fluorine content. The fluorine content is typically 57 wt%.

TFE/propylene copolymers can be represented by Aflas® TFE, produced by Asahi Glass. They are copolymers of tetrafluoroethylene (TFE) + propylene, and terpolymers of TFE + propylene + vinylidene fluoride. Fluoroelastomer dipolymer and terpolymer gums are amine or bisphenol-cured and peroxide-cured for covulcanizable blends with other peroxide curable elastomers. They can contain cure accelerators for faster cures, and they are divided into three categories:

(1) gums with incorporated cures
(2) gums without incorporated cures
(3) specialty master batches used with other fluoroelastomers

Aflas products are marketed in five categories according to their molecular weight and viscosities. The five categories possess similar thermal, chemical, and electrical resistance properties but different mechanical properties. The lowest viscosity is used for chemical process industry tank and valve linings, gaskets for heat exchangers and pipe/flanges, flue duct expansion joints, flexible and spool joints, and viscosity improver additives in other Aflas grades.

The second-lowest viscosity grade is high-speed extruded into wire/cable coverings, sheet, and calendered stock. Wire and cable covering are a principal application, especially in Japan. The third grade, general-purpose, is molded, extruded, and calendered into pipe connector gaskets, seals, and diaphragms in pumps and valves. The fourth grade, with higher MW, is compression molded into O-rings and other seal applications.

The fifth grade, with the highest MW, is compression molded into oil field applications requiring resistance to high-pressure gas blistering. It is used for down-hole packers and seals in oil exploration and production. Oilfield equipment seals are exposed to short-term temperatures from 302 to 482 °F (150 to 250 °C) and pressures above 10,000 lb/in^2 (68.7 MPa) in the presence of aggressive hydrocarbons H_2S, CH_4, CO_2, amine-containing corrosion inhibitors, and steam and water.

Aircraft jet engine O-rings require fluoropolymer grades for engine cover gaskets that are resistant to jet fuel, turbine lube oils, and hydraulic fluids. Dyneon® BREs (base-resistant elastomers) are used in applications exposed to automotive fluids such as ATF, gear lubricants, engine oils shaft seals, O-rings, and gaskets.

DuPont Dow Elastomers fuel-resistant Viton® fluoroelastomers are an important source for the applications described previously. The company's Kalrez® perfluoroelastomers with reduced contamination are widely used with semiconductors and other contamination-sensitive applications. Contamination caused by high alcohol content in gasoline can cause fuel pump malfunction. The choice of polymer can determine whether an engine functions properly.

The three principal Viton categories are;

1) Viton A dipolymers composed of vinylidene fluoride (VF2) and hexafluoropropylene (HFP) to produce a polymer with 66% (wt%) fluorine content.

2) Viton B terpolymers of VF2 + HFP + tetrafluoroethylene (TFE) to produce a polymer with 68% fluorine.

3) Viton F terpolymers composed of VF2 + HFP + TFE to produce a polymer with 70% fluorine.

The three categories are based on their resistance to fluids and chemicals. Fluid resistance generally increases but low-temperature flexibility decreases with higher fluorine content. Specialty Viton grades are made with additional or different principal monomers in order to achieve specialty performance properties. An example of a specialty property is low-temperature flexibility.

FKMs are coextruded with lower-cost (co)polymers such as ethylene acrylic copolymer. They can be modified by blending and vulcanizing with other synthetic rubbers such as silicones, EPR and EPDM, epichlorohydrin, and nitriles.

Fluoroelastomers are blended with modified NBR to obtain an intermediate performance/cost balance. These blends are useful for underhood applications in environments outside the engine temperature zone such as timing chain tensioner seals. Fluoroelastomers are blended with fluorosilicones and other high temperature polymers to meet engine compartment environments and cost/performance balance. Fine-particle silica increases hardness, red iron oxide improves heat resistance, and zinc oxide improves thermal conductivity. Hardness ranges from about Shore 35 A to 70 A. Fluorosilicones are resistant to nonpolar and nominally polar solvents, diesel and jet fuel, and gasoline, but not to solvents such as ketones and esters.

Typical applications are exhaust gas recirculating and seals for engine valve stems and cylinders, crankshaft, speedometers, and o-rings for fuel injector systems.

FKMs are compounded in either water-cooled internal mixers or two-roll mills. A two-pass mixing is recommended for internally mixed compounds with the peroxide curing agent added in the second pass. Compounds press-cured 10 min @ 350 °F (177 °C) can be formulated to possess more than 2100-lb/in^2 (14.4-MPa) tensile strength, 380% elongation, 525% @ 100% modulus, and higher values when postcured 16 h. @ 392 °F (200 °C).11 Processing temperatures are >392 °F (200 °C).

Fluoroelastomers are generally made in an emulsion polymerization process. Fluoro-monomers such as HFP, VF2, and TFE are fed to a reactor under elevated temperature and pressure along with surfactants and other additives. Once the polymerization is complete the latex is removed, the polymer coagulated and washed, and the polymer is dried and packaged for use.

The main fluoroelastomer compositions are shown in Figures 2.9-2.12 [15].

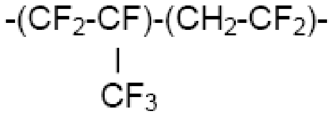

$$-(CF_2-\underset{\substack{|\\ CF_3}}{CF})-(CH_2-CF_2)-$$

Figure 2.9 Copolymer fluoroelastomer structure.

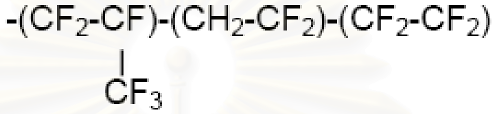

$$-(CF_2-\underset{\substack{|\\ CF_3}}{CF})-(CH_2-CF_2)-(CF_2-CF_2)$$

Figure 2.10 Terpolymer fluoroelastomer structure.

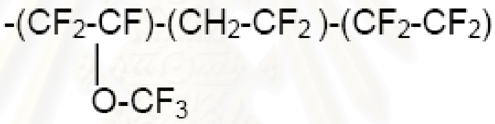

$$-(CF_2-\underset{\substack{|\\ O-CF_3}}{CF})-(CH_2-CF_2)-(CF_2-CF_2)$$

Figure 2.11 Improved low temperature fluoroelastomer terpolymer structure.

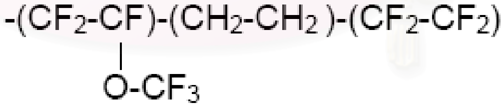

$$-(CF_2-\underset{\substack{|\\ O-CF_3}}{CF})-(CH_2-CH_2)-(CF_2-CF_2)$$

Figure 2.12 Non-VF_2 fluoroelastomer terpolymer structure.

2.5 Mechanical properties of elastomers [9]

Many polymer properties such as solvent, chemical, and electrical resistance and gas permeability are important in determining the use of a specific polymer in a specific application. However, the prime consideration in determining the general utility of a polymer is in mechanical behavior, that is, its deformation and flow characteristics under stress. The mechanical behavior of a polymer can be characterized by its stress-strain properties. This often involves observing the behavior of a polymer as one applies tension stress to it in order to elongate (strain) in to the point where if ruptures (pulls apart). The results are usually shown as a plot of the stress versus elongation (strain). The stress is usually expressed in newtons per square centimeter ($N.cm^{-2}$) or megapascals (MPa) where 1 MPa = 100 $N.cm^{-2}$. The strain is the fractional increase in the length of polymer sample (*i.e.*, $\Delta L/L$, where L is the original, unstretched sample length).

Four important quantities characterize the stress-strain behavior of a polymer:

Modulus. The resistance to deformation as measured by initial stress divided by $\Delta L/L$.

Ultimate Strength or Tensile Strength. The stress required to rupture the sample.

Ultimate Elongation. The extent of elongation at the point where the sample ruptures.

Elastic Elongation. The elasticity as measured by the extent of reversible elongation.

Polymer vary widely in their mechanical behavior depending on the degree of crystallinity, degree of crosslinking, and the values of T_g and T_m. High strength and low extensibility are obtained in polymers by having various combinations of high degrees of crystallinity or crosslinking or rigid chains (characterized by high T_g). High extensibility and low T_g values. The temperature limits of utility of a polymer are governed by its T_g and/or Tm. Strength is lost at or near T_g for an amorphous polymer and at or near T_m for crystalline polymer.

2.6 Literature reviews

In 1972, Eisner *et al* [16] studied the relationship between the structure of some fatty acid esters of varying chain length and their swelling effect on standard nitrile rubber samples. The esters evaluated were: methyl esters of caprylic, capic, lauric, myristic, palmitic and isostearic acids; n-butyl, isobutyl, n-octyl, octadecyl, “tallow” and 2,2 dimethyl-1,3-propanediol esters of luaric acid and tetradecyl acetate. Federal test methods for aircraft turbine lubricants were used for the evaluations. In the esters the swelling was higher with low nitril rubber (type L) than with high nitrile rubber (type H). The lower the equivalents weight of the ester, the higher the swelling with both types of rubber. Branching in the alcohol moiety lowered the swelling. Deswelling (desorption) in air of the swelled samples was also investigated. Methyl myristate, methyl palmitate and the long chain laurate esters meet MIL-L-23699 military specifications for type H rubbers. In type L rubbers the swelling is too high to meet specifications.

In 1994, Cusano *et al.* [17] studied swelling of elastomer when composition of diesel fuel changed. By studing the effect of difference in sulfur and aromatic content in diesel fuel on elastomer seal. The result showed that NBR seal failures which occurred soon after exposure to low sulfur fuels were resulted from change in fuel composition aromatic content and especially diaromatic content. An equation was developed which can be used to predict NBR seal swelling by using data of the fuel composition in terms of aromatics, diaromatics and cycloparaffins content, as in following equation

$$\% \text{ Swelling} = 0.20(TA) + 0.77(Di\text{-}A) - 1.1\,(CP) + 35 \qquad (2.7)$$

where:

TA = Total aromatics
Di = Diaromatics
A = Aromatics
CP = Cycloparaffins

In 1994, Robertson *et al.* [18] observed the behavior of elastomeric seals exposed to various automotive diesel fuels. The behavior is governed not only by the chemistry of the elastomer but also by the aromatic content of the fuel and is typical of elastomer/fluid interactions occurring under diffusion control. The result showed that significant variations in elastomer behaviors occur when they are exposed to different types of diesel fuel, and that major differences in response can exist between environmentally adapted and standard automotive diesel oil. These responses depend on elastomer chemistry and automotive diesel oil. In case of diesel oil, it also depends on aromatic content and type of aromatic content.

In 1997, Beesee *et al.* [5] studied the compatibility of four base fuels and six blends with elastomer and metallic components commonly found in fuel systems such as seal, gaskets, o-rings and fuel tank. The physical properties of the elastomers were measured according to American Society of Testing and Materials (ASTM) D471, “Standard Test Method for Rubber Property-Effect of Liquids” and ASTM D412, “Standard Test Methods for Rubber Properties in Tension.” These evaluations were performed at 51.7 ^{o}C for 0, 22, 70, and 694 hours. Tensile strength, hardness, swelling, and elongation were determined for all specimens. Six metal specimens were stored for 6 months at 51.7 ^{o}C. Visual inspection of the specimens was performed, and total acid number (TAN) was determined using ASTM D664, “Standard Test Method for Acid Number of Petroleum Products by Potentiometric Titration.” The results showed that effect certain physical properties in nitrile rubber, nylon 6/6, and high-density polypropylene. Teflon®, Viton®401-C and Viton® GFLT appear to have good resistance and minimal changes in the physical properties when exposed to this fuel matrix. Copper-containing metals exhibit severe corrosion when exposed to biodiesel and its blends; they also form large amounts of gum when stored at elevated temperatures. The steel and aluminum samples exhibit exceptionally high total acid numbers which could corrode various parts of the fuel system.

In 2003, Kumnuantip *et al.* [19] studied dynamic mechanical properties and swelling behaviour of two natural rubber (NR) (STRVS60 and STR20CV) vulcanizates filled with different reclaimed rubber contents. They were examined with respect to loss tangent (tanδ) and the change in glass transition temperature. $\text{Tan}\delta_{max}$ was found to shift to higher temperature, and the peak height reduced with increasing reclaimed rubber content. An increase in the overall width of the tanδ peaks was associated with the presence of styrene butadiene rubber (SBR) in the reclaimed rubber. Tg was found to increase with reclaim content due to an increased cross-link density, and presence of carbon black in the reclaim. The change in cross-link density was more dependent on the vulcanizing recipe than the initial molar mass of the rubber. The equilibrium swelling of the NR vulcanizates was observed to reduce with increasing reclaimed rubber content due to the increases in cross-link density and the polymer–solvent interaction.

In 2004, Jianbo *et al.* [20] studied solvent power of biodiesel. Refined methyl, ethyl, propyl, 1-butyl, and 2-butyl biodiesels as well as unrefined methyl biodiesels containing glycerides were prepared, and their solvent power was evaluated by measuring the kauri-butanol value. By analysis of the kauri-butanol values of bidoiesel with different alcohol types, some interesting results were obtained. The pure methyl esters have larger kauri-butanol values than those containing glycerides. The unsaturated fatty acid esters have larger kauri-butanol values than the saturated ones, while the number of double bonds of the unsaturated fatty acid has little effect on the value. The shorter the carbon chain of the fatty acid group or alcohol group, the larger the kauri-butanol value of biodiesel. Biodiesel with straight chains has a larger kauri-butanol value than that with branched chains.

In 2005, Nielsen *et al.* [21] studied swelling and Hansen solubility parameters (HSP) of two types of elastomers: EPDM and FKM elastomers. They were determined before vulcanization by correlating solubility in solvents that fully dissolved the polymers. These values were then used to generate plots of solvent swelling after the same elastomers were vulcanized. HSP correlations were also established for the same vulcanized elastomers at different levels of swelling. This makes it possible to predict the swelling of the elastomers studied in contact with many untested solvents.

In 2005, Terry *et al.* [22] studied impact of biodiesel on fuel system component durability using B5 and B20 of rapeseed methyl ester (RME), soy methyl ester (SME) and oxidized SME as biodiesel sample. Elastomer specimen tested were NBR medium content of acrylonitrile, NBR high content of acrylonitrile, HNBR, fluorocarbon polymer (medium fluorine content) and fluorocarbon polymer (high fluorine content). Elastomers were immersed in biodiesel at 60^{o}C for 1000 hours. Control sample was conditioned in air 23 ^{o}C for the same period. Result showed that fluorocarbon elastomers of medium to high fluorine content are most compatible with the test fuels under the specified conditions at concentrations of 20% or below. The other elastomer tested exhibited good resistance to changes in physical properties but exceeded the typically acceptable levels of degradation in one or more tests. These materials may be less compatible with biodiesel blends under certain applications.

CHAPTER III

EXPERIMENTAL

3.1 Materials

3.1.1 Diesel and biodiesel blends

Biodiesel of palm oil produced from transesterification of crude palm oil, was supplied by Thailand Institute of Scientific and Technological Research. Biodiesel of used cooking oil was produced from transesterification of used frying potato oil from in Frito-Lay (Thailand) Co.,Ltd. and supplied by Department of Alternative Energy Development and Efficiency. Diesel PTT Alpha-X from PTT Public Co.,Ltd was used as a blending component. Ratios of diesel and biodiesel blends are assigned code as in Table 3.1.

Table 3.1 Ratio of diesel and biodiesel blends

Sample code	Biodiesel / diesel (vol/vol)
B0	Diesel 100%
B5-P	Biodiesel palm oil 5% /Diesel 95%
B10-P	Biodiesel palm oil 10% /Diesel 90%
B100-P	Biodiesel palm oil 100%
B5-C	Biodiesel used cooking oil 5% /Diesel 95%
B10-C	Biodiesel used cooking oil 10%/Diesel 90%
B100-C	Biodiesel used cooking oil 100%

3.1.2 Elastomers

The elastomeric materials used in automotive fuel system were chosen for this study. All of them were obtained form Inoue Rubber (Thailand) Co.,Ltd.. Its type and application were listed in Table 3.2.

Table 3.2 Type of elastomer used in this study and application

Material type	Application
NBR	Pump seal, oil handling hose
HNBR	Fuel system seal
NBR PVC	Fuel hose
Acrylic rubber	Fuel filter
Copolymer FKM	Injection pump seal
Terpolymer FKM	Fuel system seal

3.2 Instrument and Apparatus

3.2.1 Density meter : Anton Paar DMA4500, Austria
3.2.2 Automatic distillation tester : ISL AD 86 5G, France
3.2.3 Viscometer tube : Canon viscometer, England
3.2.4 Flash point tester : Petrotest PMA4, Austria
3.2.5 Micro carbon residue tester : Alcor MCRT-130, USA
3.2.6 Cloud point and pour point tester : ISL CPP 5G, France
3.2.7 High performance liquid chromatograph : Agilent HP-Series 1100, USA
3.2.8 X-Ray fluorescence spectrometer : Oxford Lab-X 3000, England
3.2.9 Gas chromatograph : Agilent HP6890 series, USA
3.2.10 Vacuum distillation tester : i-Fischer Dist D-1160CC, Germany
3.2.11 Viscometer bath : Precision 75943-1, England
3.2.12 Oxidation stability tester for biodiesel : Metrohm 743 Rancimat, Switzerland
3.2.13 Total acid number tester : Metrohm 808 Titrando, Switzerland
3.2.14 Balance : Mettler Toledo AG204, Switzerland
3.2.15 Durometer : Rex durometer, USA
3.2.16 Digital meter : Mitutoyo, Japan
3.2.17 Oven : WTB Binder FEO240, Germany
3.2.18 Universal tester : Instron 5500 Series, USA

3.3 Determination of the properties of diesel, biodiesel and biodiesel blends

3.3.1 Density (ASTM D4052; Standard test method for density and relative density of liquids by digital density meter)

Figure 3.1 Density meter.

A small volume (approximately 0.7 ml) of liquid sample is introduced into an oscillating sample tube and the change in oscillating frequency caused by the change in the mass of the tube is used in conjunction with calibration due to determine the density of sample.

3.3.2 Cetane index (ASTM D 976; Standard test method for calculated cetane index of distillate fuels)

The calculated cetane index is determined from the following equation:

$$\text{Cetane index} = 454.74 - 1641.416D + 774.74D^2 - 0.554B + 97.803(\log B)^2$$

where:

D = density at 15°C, g/mL, determined by test method D 4052 (see 3.3.1), and
B = mid-boiling temperature, °C, determined by test method D 86 and corrected to standard barometric pressure

3.3.3 Distillation temperature (ASTM D 86; Standard test method for distillation of petroleum products at atmospheric pressure)

Figure 3.2 Automatic distillation tester.

Sample is defined in one of five group depend on vapor pressure, initial boiling and end point. Apparatus condition and sample preparation in distillation 100 ml of sample are depend on group of sample. The distillation is performed in a laboratory batch distillation unit at ambient pressure under conditions that are designed to provide approximately one theoretical plate fractionation. Systematic observations of temperature readings and volumes of condensate are made. The volume of the residue and the losses are also recorded.

Test results are commonly expressed as percent evaporated or percent recovered versus corresponding temperature, either in a table or graphically, as a plot of the distillation curve.

3.3.4 Viscosity (ASTM D 445; Standard test method for kinematic viscosity of transparent and opaque liquids)

Figure 3.3 Viscometer bate and tube.

The time is measured for a fixed volume of liquid to flow under gravity through the capillary of a calibrated viscometer under a reproducible driving head at temperature 40 ^{o}C. The kinematic viscosity (determined value) is the product of the measured flow time and the calibration constant of the viscometer. Two such determinations are needed from which to calculate a kinematic viscosity result that is the average of two acceptable determined values.

3.3.5 Flash point (ASTM D 93; Standard test methods for flash point by pensky-martens closed cup tester)

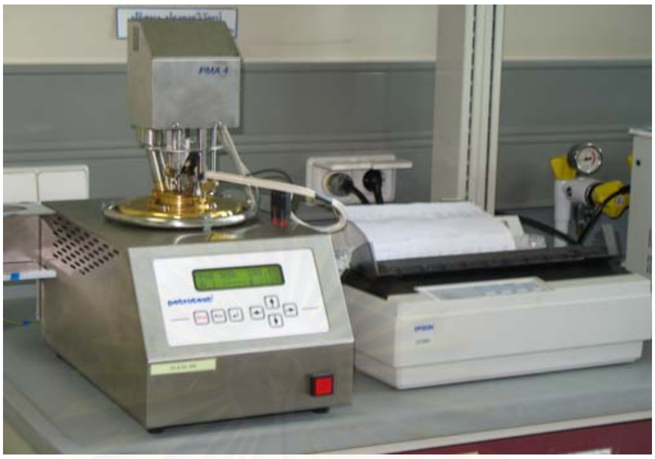

Figure 3.4 Automatic flash point tester.

A brass test cup of specified dimensions, filled to the inside mark with test specimen and fitted with a cover of specified dimensions, is heated and the specimen stirred at 5-6 ^{o}C/min. An ignition source is directed into the test cup at regular intervals with simultaneous interruption of the stirring, until a flash is detected.

3.3.6 Carbon residue (ASTM 4530; Standard test method for determination of carbon residue (micro method))

Figure 3.5 Microcarbon residue tester.

A weighed quantity of sample is placed in a glass vial and heated to 500 °C under an inert (nitrogen) atmosphere in a controlled manner for a specific time. The sample undergoes coking reactions, and volatiles formed are swept away by the nitrogen. The carbonaceous-type residue remaining is reported as a percent of the original sample as “carbon residue (micro)”.

3.3.7 Pour point (ASTM D 97; Standard test method for pour point of petroleum products)

Figure 3.6 Automatic cloud and pour point tester.

After preliminary heating, the sample is cooled at a specified rate and examined at intervals of 3 °C for flow characteristics. The lowest temperature at which movement of the specimen is observed is recorded as the pour point.

3.3.8 Cloud point (ASTM D 2500; Standard test method for cloud point of products)

The specimen is cooled at a specified rate and examined periodically. The temperature at which a cluster of wax crystals first appears observed at the bottom of the test jar is recorded as the cloud point.

3.3.9 Aromatic (IP 391; Determination of aromatic hydrocarbon types in middle distillates)

A Known mass of sample is diluted in the mobile phase and a fixed volume of this solution injected into a high performance liquid chromatograph fitted with a polar column. This column has little affinity for the nonaromatic hydrocarbons whilst exhibiting a pronounced selectivity for aromatic hydrocarbons. As a result of this selectivity, the aromatic hydrocarbons are separated from the non-aromatic hydrocarbons into distinct bands according to their ring structure, i.e. MAHs, DAHs and PAHs compounds. At a predetermined time, after the elution of the DAHs, the column is backfulshed to elute the PAHs as a single sharp band.

The column is connected to a refractive index detector which detects the components as they elute from the column. The electronic signal from the detector is continually monitored by a data processor. The amplitudes of the signals from the sample aromatics are compared with those obtained from previousty rin calibration standards in order to calculate percent mass of MAHs, DAHs and PAHs in the sample. The sum of MAHs, DAHs and PAHs, is repoted as the total content of aromatic compounds in the sample.

3.3.10 Sulfur content (ASTM D 4294; Standard test method for sulfur in petroleum and petroleum products by energy-dispersive X-ray fluorescence spectrometry)

Figure 3.7 X-Ray fluorescence spectrometer.

The sample is placed in the beam emitted from an X-ray source. The resultant excited characteristic *X* radiation is measured, and the accumulated count is compared with counts from previously prepared calibration standards in concentration range of interest to obtain the sulfur concentration in mass %.

3.3.11 Acid number (ASTM D 664; Standard test method for acid number of petroleum products by potentiometric titration)

Figure 3.8 Potentiometric tritator

The sample is dissolved in a mixture of toluene and propan-2ol containing a small amount of water and titrated potentiometrically with alcoholic potassium hydroxide using a glass indicating electrode and a calomel reference electrode. The meter readings are plotted against the respective volumes of titrating solution and the end points are taken only at well defined inflections in the resulting curve. When no definite inflections are obtained end points are taken at meter readings corresponding to those found for freshly prepared nonaqueous acidic and basic buffer solutions.

3.3.12 Oxidation stability (EN 14112; Determination of oxidation stability of fatty acid methyl esters (accelerated oxidation test))

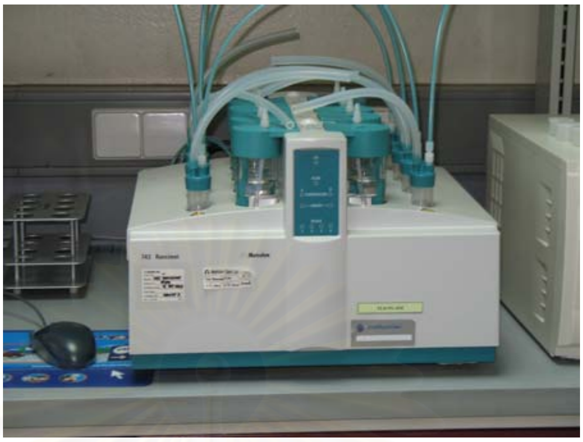

Figure 3.9 Rancimat for oxidation stability of biodiesel

A stream of purified air is passed through the sample wish has been brought to a specified temperature. The vapours released during the oxidation process, together with the air, are passed into a flask containing water which has been demineralized or distilled and contains an electrode for measuring the conductivity. The electrode is connected to a measuring and recording device. It indicates the end of the induction period when the conductivity begins to increase rapidly. This accelerated increase is caused by the dissociation of volatile carboxylic acids produced during the oxidation process and absorbed in the water.

3.3.13 Methyl ester content (EN 14103; Determination of ester and linolenic acid methyl ester contents in fatty acid methyl esters)

Determination of the percentage of methyl esters and linolenic acid of fatty acids present in the sample in n-heptane with methyl heptadeconoate as internal standard by gas chromatography according to following condition:

Column: FAMEWAX^{TM}, restek, 30m, 0.25mm ID, 0.25 µm
Inlet: split/splitless, split ratio 200:1, 250 ^{o}C
Detector: FID, 250 ^{o}C, H_2 flow 40 ml/min, make up flow 30 ml/min

Oven: 150^{o}C (hold 15 min.) to 190^{o}C @ 1.5^{o}C/min. (hold 5 min.) to 220 ^{o}C @ 1.5^{o}C/min

Carrier: He, flow 1 ml/min

Volume injected: 1 μl

3.3.14 Distillation temperature (ASTM D 1160; Standard test method for distillation of petroleum products at a reduced pressure)

Figure 3.10 Vacuum distillation tester

The sample is distilled at an accurately controlled pressure 10 mm Hg under conditions that are designed to provide approximately one theoretical plate fractionation. Data are obtained from which the initial boiling point, the final boiling point, and a distillation curve relating volume percent distilled and atmospheric equivalent boiling point temperature can be prepared.

3.3.15 Iodine value (EN 14111; Determination iodine value in fatty acid methyl esters)

Sample 0.2 g is dissolved in a mixed solvent (cyclohexane and acetic acid) and then Wijs (Iodine monochloride in acetic acid) reagent is added. After a specified time, potassium iodide and water are added to the sample and the liberated iodine is titrated using a sodium thiosulfate standardized solution and starch solution indicator.

3.3.16 Free and total glycerol and mono-, di-, triglyceride contents (EN 14105; Determination free and total glycerol and mono-, di-, triglyceride contents of fat and oil derivatives- fatty acid methyl esters)

The percentage of free and total glycerol an mono-, di-, tri-glyceride was determined by transformation of the glycerol and of the mono- and di-glycerieds into more volatile silylated derivatives in presence of pydidine and of N-methyl-N-trimethylsilyltrifluoroacetamide (MSTFA). After a calibration procedure, the quantification is carried out in the presence of two internal standard; 1,2,4-butanetriol intended for the determination of the free glycerol and 1,2,3 –tricaproyloglycerol (tricaprin) intended for the determination of the mono-, di-, tri-glycerides. Analysis of the silylated derivates by gas chromatography according to following condition :

Column: DB-5, J&W, 10m, 0.32mm ID, 0.1 μm
Inlet: cool on column
Detector: FID, 380 ^{o}C, H_2 flow 40 ml/min, make up flow 30 ml/min
Oven: 50^{o}C (hold 1 min.) to 180^{o}C @ 15^{o}C/min. to 230 ^{o}C @ 7^{o}C/min. to 370 ^{o}C @ 10 ^{o}C/min.
Carrier: He, flow 1 ml/min.
Volume injected: 1 μl

3.4 Mechanical testing

3.4.1 Durometer hardness (ASTM D 2240; Standard test method for rubber property durameter hardness)

This method is hardness measurement based on either initial indentation or indentation after a 15 second. The test specimen shall be at least 6.0 mm. in thickness. The indentor type A was used to observed hardness. The shape of indentor is shown in Figure 3.11.

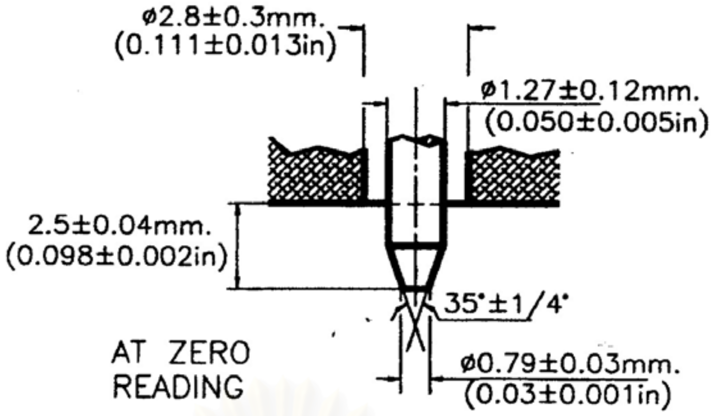

Figure 3.11 Indentor for type A durometer.

3.4.2 Tensile and elongation (ASTM D 412; Standard test methods for vulcanized rubber and thermoplastic rubber and thermoplastic elastomers-tension)

The tensile and elongation were determined by tensile tester. The rate of grip separation was 500 ± 50 mm/min. Dumbbell shape specimen in Die C, as shown in Figure 3.12 was used in this measuring. The elongation measurements were made by noting the distance between the bench marks in narrow portion of specimen. At rupture, measure and record the elongation. Elongation was calculated by equation 3.1.

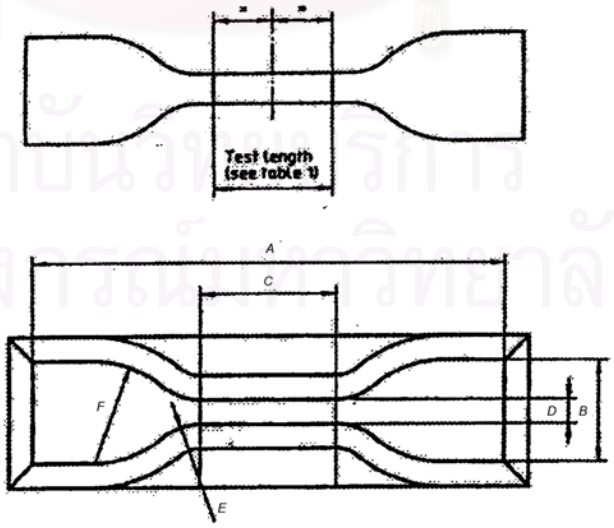

Figure 3.12 Schematic of tensile test specimen.

	Dimension	Type C (mm.)
A	Overall length (minimum)	115
B	Width of ends	25.0 ± 1.0
C	Length of narrow portion	33.0 ± 2.0
D	Width of narrow portion	6.0 ± 0.4
E	Transition radius outside	14.0 ± 1.0
F	Transition radius inside	25.0 ± 2.0

$$E = \left(\frac{L - L_o}{L_o} \right) \times 100 \tag{3.1}$$

where;

E = the elongation in percent (of original bench mark distance),

L = observed distance between end marks on the extended specimen, and

L_o = original distance between bench marks (use same units for L and L_o).

3.5 Determination of the properties of elastomers change in liquid

The tensile bar specimen of each material was placed in a sealed glass container of each fuel sample and stored at 50 ^{o}C and 100 ^{o}C for 0, 22, 670 and 1008 hours. After completion of the storage period, the test specimen was cooled to room temperature by transferring to a cool clean portion of test liquid for 30 to 60 minutes. Then it was dipped the specimen quickly in toluene and acetone, respectively. The changing of elastomer properties; the tensile strength, elongation, hardness, mass and swelling by effect of fuel were determined.

3.5.1 Mass change

Weigh each specimen in air to the nearest 1 mg, record the mass, and immerse in the fuel container. After immersion has proceeded for the required length of time, weigh the mass after test of each specimen to nearest 1 mg. Percent change in mass was calculated as in equation (3.2);

$$\textbf{\% Mass change} = \frac{(M_2 - M_1)}{M_1} \times 100 \tag{3.2}$$

where:

M_1 = initial mass of specimen in air (g)

M_2 = mass of specimen in air after immersion (g)

3.5.2 Volume change

Weigh specimen in air to the nearest 1 mg and then obtain the mass of each specimen immersed in distilled water at room temperature. Quickly dip each specimen in alcohol to remove water, blot dry with filter paper free of lint and foreign material, and place in the immersion apparatus described in 3.5. After immersion has proceeded for the required length of time, clean specimen described in 3.5. Weigh specimen in air and in distilled water again. The percentage in volume was calculated in equation (3.3);

$$\textbf{\%Volume change} = \frac{(M_3 - M_4) - (M_1 - M_2)}{(M_1 - M_2)} \times 100 \tag{3.3}$$

where;

M_1 = initial mass of specimen in air (g)

M_2 = initial mass of specimen in water (g)

M_3 = mass of specimen in air after immersion (g)

M_4 = mass of specimen in water after immersion (g)

3.5.3 Hardness change

Before and after immerse specimen, determine the hardness of specimen accordance with method ASTM D 2240. Changing of hardness in each period was calculated in equation (3.4);

$$\textbf{Hardness change} = H_i - H_o \qquad (3.4)$$

where;

H_o = original hardness before immersion (units)

H_i = hardness after immersion (units)

3.5.4 Tensile change

Determine changing in tensile strength of specimen by using Die C specimen in test method ASTM D 412 by compare result of new specimen and tested specimen. It may be desirable to calculate the tensile strength based on the swollen cross-sectional area. In that case shall be use equation (3.5);

$$TS_s = \frac{F}{A\left(1+\frac{\Delta V}{100}\right)^{\frac{2}{3}}} \qquad (3.5)$$

where;

TS_s = tensile stress based on swollen unstretched cross sectional area

F = observed force

A = original unstretched cross-sectional area of the test specimen before immersion

ΔV = volume swell after immersion (%)

To express tensile strength after immersion as a percentage change from the original properties, use equation (3.6);

$$\textbf{\%Tensile change} \quad = \frac{TS_s - TS_o}{TS_o} \times 100 \qquad (3.6)$$

where;

ΔTS = change in tensile strength after immersion (%)

TS_o = tensile stress based on original unstretched cross-sectional area

3.5.5 Elongation change

Determine changing in elongation of specimen by using Die C specimen in test method ASTM D 412 by compare result of new specimen and tested specimen. To express elongation after immersion as a percentage change from the original properties, use equation (3.7);

$$\textbf{\%Elongation change} = \frac{E_s - E_o}{Eo} \times 100 \qquad (3.7)$$

where;

E_o = original elongation before immersion

E_s = elongation after immersion

3.6 Dynamic Mechanical Analysis (DMA)

The dynamic mechanical properties of grafted natural rubber were measured on a Dynamic Mechanical Analyzer (Perkin-Elmer 7e) with a liquid nitrogen cooling system. The Parallel Plate mode was used in a temperature range of -80 to +20 ^{o}C at a heating rate of 5 ^{o}C min^{-1} and at a frequency of 1 Hz.

CHAPTER IV

RESULTS AND DISCUSSION

4.1 Biodiesel properties

Biodiesels produced from palm oil and used cooking oil, used as sample fuel in the testing of elastomers, were analyzed for their physical and chemical properties according to American standard (ASTM) and European standard (EN). The properties were compared with the specification of European standard; EN 14214.

Chemical and physical properties of biodiesels (B100-P and B-100C) are shown in Table 4.1. Their properties are within the specification. Most of them are not different, except methyl ester content, flash point, oxidation stability, triglyceride iodine value, sulfur content and cloud point. B100-C shows lower oxidation stability than B100-P because it has high unsaturated fatty acid in composition.   This was also confirmed by the iodine value.

Table 4.1 Methyl ester properties

Properties	Method	Specification EN14214	B100-P	B100-C
Density @15 °C, kg/m^3	ASTM D 4052	860-900	875.9	877.6
Specific gravity @15.6/15.6 °C	ASTM D 4052	report	0.8768	0.8785
Cetane index	ASTM D 976		50	50
Methyl ester content, % w/w	EN14103	>96.5	96.91	98.38
Kinematic Viscosity, @40°C, mm^2/s	ASTM D 445	3.5-5.0	4.5187	4.6524
Flash point, °C	ASTM D 93	>120	142	172
Oxidation stability, h.	EN14112	>6	8.3	6.7
Total acid number, mg KOH/g	ASTM D 664	<0.5	0.20	0.37
Distillation, °C				
90%	ASTM D 1160	<360	353.2	353.5
Monoglyceride, % w/w	EN14105	<0.8	0.199	0.195
Diglyceride,% w/w	EN14105	<0.2	0.063	0.041
Triglyceride, %w/w	EN14105	<0.2	0.166	0.058
Free glycerol, %w/w	EN14105	<0.02	ND	0.006
Iodine value	EN14111	<120	48.95	60.76
Sulfur content, ppm	ASTM D 5453	<10	2.41	4.40
Cloud point, °C	ASTM D 1500	report	12.6	20.5

4.2 Diesel and biodiesel blend properties

Diesel in this study has specific gravity, viscosity, total acid number, and flash point lower than both biodiesels (Table 4.2) but its sulfur content is higher.

Physical and chemical properties of biodiesel blends (in four ratios) were measured as shown in Table 4.2. All of the properties are within the specification of diesel of Department of Energy Business, Ministry of Energy. Biodiesel blends with increased volume of biodiesel, shows a change in property, such as total acid number form oxidation product of biodiesel after long term storage. Biodiesel has lower sulfur content than diesel.

4.3 Effect of biodiesel and biodiesel blends on elastomer

Six types of elastomers were immersed in biodiesel and biodiesel blends samples at temperature of 50°C for 23, 670 and 1008 hours. After immersion, the elastomers were measured for change of mechanical properties. The results are shown in Figures 4.1- 4.10.

Table 4.2 Diesel and biodiesel blends properties

Properties	Method	Specification*	Diesel	B5-P	B10-P	B5-C	B10-C
Specific gravity @15.6/15.6 ^{o}C	ASTM D 4052	>0.81	0.8296	0.8318	0.8352	0.8319	0.8350
Cetane index	ASTM D 976	>47	59	59	57	58	57
Kinematic Viscosity@40^{o}C, mm^{2}/s	ASTM D 445	3.5-5.0	3.44	3.43	3.46	3.41	3.47
Flash point, ^{o}C	ASTM D 93	>52	63	66	65	62	64
Total acid number, mg KOH/g	ASTM D 664	report	0.03	0.04	0.06	0.06	0.06
Distillation, ^{o}C							
90%	ASTM D 86	<357	354.9	351.7	347.7	350.8	348.1
Carbon residue, % w/w	ASTM D 4530	<0.05	0.02	0.02	0.02	0.02	0.02
Sulfur content, ppm	ASTM D 4294	<0.05	0.032	0.030	0.028	0.030	0.028
Pour point, ^{o}C	ASTM D 97	<10	3.0	3.0	3.0	3.0	3.0
Total Aromatic content,% wt	IP391	report	24.38	24.01	24.17	24.12	24.09
Monoaromatics			18.83	18.86	18.76	18.80	18.82
Diaromatics			3.76	3.75	3.68	3.71	3.60
Polyaromatics			1.79	1.77	1.73	1.61	1.67

*Specification of Department of Energy Business, Ministry of Energy

4.3.1 Mass change

Percent mass change of elastomers after immersed in diesel, biodiesel blends and biodiesel at 50°C for each period of time (23, 670 and 1008 hours) are presented in Figures 4.1- 4.2.

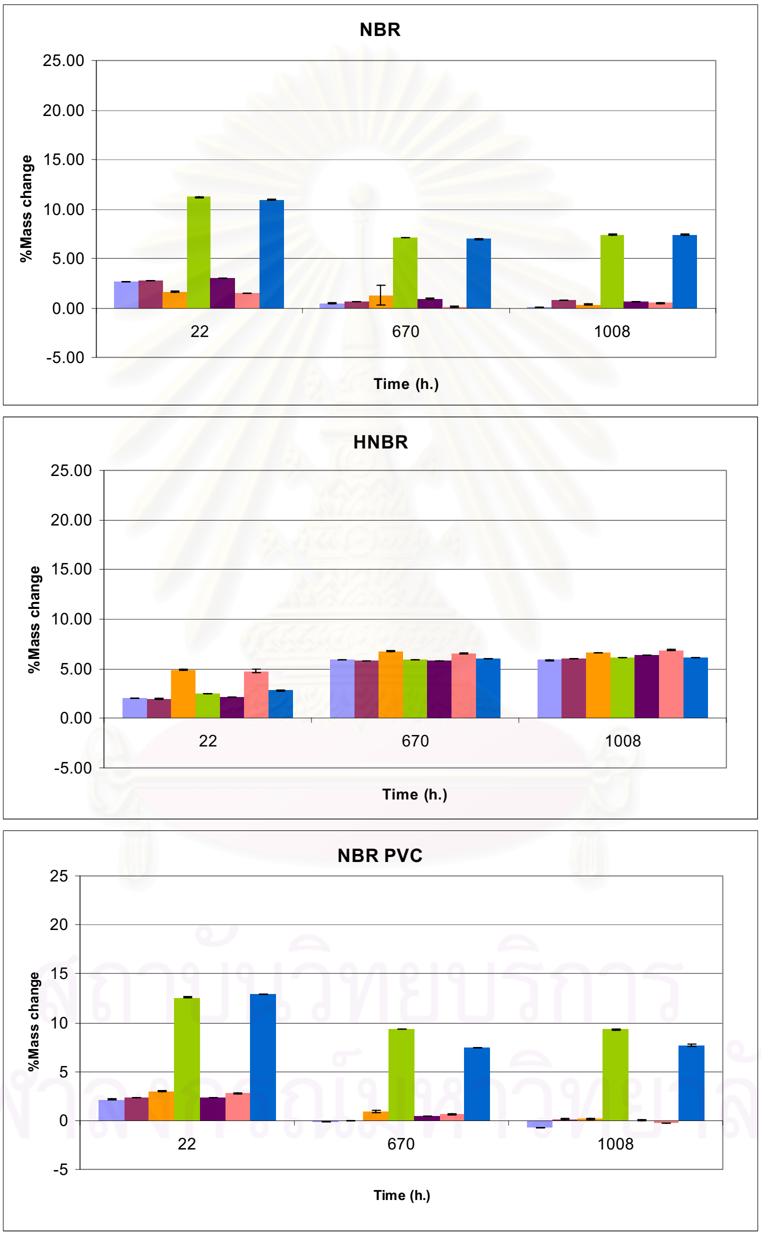

Figure 4.1 Effect of biodiesel and biodiesel blends :(■) Diesel; (■) B5-P; (■) B10-P; (■) B 100-P; (■) B5-C; (■) B10-C; (■) B100-C on percent mass change of NBR, HNBR and NBR PVC elastomers at 50 °C.

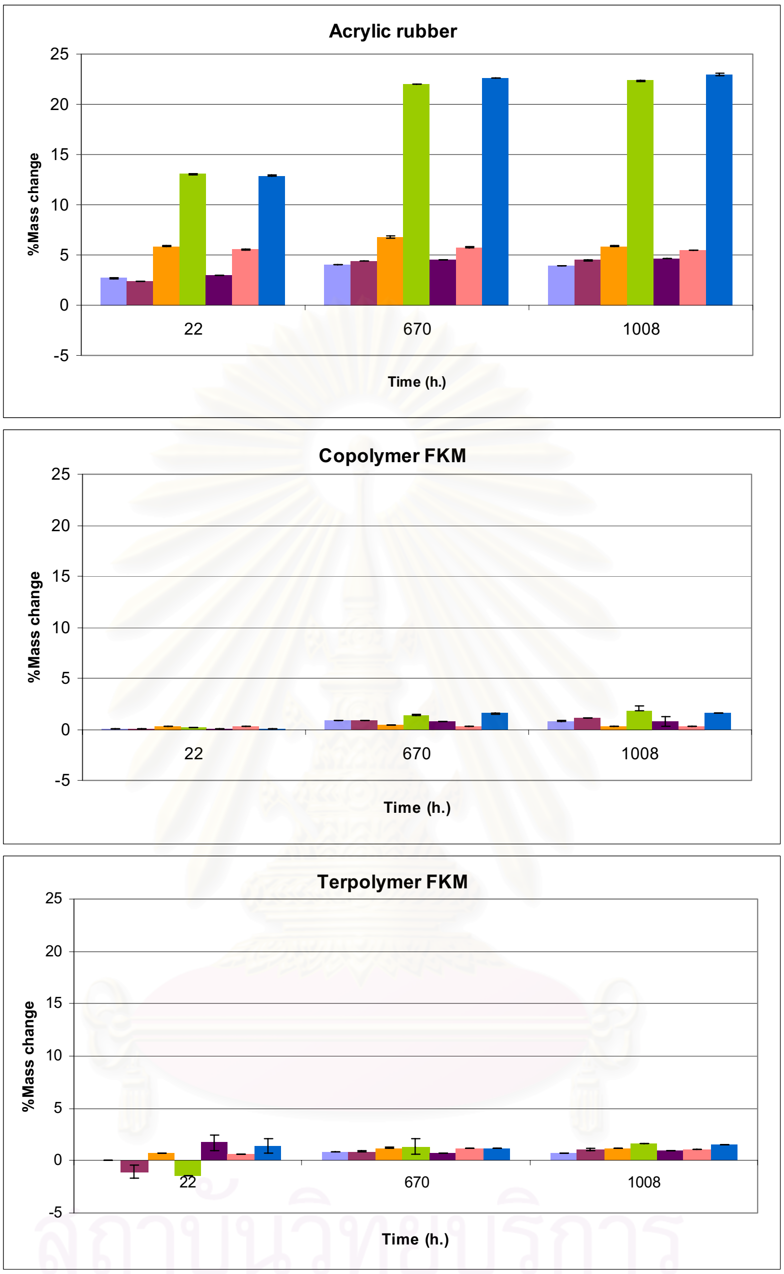

Figure 4.2 Effect of biodiesel and biodiesel blends :(🟪) Diesel; (🟥) B5-P; (🟧) B10-P; (🟩) B 100-P; (🟫) B5-C; (🟥) B10-C; (🟦) B100-C on percent mass change of acrylic rubber, copolymer FKM and terpolymer FKM elastomers at 50 °C.

Percentage of mass change for NBR immersed in the biodiesel blends was not different from that in diesel, in 5 and 10 percentage of biodiesel blending ratios. However, it can be seen that in pure biodiesel (B100-P, B100-C), mass change is high. This is because NBR added plasticizer that dissolved by biodiesel. So, NBR is soluble in biodiesel and permeation takes place. In addition, it should be noted that mass change increased in the first 22 hours and then decreased when immersion time was prolonged. This can be explained by elastomers loss of plasticizer because extracted by fuel sample.

Mass change percentages for HNBR immersed in biodiesel blends were similar to NBR. When the immersion time increased to 670 hours, percentage of mass change increased and became constant afterward. It shows that oil permeated in to HNBR in first period until equilibrium was reached at 670 hours. At the equilibrium there is no more absorption of oil as the intake and exclusion of fuel molecule reaches the same rate [23].

Mass change percentage for NBR PVC immersed in biodiesel blends is similar to that for NBR as NBR PVC has NBR in molecule.

Percentage of mass change for acrylic rubber immersed in biodiesel blends increased when increasing biodiesel content in diesel. Acrylic rubber molecule has carboxylic group like composition of biodiesel which absorb oil. Absorption increased with the number of active groups. Increase of mass change was higher when time of immersion increased. Highest mass change was observed with pure biodiesel.

Effect of biodiesel and biodiesel blended on percentage mass change of copolymer FKM elastomer at 50 ^{o}C was shown in Figure 4.2. Very little mass change was observed. Even when increasing immersion time, % change was not significant. Copolymer FKM is a type of fluoroelastomer. It has high ratio of fluorine-hydrogen and absence of unsaturated component. So, it makes elastomer not change in fuel sample.

For terpolymer FKM, changing in mass was similar to copolymer FKM.

4.3.2 Volume change

Percent volume change of elastomer after immersed in diesel, biodiesel blended and biodiesel at 50°C for each period of time (23, 670 and 1008 hours) are presented in Figures 4.3- 4.4.

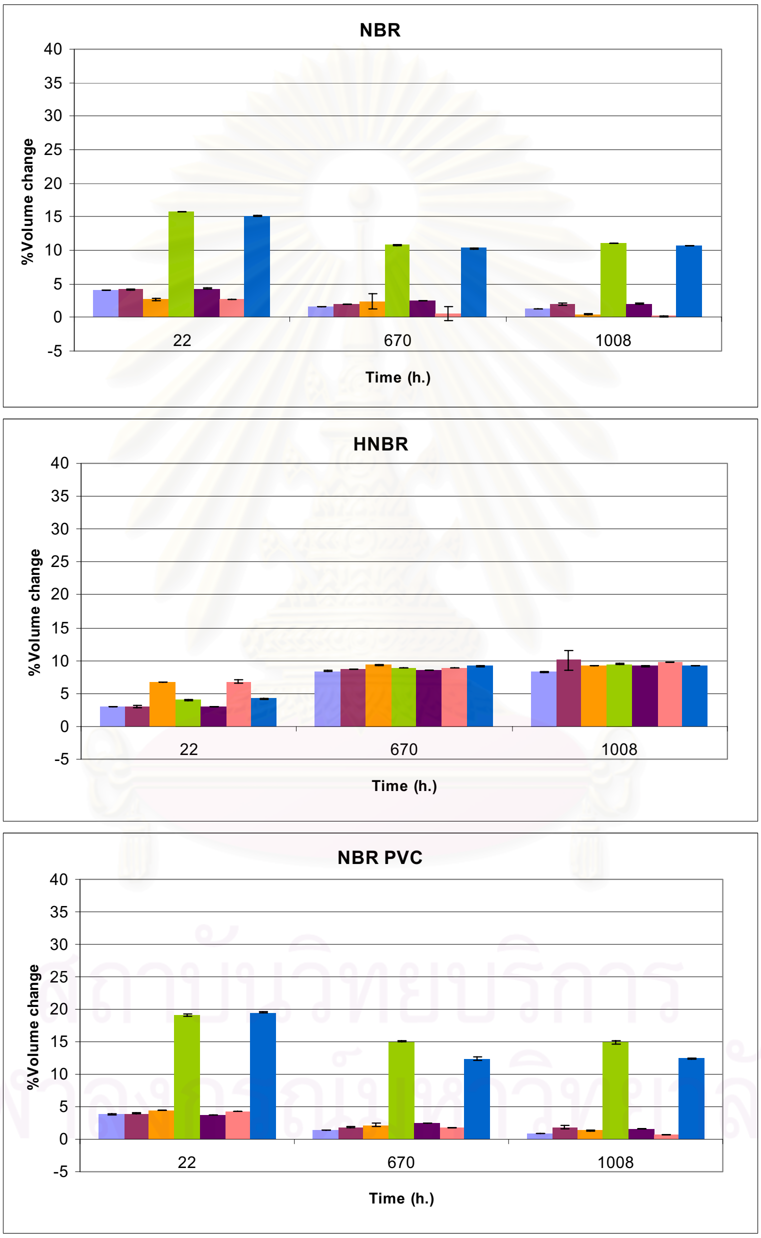

Figure 4.3 Effect of biodiesel and biodiesel blended:(🟪) Diesel; (🟥) B5-P; (🟧) B10-P; (🟩) B 100-P; (🟪) B5-C; (🟥) B10-C; (🟦) B100-C on percent volume change of NBR, HNBR and NBR PVC elastomers at 50 °C.

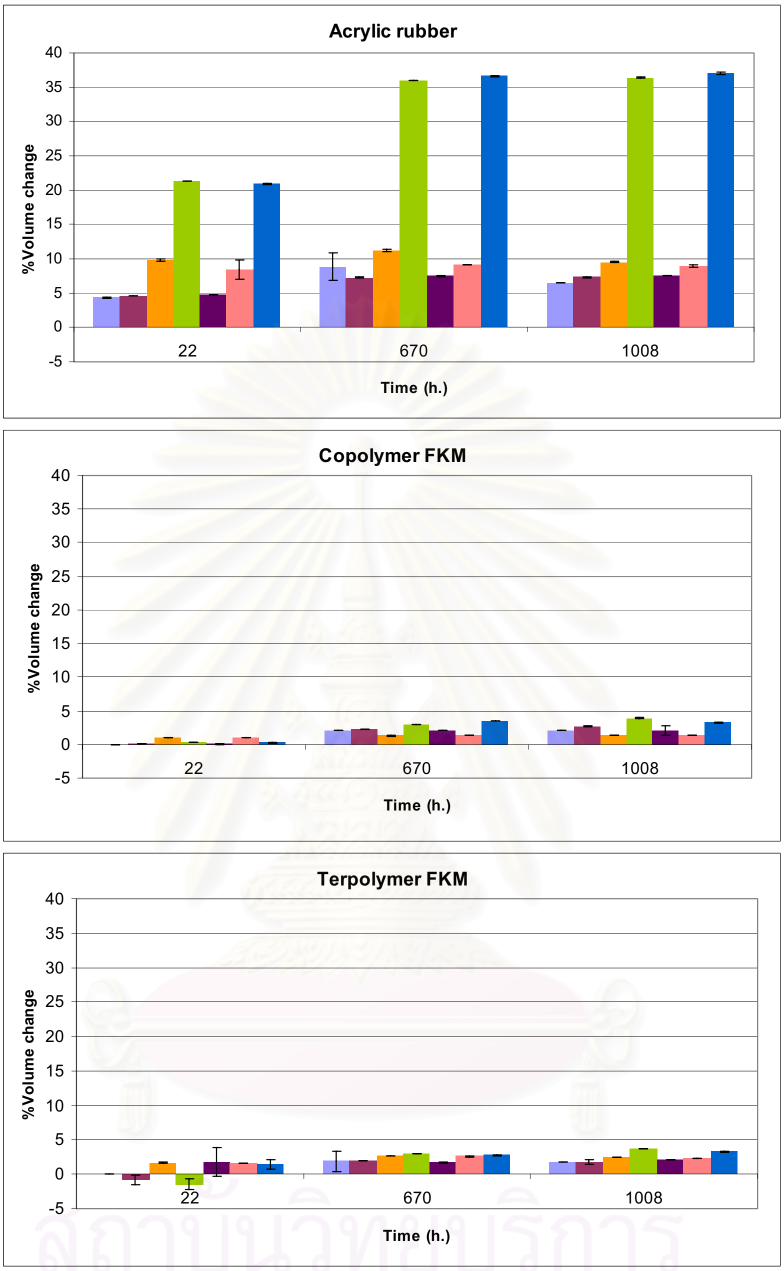

Figure 4.4 Effect of biodiesel and biodiesel blends :(🟪) Diesel; (🟥) B5-P; (🟧) B10-P; (🟩) B 100-P; (🟪) B5-C; (🟥) B10-C; (🟦) B100-C on percent volume change of acrylic rubber, copolymer FKM and terpolymer FKM elastomers at 50 °C.

The percent volume changes for in different elastomers were correlated with the change in percent mass change. When fuel diffused and was absorbed into the polymers, mass and the volume increased at the same time. This process is called swelling of elastomer.

4.3.3 Hardness change

Hardness change of elastomer after immersed in diesel, biodiesel blends and biodiesel at 50 ^{o}C for each period of time (23, 670 and 1008 hours) are presented in Figures 4.5- 4.6.

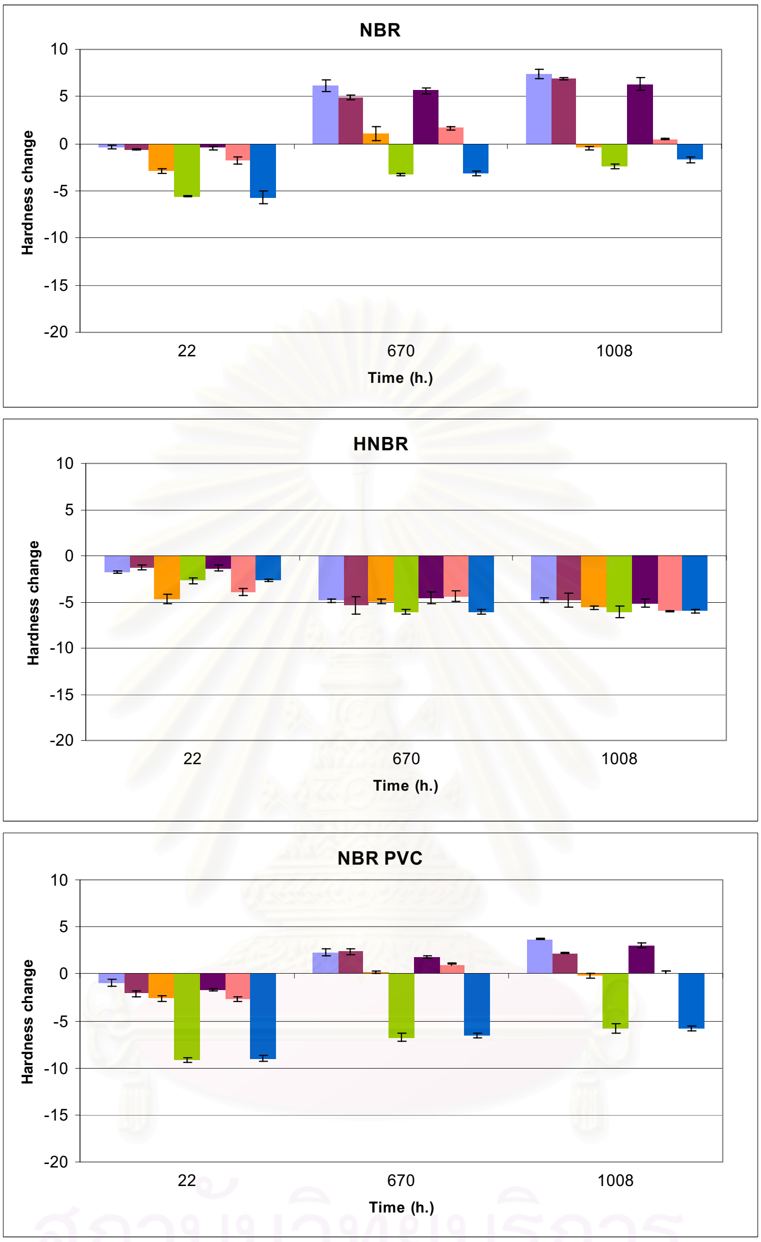

Figure 4.5 Effect of biodiesel and biodiesel blends :(🟪) Diesel; (🟥) B5-P; (🟧) B10-P; (🟩) B 100-P; (🟪) B5-C; (🟥) B10-C; (🟦) B100-C on percent hardness change of NBR, HNBR and NBR PVC elastomers at 50 °C.

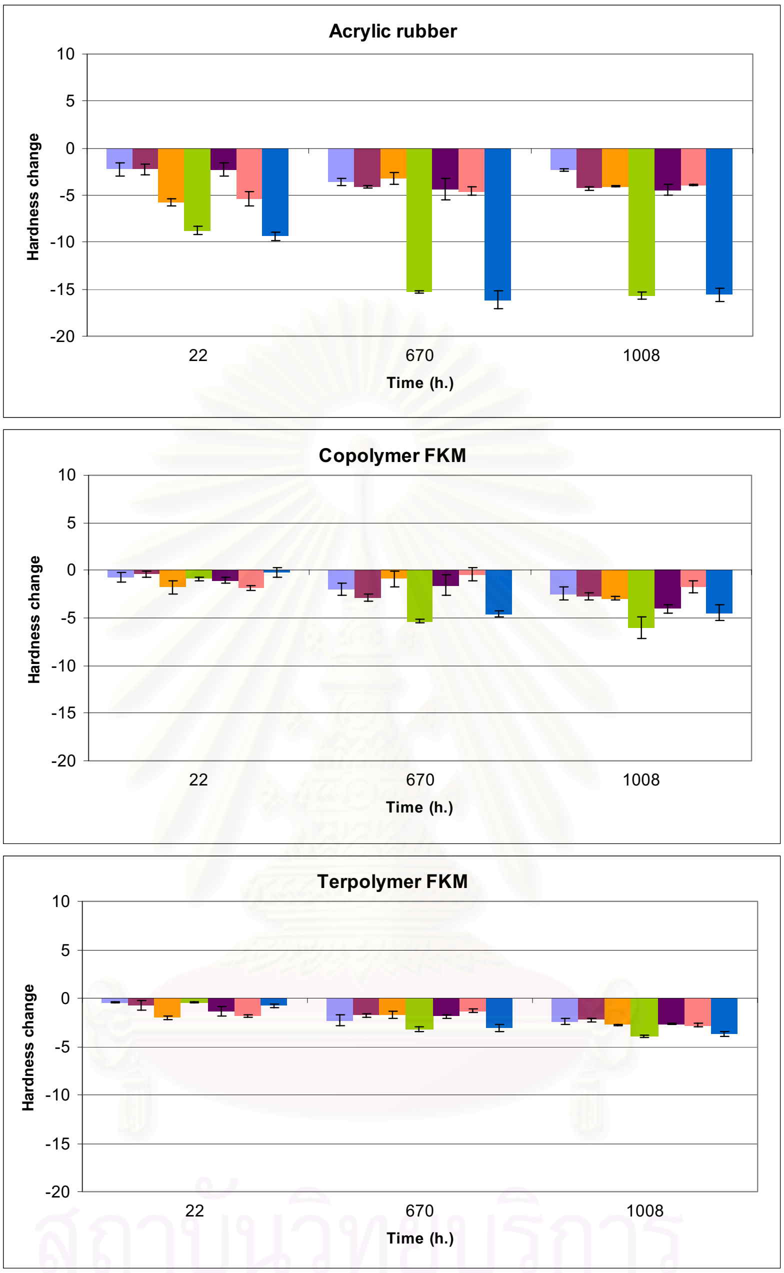

Figure 4.6 Effect of biodiesel and biodiesel blends :(🟪) Diesel; (🟫) B5-P; (🟧) B10-P; (🟩) B 100-P; (🟪) B5-C; (🟥) B10-C; (🟦) B100-C on hardness change of acrylic rubber, copolymer FKM and terpolymer FKM elastomers at 50 °C.

Effect of biodiesel and biodiesel blends on hardness of NBR is shown in Figure 4.5. Hardness change of NBR was decreased with the increasing biodiesel content in diesel. Both types of biodiesel tested in this work gave similar results.

From the beginning of the test to 22 hours, hardness of NBR decreased upon immersion into biodiesel blends. But for longer time of immersion, the hardness increased. This can be explained similarly to mass change. Elastomer swelled, therefore it becomes soften. But when time increased elastomer becomes harder because plasticizer was dissolved by diesel.

Effect of biodiesel and biodiesel blends on hardness of HNBR is shown in Figure 4.5. Hardness change of HNBR was decreased slightly with increased biodisel content in diesel.

Effect of biodiesel and biodiesel blends on hardness of NBR PVC is shown in Figure 4.5. The result was similar to that of NBR because in NBR PVC has composed by NBR in molecule.

Effect of biodiesel and biodiesel blends on hardness of acrylic rubber is shown in Figure 4.6. The hardness was decreased when biodiesel content in diesel and immersion time increased. This is due to the swelling.

Effect of biodiesel and biodiesel blends on hardness of copolymer FKM is shown in Figure 4.6. Hardness change was not significantly different in each fuel type.

In case of terpolymer FKM, the same result with copolymer FKM was obtained.

4.3.4 Tensile change

Percent tensile changes of elastomer after immersed in diesel, biodiesel blends and biodiesel at 50 ^{o}C for each period of time (23, 670 and 1008 hours) are presented Figures 4.7-4.8.

Figure 4.7 Effect of biodiesel and biodiesel blends :(🟪) Diesel; (🟥) B5-P; (🟧) B10-P; (🟩) B 100-P; (🟪) B5-C; (🟥) B10-C; (🟦) B100-C on percent tensile change of NBR, HNBR and NBR PVC elastomers at 50 °C.

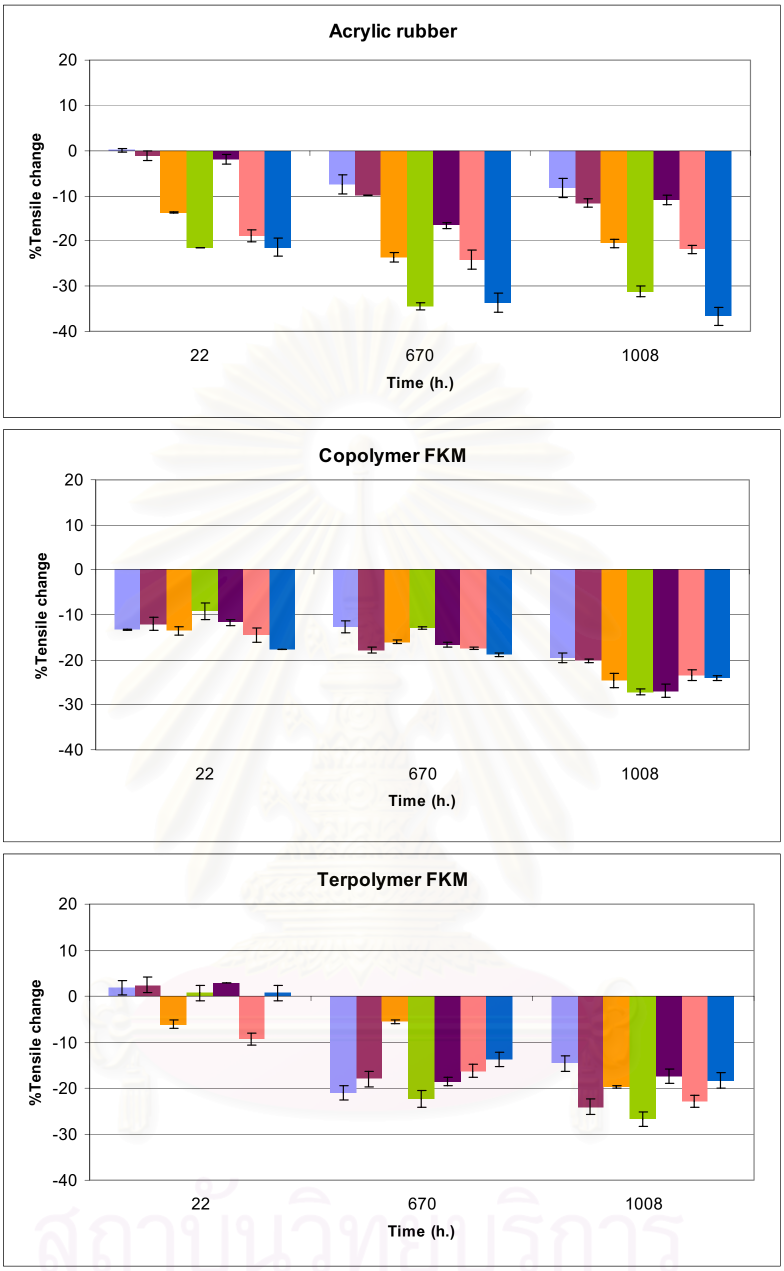

Figure 4.8 Effect of biodiesel and biodiesel blends :(🟪) Diesel; (🟥) B5-P; (🟧) B10-P; (🟩) B 100-P; (🟪) B5-C; (🟥) B10-C; (🟦) B100-C on percent tensile change of acrylic rubber, copolymer FKM and terpolymer FKM elastomers at 50 °C.

In Figure 4.7 tensile change of NBR was decreased when biodiesel content in diesel was increased. All fuel show decreased tensile when time increased except biodiesel from palm oil.

Effect of biodiesel and biodiesel blends on tensile of HNBR is shown in Figure 4.7. Tensile was found little change in all fuel types.

Effect of biodiesel and biodiesel blends on tensile of NBR PVC is shown in Figure 4.7. The tensile change was decreased from the start to the end of test. Differences in tensile change of each fuel were not significant [24].

Effect of biodiesel and biodiesel blends on tensile of acrylic rubber is shown in Figure 4.8. It's tensile change tended to decrease after immersed in the fuels. Changing in tensile was decreased if increased biodiesel content in diesel and increasing time.

Effect of biodiesel and biodiesel blend on tensile of copolymer FKM is shown in Figure 4.8. Its tensile change was decreased throughout the test. But decreasing of tensile was not different in every type of fuel. Tensile decreased with time [5].

Effect of biodiesel and biodiesel blends on tensile of terpolymer FKM is shown in Figure 4.8. It shows the same trend as in copolymer FKM.

From result of tensile change percentage was decreased after test because after polymer swollen, the polymer chains tend to have reduced entanglements. The polymer-polymer interaction is low in the swollen state. The elongation at break values also decreased due to swelling [25].

4.3.5 Elongation change

Percent elongation change of elastomers after immersed in diesel, biodiesel blends and biodiesel at 50^{o}C for each period of time (23, 670 and 1008 hours) are presented in Figures 4.9-4.10.

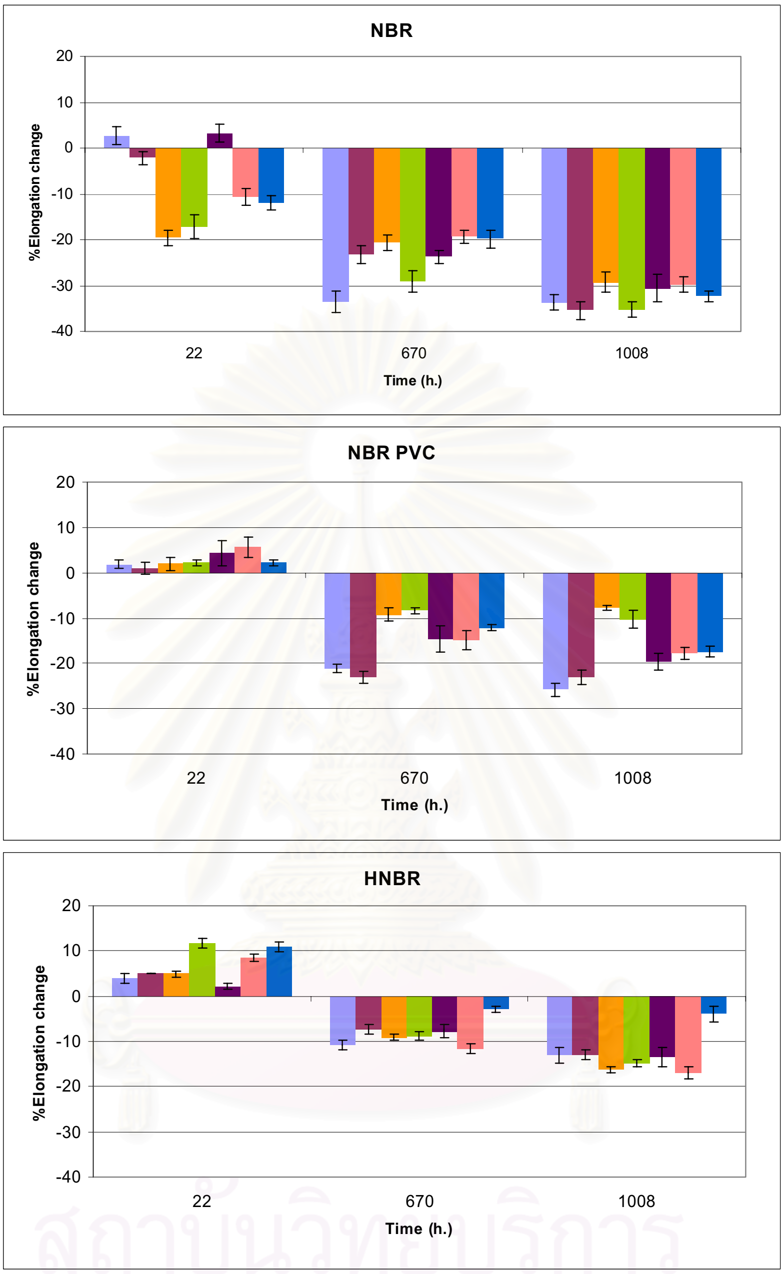

Figure 4.9 Effect of biodiesel and biodiesel blends :(🟪) Diesel; (🟥) B5-P; (🟧) B10-P; (🟩) B 100-P; (🟪) B5-C; (🟥) B10-C; (🟦) B100-C on percent elongation change of NBR, HNBR and NBR PVC elastomers at 50 ^{o}C.

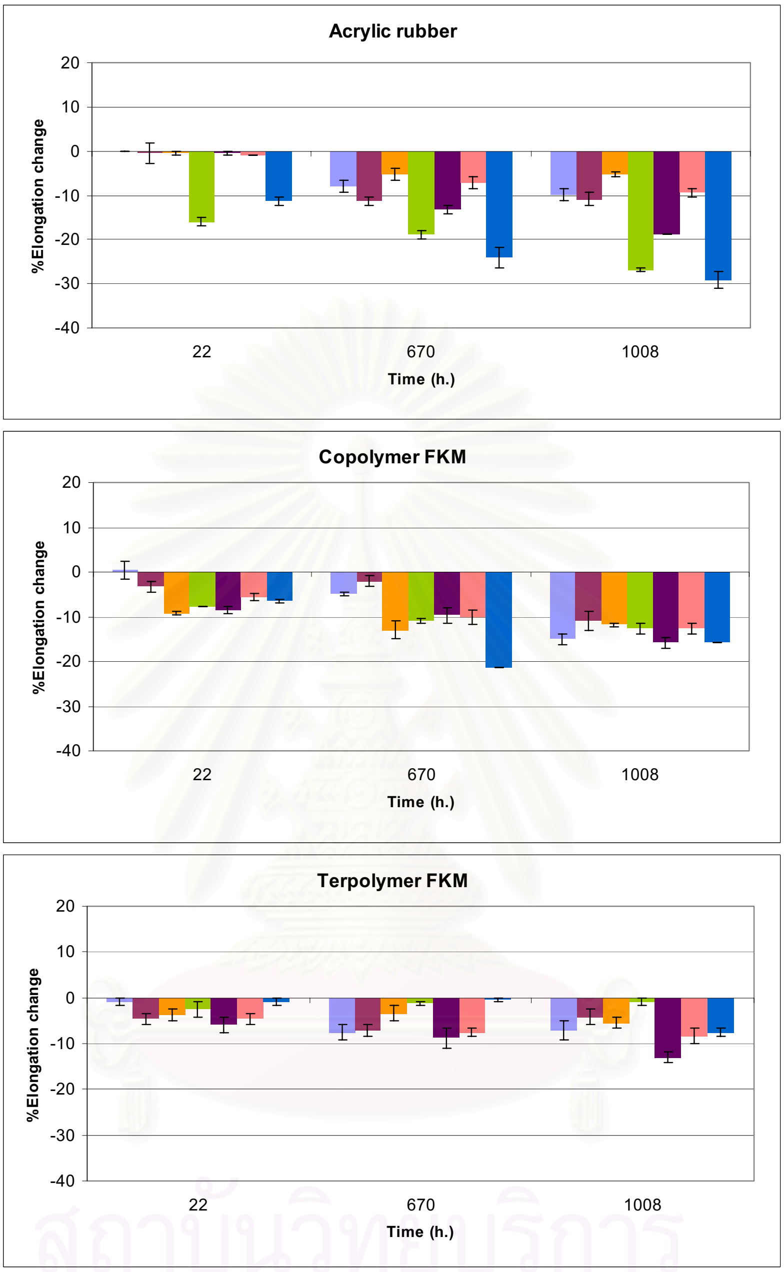

Figure 4.10 Effect of biodiesel and biodiesel blends :(🟪) Diesel; (🟥) B5-P; (🟧) B10-P; (🟩) B 100-P; (🟪) B5-C; (🟥) B10-C; (🟦) B100-C on percent elongation change of acrylic rubber, copolymer FKM and terpolymer FKM elastomers at 50 °C.

For NBR, elongation after immersion decreased when time of immersion increased. In 22 hours the change was higher when blending biodiesel content more than 10%.

Effect of biodiesel and biodiesel blends on elongation change of HNBR at 50 ^{o}C is shown in Figure 4.9. HNBR elongation change was found to decrease when time of test increased.

Effect of biodiesel and biodiesel blends on elongation change of NBR PVC at 50^{o}C is shown in Figure 4.9. For NBR PVC elongation was not changed in 22 hours. After that, it tended to decrease.

Effect of biodiesel and biodiesel blends on elongation change of acrylic rubber at 50 ^{o}C is shown in Figure 4.10. Elongation of acrylic rubber was decreased from beginning to the end of test. Obvious change was observed for B100-P and B100-C in 22 hours. For 670 hours, for diesel and biodiesel blends, the elongation was affected.

Effect of biodiesel and biodiesel blends on elongation change of copolymer FKM and terpolymer FKM at 50 ^{o}C is shown in Figure 4.10. Little change was observed.

4.4 Effect of temperature

Elastomers were immersed in biodiesel and biodiesel blends sample at temperature 100^{o}C for 23, 670 and 1008 hours. After immersion, elastomers were measured mechanical properties change. The results are shown in Figures 4.11- 4.25.

4.4.1 Mass change

Percent mass change of elastomer after immersed in diesel, biodiesel blends and biodiesel at 100 ^{o}C for each period of time are presented in Figure 4.11-4.13.

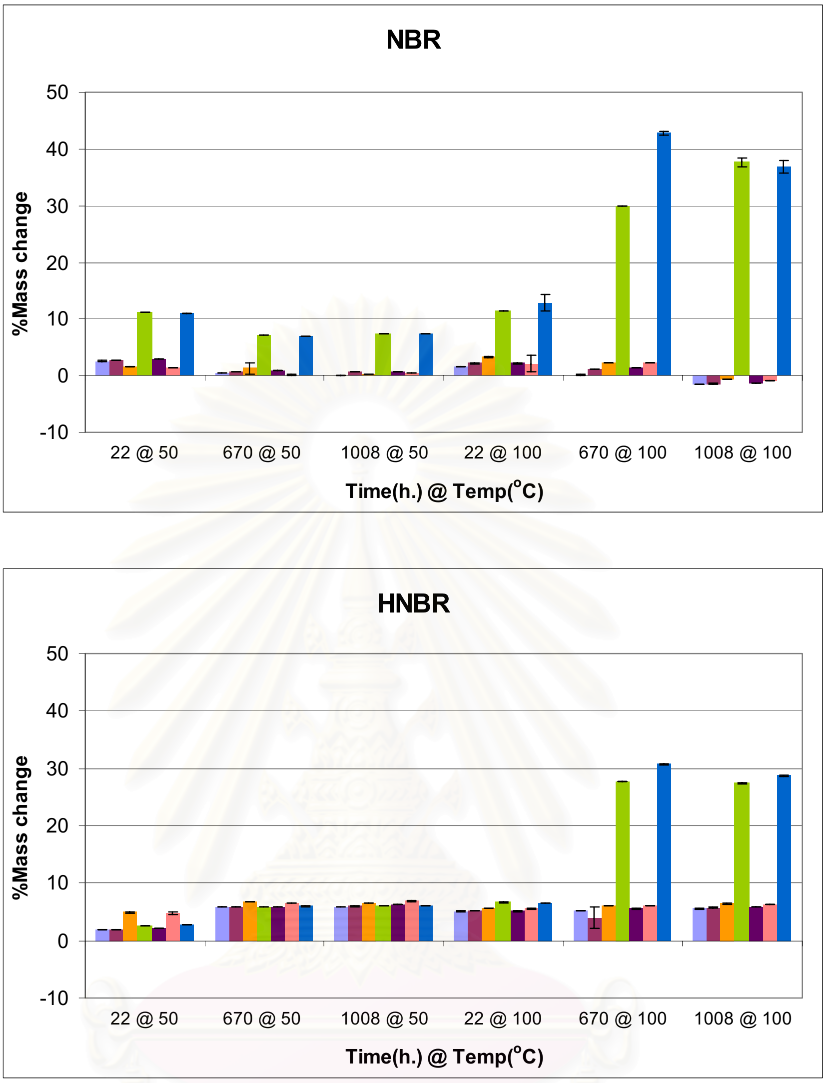

Figure 4.11 Effect of biodiesel and biodiesel blends :(🟪) Diesel; (🟫) B5-P; (🟧) B10-P; (🟩) B 100-P; (■) B5-C; (🟥) B10-C; (🟦) B100-C on percent mass change of NBR and HNBR elastomers at 100 °C.

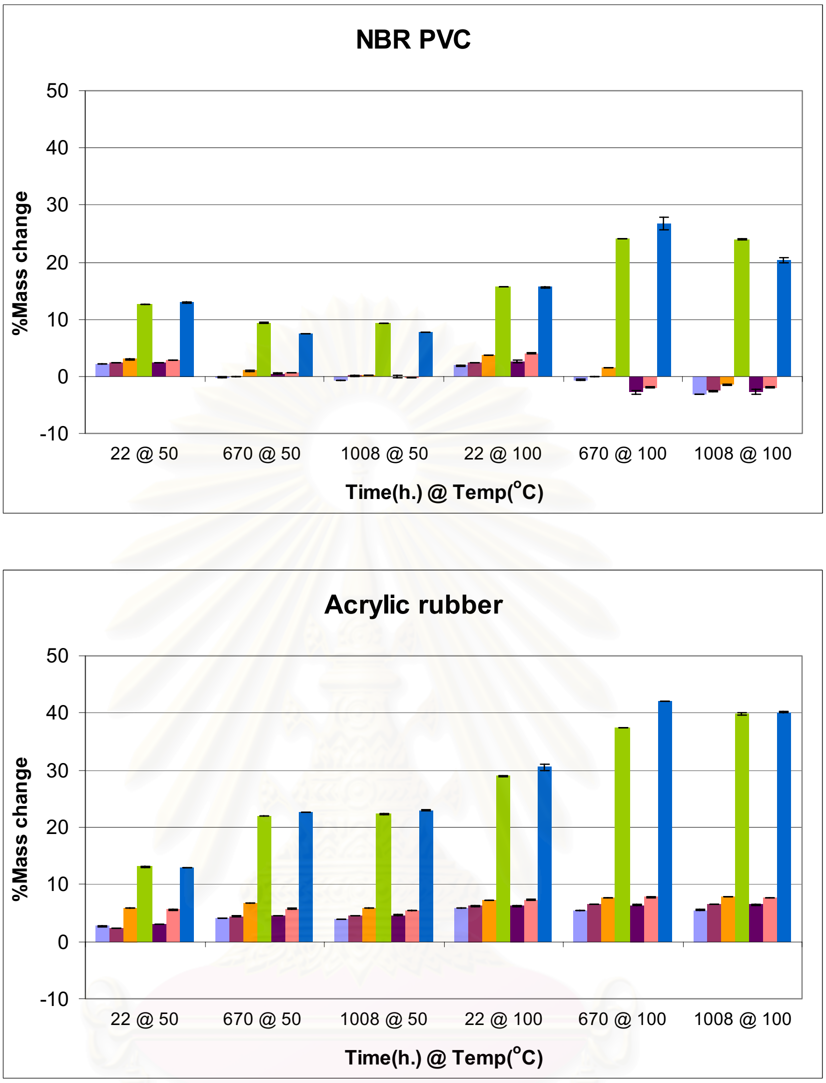

Figure 4.12 Effect of biodiesel and biodiesel blends :(🟪) Diesel; (🟥) B5-P; (🟧) B10-P; (🟩) B 100-P; (🟪) B5-C; (🟥) B10-C; (🟦) B100-C on percent mass change of NBR PVC and acrylic rubber elastomers at 100 °C.

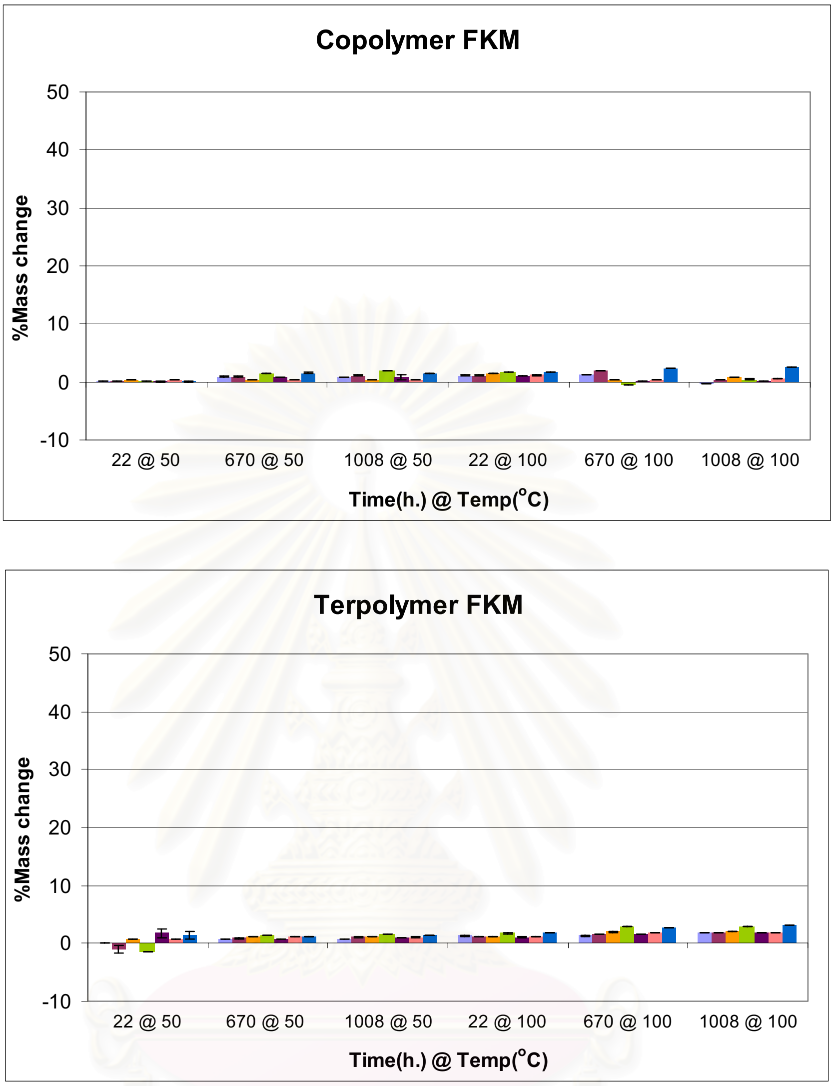

Figure 4.13 Effect of biodiesel and biodiesel blends :(🟪) Diesel; (🟫) B5-P; (🟧) B10-P; (🟩) B 100-P; (🟪) B5-C; (🟥) B10-C; (🟦) B100-C on percent mass change of copolymer FKM and terpolymer FKM elastomers at 100°C.

Effect of biodiesel and biodiesel blends on mass change of NBR at 100 °C is shown in Figure 4.11. In diesel and biodiesel blends, the mass change was little higher than with 50 °C. Changing of percent mass showed negative value; it was lower than the original mass. Decreasing of mass took place because desorption occurs at a rapid rate compared to sorption [25]. It can be explained by higher loss of plasticizer when the temperature was raised higher[26] than in the case of biodiesel. Changing of mass was higher when temperature increased and the mass change was increased after immersion time increased. Because at higher temperature the molecular motion associated with the chain flexibility allows biodiesel molecules to penetrate the polymer. As the temperature is increased the segmental motion is also increased with the result of more diffusion of the biodiesel molecules.

Effect of biodiesel and biodiesel blends on percentage of the mass change of HNBR at 100 ^{o}C is shown in Figure 4.11. HNBR in 22 hours at 100 ^{o}C showed the same result with 1008 hours at 50 ^{o}C. It gave in the same result in all fuel type. After that, it showed mass increased in both of biodiesel but in diesel and biodiesel not increased.

Effect of biodiesel and biodiesel blends on the mass change of NBR PVC at 100 ^{o}C is shown in Figure 4.12. For the mass change of NBR PVC at 100 ^{o}C was higher than at 50 ^{o}C. It changing was in same trend with NBR but less than NBR. Because PVC in NBR PVC that improves thermal aging resistance of NBR [27].

Effect of biodiesel and biodiesel blends on the mass change of acrylic rubber at 100 ^{o}C is shown in Figure 4.12. Result of the mass change in acrylic rubber was increased after temperature increased from 50 ^{o}C to 100 ^{o}C. Increasing of acrylic rubber mass in B100-P and B100-C was higher effected than diesel and biodiesel blends. In mass change of acrylic rubber was slightly increased when biodiesel content increased.

Effect of biodiesel and biodiesel blends on the mass change of terpolymer FKM and copolymer FKM at 100 ^{o}C is shown in Figure 4.13. Both type of elastomers observed change in mass similar to changing at 50 ^{o}C.

From the result at 100 ^{o}C, the mass of rubber was increased higher than 50 ^{o}C almost of all result because at higher temperature the molecular motion associated with the chain flexibility allows biodiesel molecules to penetrate the polymer. As the temperature is increased the segmental motion is also increased with the result of more diffusion of the biodiesel molecules [23].

4.4.2 Volume change

Percent volume change of elastomer after immersed in diesel, biodiesel blended and biodiesel at 100 °C for each period of time are presented in Figures 4.14-4.16.

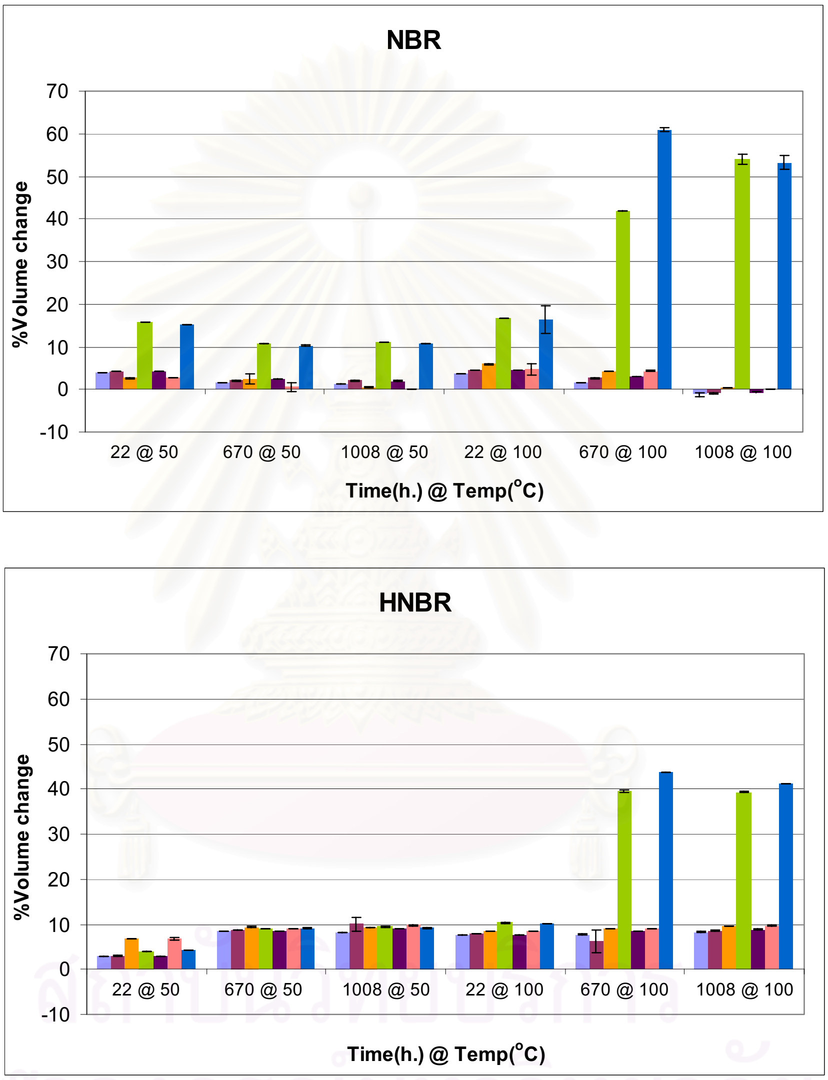

Figure 4.14 Effect of biodiesel and biodiesel blends :(🟪) Diesel; (🟫) B5-P; (🟧) B10-P; (🟩) B 100-P; (🟪) B5-C; (🟥) B10-C; (🟦) B100-C on percent volume change of NBR and HNBR elastomers at 100 °C.

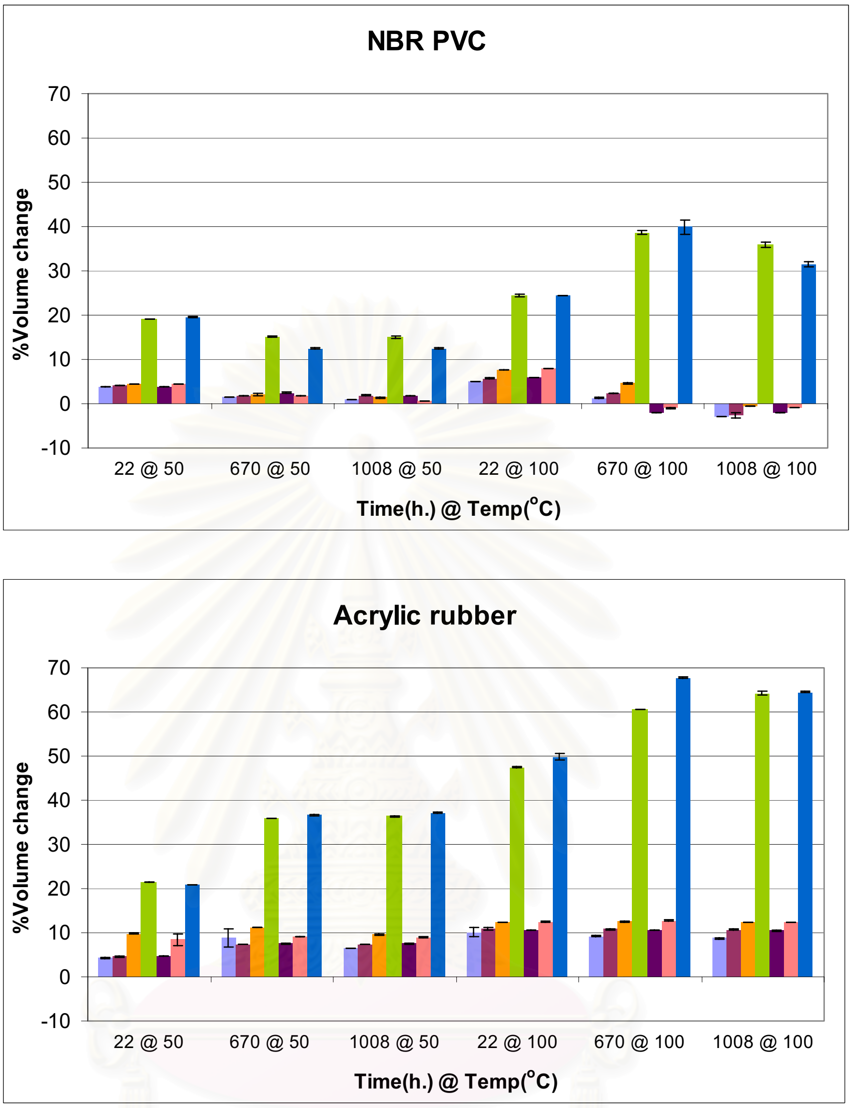

Figure 4.15 Effect of biodiesel and biodiesel blends :(🟪) Diesel; (🟥) B5-P; (🟧) B10-P; (🟩) B 100-P; (🟪) B5-C; (🟥) B10-C; (🟦) B100-C on percent volume change of NBR PVC and acrylic rubber elastomers at 100 °C.

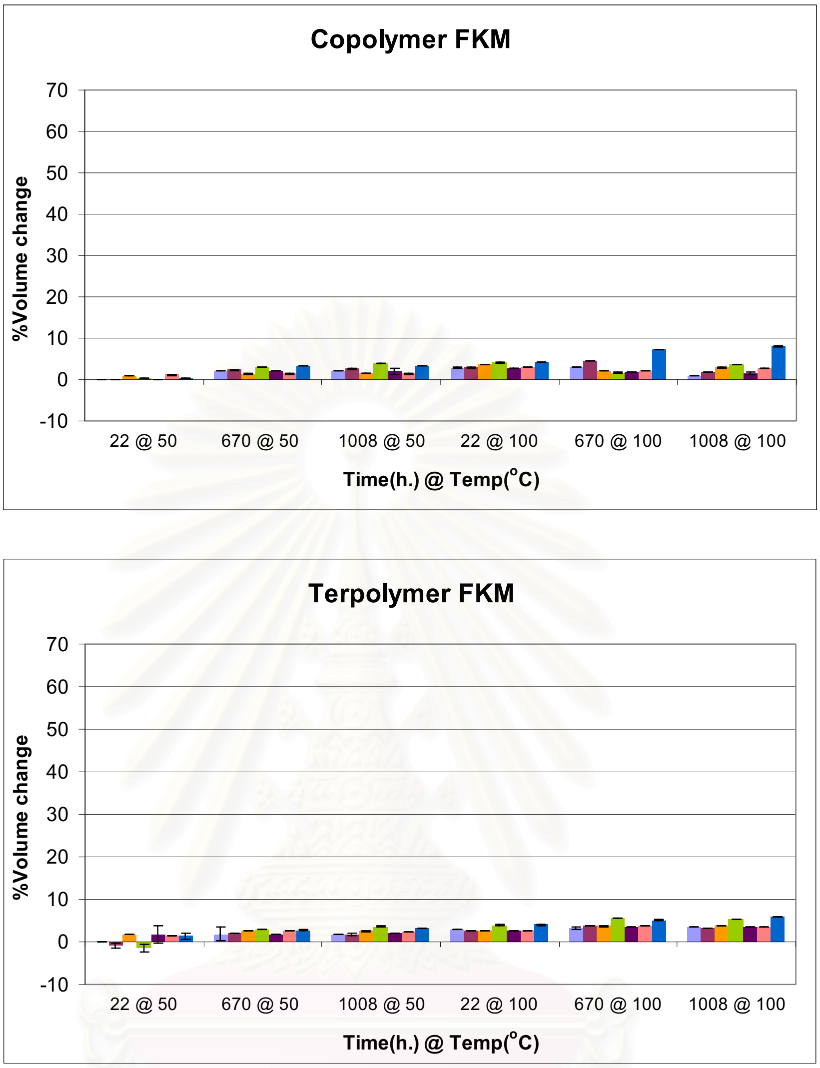

Figure 4.16 Effect of biodiesel and biodiesel blends :(🟪) Diesel; (🟥) B5-P; (🟧) B10-P; (🟩) B 100-P; (🟪) B5-C; (🟥) B10-C; (🟦) B100-C on percent volume change of copolymer FKM and terpolymer FKM elastomers at 100 °C.

From percentage of the volume change of elastomers, it was correlated with to the mass change but it’s higher. Volume of elastomers increased until 22 hours and constant to the end of test. If biodiesel content increased, the volume of elastomers will increase and highest increase when elasomers immersed in biodiesel. The highest volume change was acrylic rubber that immersed in B100-P and B100-C. Volume change at 100 °C was increased about two times when compared with volume change at 50 °C except copolymer FKM and terpolymer FKM. It showed same result between two temperatures.

4.4.3 Hardness change

Hardness change of elastomer after immersed in diesel, biodiesel blends and biodiesel at 100 °C for each period of time are presented in Figure 4.17-4.19.

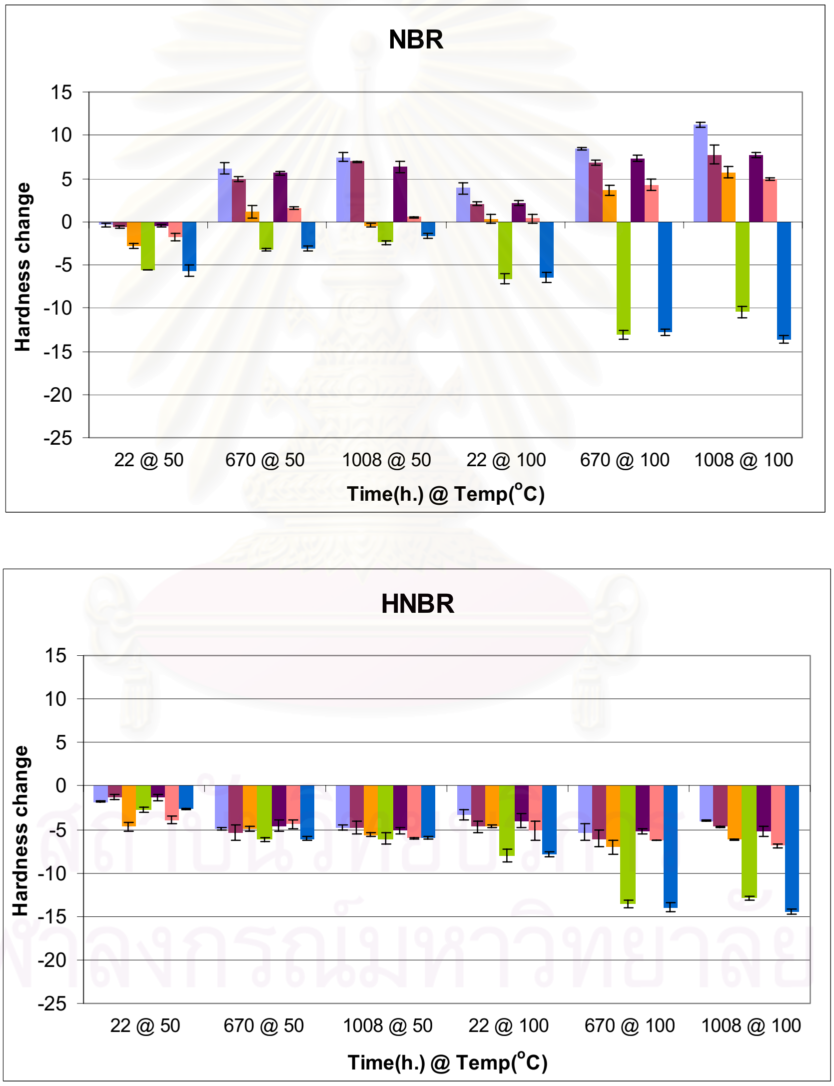

Figure 4.17 Effect of biodiesel and biodiesel blends :(🟪) Diesel; (🟥) B5-P; (🟧) B10-P; (🟩) B 100-P; (🟪) B5-C; (🟥) B10-C; (🟦) B100-C on percent hardness change of NBR and HNBR elastomers at 100 °C.

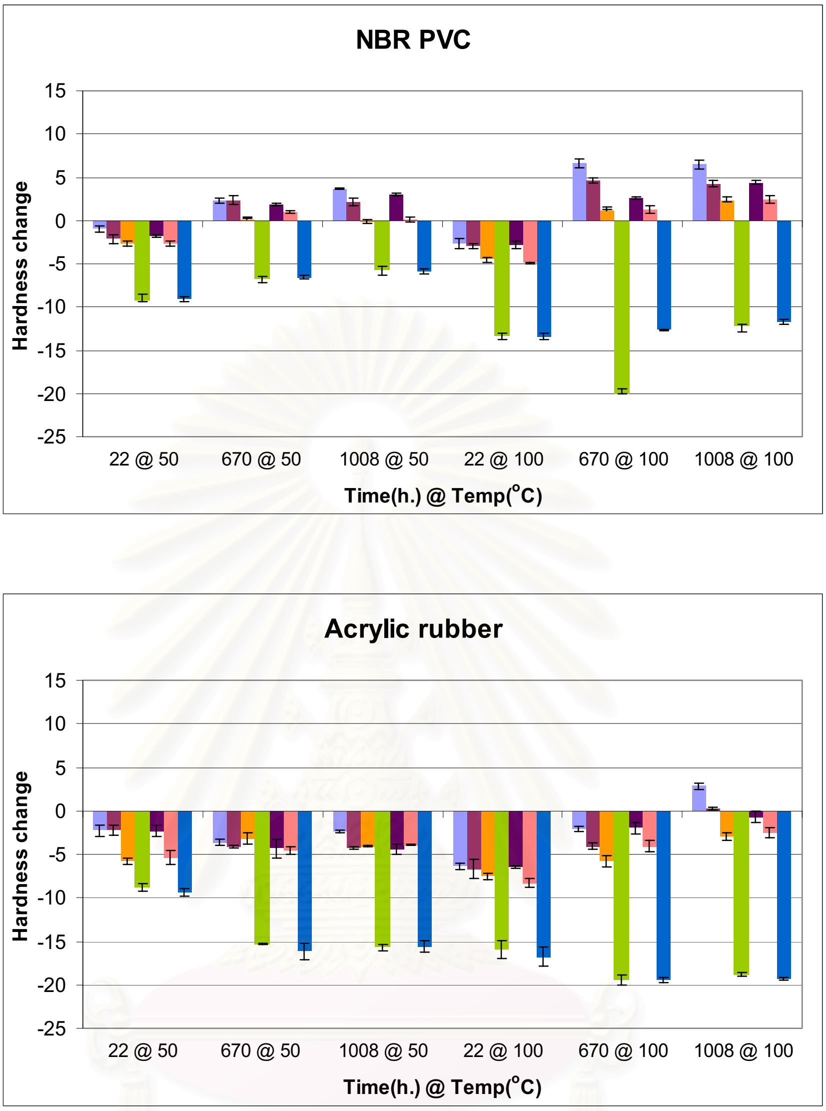

Figure 4.18 Effect of biodiesel and biodiesel blends :(🟪) Diesel; (🟫) B5-P; (🟧) B10-P; (🟩) B 100-P; (🟪) B5-C; (🟥) B10-C; (🟦) B100-C on percent hardness change of NBR PVC and acrylic rubber elastomers at 100 °C.

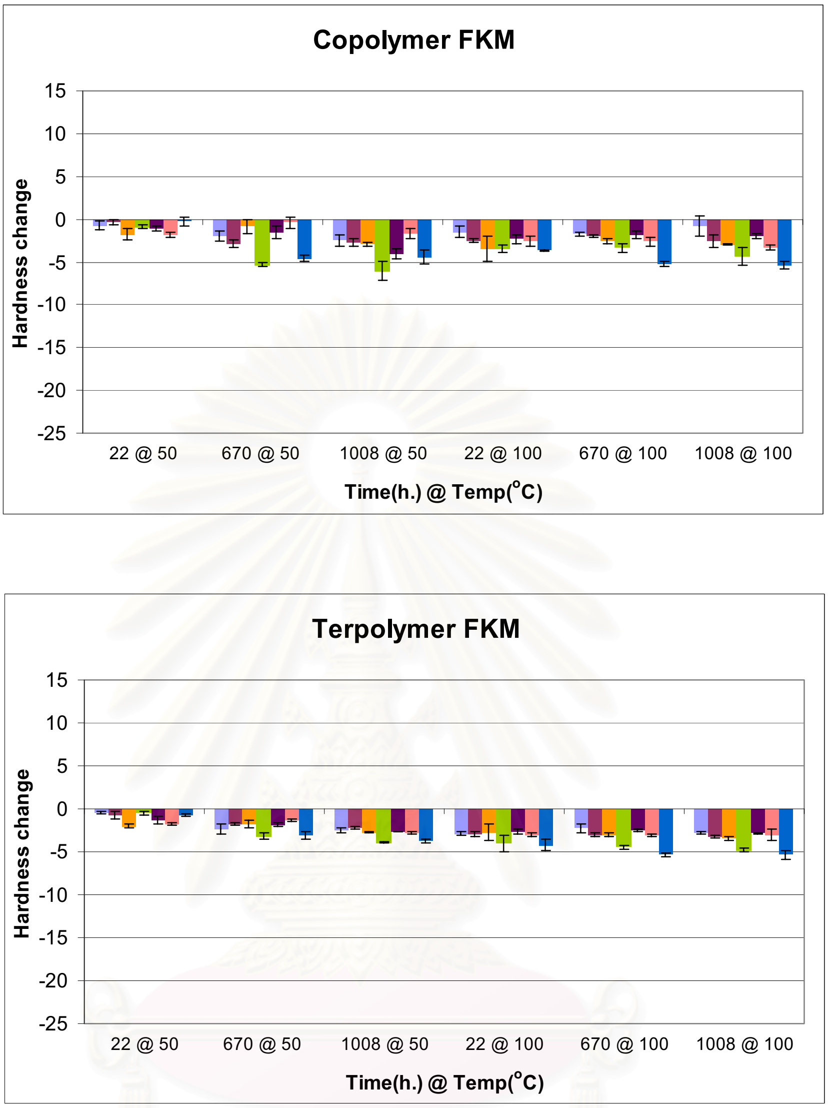

Figure 4.19 Effect of biodiesel and biodiesel blends :(🟪) Diesel; (🟥) B5-P; (🟧) B10-P; (🟩) B 100-P; (🟪) B5-C; (🟥) B10-C; (🟦) B100-C on percent hardness change of copolymer FKM and terpolymer FKM elastomers at 100 °C.

Effect of biodiesel and biodiesel blends on the hardness change of NBR at 100 °C is shown in Figure 4.17. Hardness of NBR after the temperature raised to 100 °C was increased only that immersed in diesel and biodiesel blends and it increased higher when the time of test increased. Compare it with temperature 50 °C, the hardness was little higher. The hardness decreased when increased biodiesel content.

So, it made hardness decreased if immersed in B100-P and B100-C. It decreased to 670 hours and then kept constant to 1008 hours.

Effect of biodiesel and biodiesel blends on the hardness change of HNBR at 100 ^{o}C is shown in Figure 4.17. The hardness of HNBR was tended decreased higher than at temperature 50 ^{o}C. It made decreased in hardness if biodiesel content decreased and it highest decreased after immersed in B100-P and B100-C.

Effect of biodiesel and biodiesel blends on the hardness change of NBR PVC at 100 ^{o}C is shown in Figure 4.18. For NBR PVC was tended to change in hardness at temperature 100 ^{o}C like NBR. The result compare with temperature 50 ^{o}C was given in the same trend with NBR. Because it main structure is NBR.

Effect of biodiesel and biodiesel blends on hardness change of acrylic rubber at 100 ^{o}C is shown in Figure 4.18. Acrylic rubber showed result in same trend with NBR and NBR PVC but it effect was less than them. But it was given in different result if immersed in B100-P and B100-C. It change was in same characteristic but with changing in temperature 50 ^{o}C but higher in all period of time. It changing happen with acrylic rubber was highest.

Effect of biodiesel and biodiesel blends on hardness change of copolymer FKM and terpolymer FKM at 100 ^{o}C is shown in Figure 4.19. Copolymer FKM and terpolymer FKM were given in the same result after test. It was observed little change in hardness in both temperatures. It hardness were tended to decreased until time pass through 670 hours after that it kept constant though 1008 hours. The both type of rubber was decreased in hardness when biodiesel content increased.

From result of all type material showed decreased of hardness higher after increased biodiesel content. The hardness of elastomers will decreased little higher when immersed in B100-C.

4.4.4 Tensile change

Percent tensile change of elastomer after immersed in diesel, biodiesel blends and biodiesel at 100 °C for each period of time are presented in Figures 4.20-4.22.

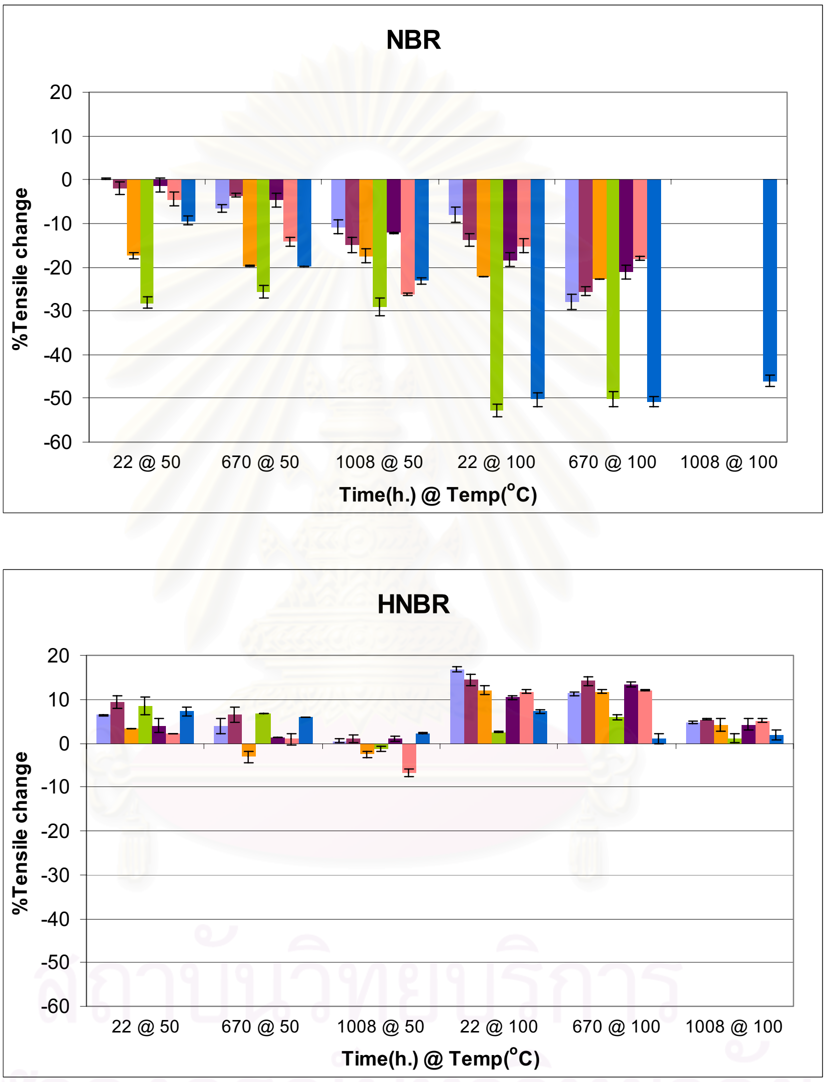

Figure 4.20 Effect of biodiesel and biodiesel blends :(🟪) Diesel; (🟫) B5-P; (🟧) B10-P; (🟩) B 100-P; (🟪) B5-C; (🟥) B10-C; (🟦) B100-C on percent tensile change of NBR and HNBR elastomers at 100 °C.

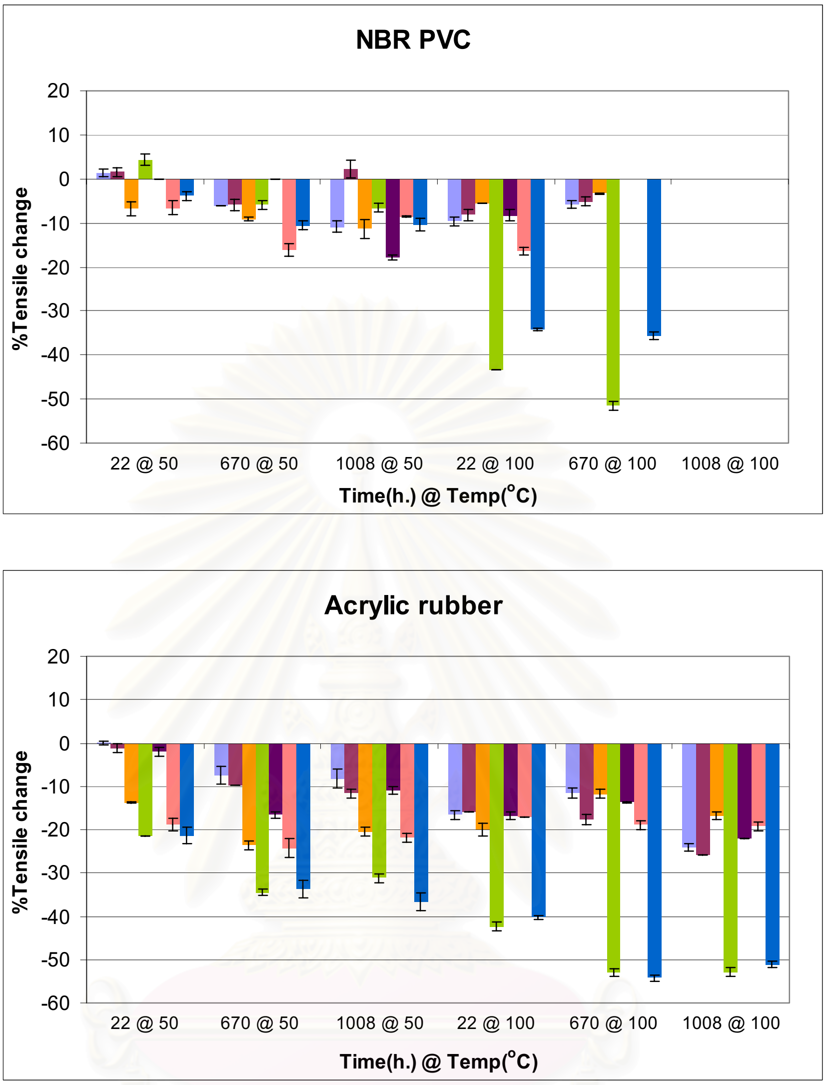

Figure 4.21 Effect of biodiesel and biodiesel blends :(🟪) Diesel; (🟫) B5-P; (🟧) B10-P; (🟩) B 100-P; (🟪) B5-C; (🟥) B10-C; (🟦) B100-C on percent tensile change of NBR PVC and acrylic rubber elastomers at 100 °C.

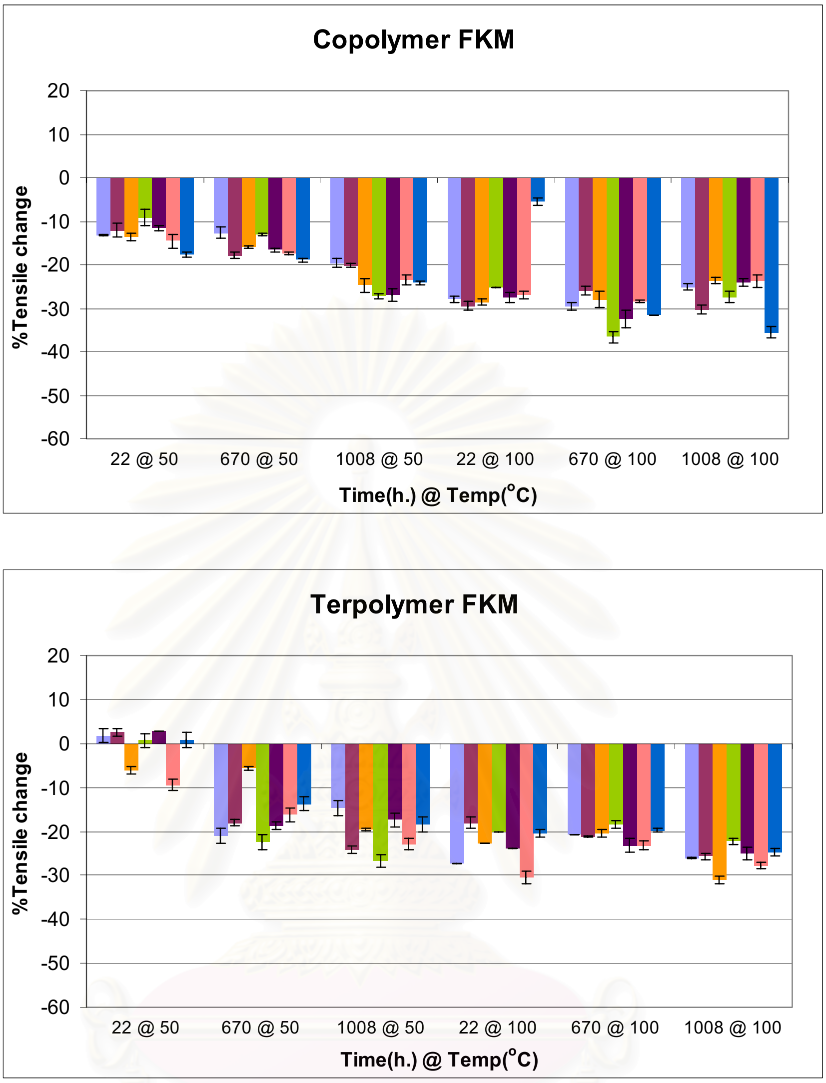

Figure 4.22 Effect of biodiesel and biodiesel blends :(🟪) Diesel; (🟥) B5-P; (🟧) B10-P; (🟩) B 100-P; (🟪) B5-C; (🟥) B10-C; (🟦) B100-C on percent tensile change of copolymer FKM and terpolymer FKM elastomers at 100 °C.

Effect of biodiesel and biodiesel blends on percentage of the tensile change of NBR at 100 °C is shown in Figure 4.20.The tensile change of NBR after immersed at 100 °C was lower than at 50 °C in all type of fuel. It was tended slightly increased in diesel and biodiesel blends. For the tensile change of NBR in biodiesel, it was highest decreased when compare with after immersed in diesel and biodiesel blends. It changing was two time of 50 °C. The result of changing was not different between the two types of biodiesel.

Effect of biodiesel and biodiesel blends on the percentage of tensile change of HNBR at 100 °C is shown in Figure 4.20. The result of changing in tensile of HNBR was tended decrease after the temperature increased. Changing in all fuel type of HNBR was not different. It means that no effect of biodiesel with HNBR at high temperature. It was similar to result at 50 °C.

Effect of biodiesel and biodiesel blends on percentage of tensile change of NBR PVC at 100 °C is shown in Figure 4.21. For NBR PVC, that elastomer in diesel and biodiesel blends was given result like immersed in temperature 50 °C. It tensile change of in diesel and biodiesel blends was not different. But, it showed the different result in both of biodiesel. Immersed elastomer in B100-P and B100-C was highest decreased. The decreasing of elastomer in B100-P was decreased little higher than B100-C.

Effect of biodiesel and biodiesel blends on the tensile change percent of acrylic rubber at 100 °C is shown in Figure 4.21. It tensile change was decreased higher than at 50 °C in all type of fuel. It tensile was slightly decreased when time of immersion increased. It highest tensile decrease was material in biodiesel. It decreased tended to higher until 670 hours and after that kept constant to 1008 hours. Characteristic of decreased was the same in both of biodiesels.

Effect of biodiesel and biodiesel blends on percentage of tensile change of copolymer FKM at 100 °C is shown in Figure 4.22. Copolymer FKM was decreased the tensile after the temperature 100 °C higher than 50 °C. But it decrease was kept constant from 22 hours to 1008 hours. It changing different was no significant in each type of fuel.

Effect of biodiesel and biodiesel blends on percentage of tensile change of terpolymer FKM at 100 °C is shown in Figure 4.22. For terpolymer FKM changing in tensile, it showed decrease like tensile change at 1008 hours of 50 °C and it change of terpolymer FKM in biodiesel and biodiesel blend was given not different from terpolymer FKM in diesel. In case of different source of biodiesel, it showed the same trend. Decreasing of tensile kept constant through the time of test.

4.4.5 Elongation change

Percent elongation change of elastomer after immersed in diesel, biodiesel blended and biodiesel at 100 °C for each period of time are presented in Figures 4.23-4.25.

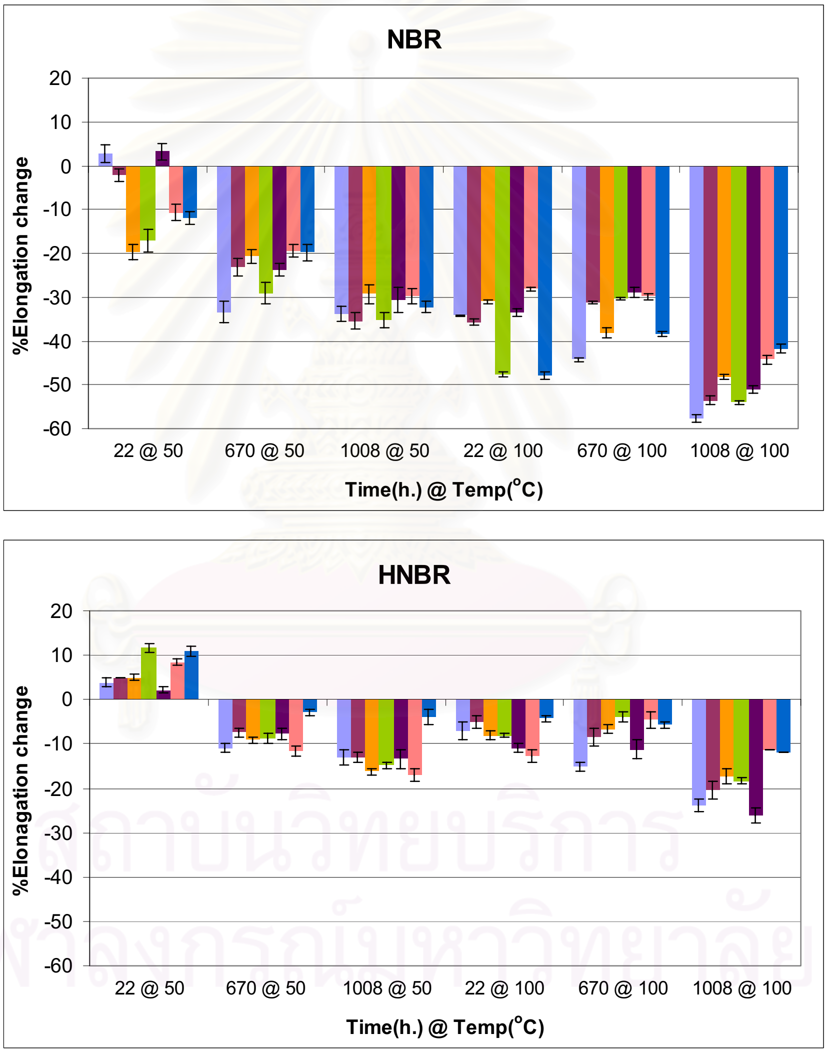

Figure 4.23 Effect of biodiesel and biodiesel blends :(■) Diesel; (■) B5-P; (■) B10-P; (■) B 100-P; (■) B5-C; (■) B10-C; (■) B100-C on percent elongation change of NBR and HNBR elastomers at 100 °C.

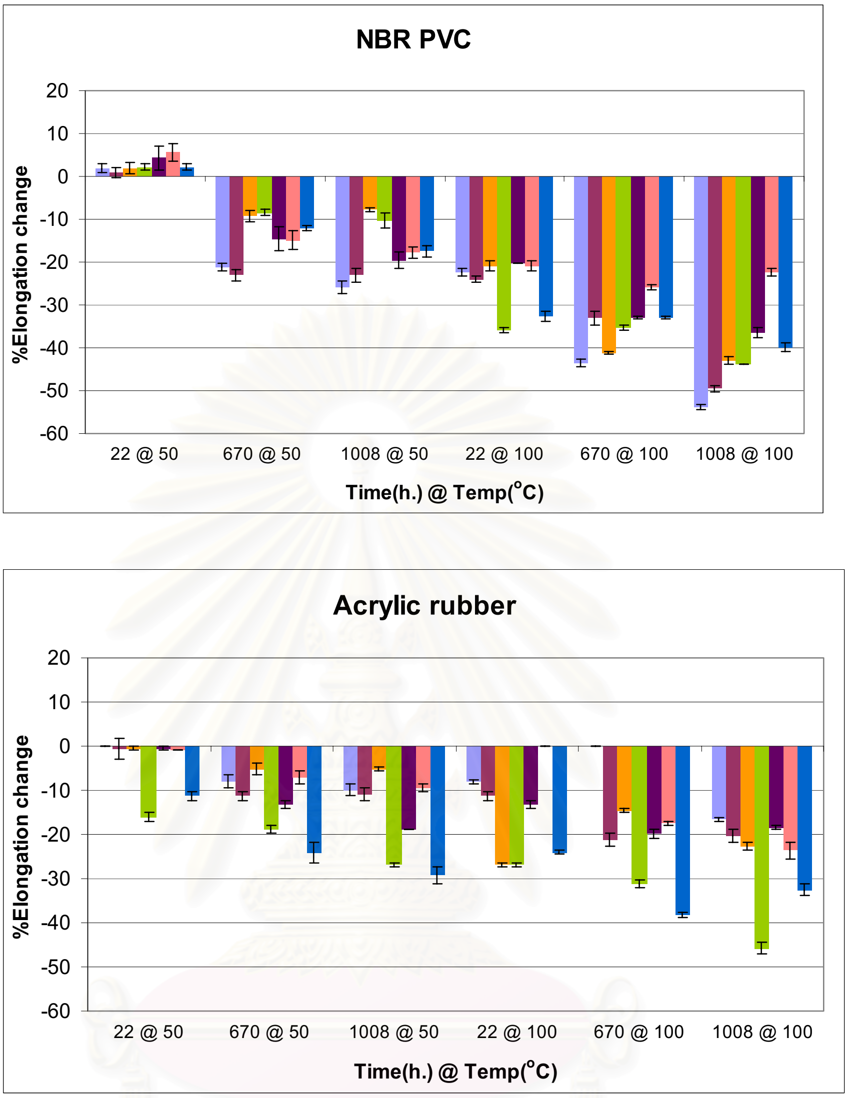

Figure 4.24 Effect of biodiesel and biodiesel blends :(🟪) Diesel; (🟥) B5-P; (🟧) B10-P; (🟩) B 100-P; (🟪) B5-C; (🟥) B10-C; (🟦) B100-C on percent elongation change of NBR PVC and acrylic rubber elastomers at 100 °C.

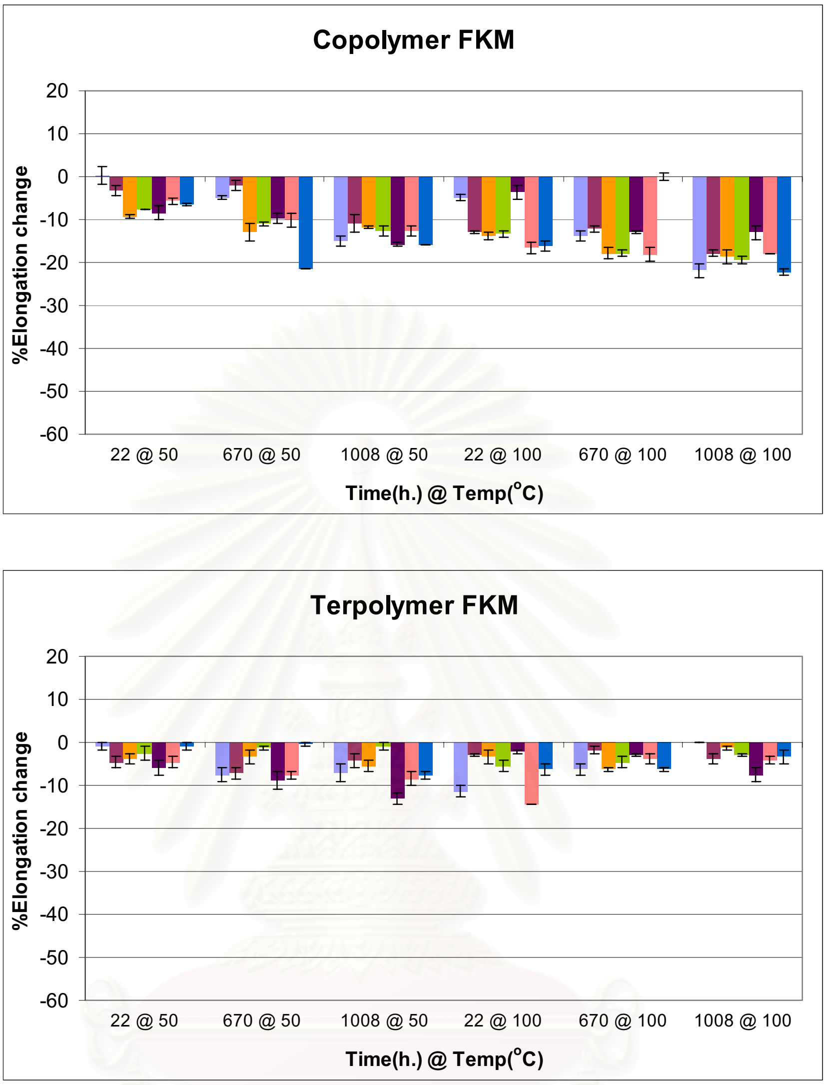

Figure 4.25 Effect of biodiesel and biodiesel blends :(🟪) Diesel; (🟥) B5-P; (🟧) B10-P; (🟩) B 100-P; (🟪) B5-C; (🟥) B10-C; (🟦) B100-C on percent elongation change of copolymer FKM and terpolymer FKM elastomers at 100 °C.

Effect of biodiesel and biodiesel blend on percentage of the elongation change of NBR at 100 °C is shown in Figure 4.23. Elongation of NBR showed more decrease at 100 °C than 50 °C in each period of time. At 22 and 670 hours, its change was took place only biodiesel. At 1008 hours, it change more decreased and the elongation change of diesel showed not different from biodiesel and biodiesel blends. It trend of elongation change of both of biodiesel was no different.

For percentage of the elongation change of HNBR at 100 °C is shown in Figure 4.23. Changing of HNBR in fuel at 100 °C was given in the same result with in fuel at 50 °C except at 1008 hours. It changing was more decreased. Decreased in elongation change of HNBR at 100 °C showed not different in each fuel.

Effect of biodiesel and biodiesel blends on percentage of the elongation change of NBR PVC at 100 °C is shown in Figure 4.24. For elongation change of NBR PVC was tended to decrease elongation after immersed in fuel at 100 °C more than at 50 °C in each time period. In 22 hours, changing of sample test with biodiesel was more than diesel and biodiesel blended.

Effect of biodiesel and biodiesel blend on percentage of the elongation change of acrylic rubber at 100 °C is shown in Figure 4.24. Acrylic rubber at the temperature 100 °C showed decreased in elongation more than temperature in each period . Acrylic rubber that immersed in biodiesel showed the highest decreased elongation. It was shown decreased in elongation when biodiesel content increased.

Effect of biodiesel and biodiesel blends on percentage of the elongation change of copolymer FKM at 100 °C is shown in Figure 4.25. It was tended to decrease if temperature rose. It tended to more decreased when the time of testing. Biodiesel content in diesel was not affect on elongation of copolymer FKM because the elongation changes not significant with biodiesel content in diesel.

Effect of biodiesel and biodiesel blends on percentage of the elongation change of terpolymer FKM at 100 °C is shown in Figure 4.25. For elongation change of terpolymer FKM in temperature 100 °C was no different from temperature 50 °C and it change was given result no different in elongation after increased biodiesel content and time of testing.

4.5 Dynamic Mechanical Analysis (DMA)

Dynamic mechanical analysis is important way to characterize elastomer. The tension mode was used to determine the dynamic mechanical properties of elastomer that immersed in biodiesel at temperature range of -50 to +30, heating rate of 3 K. min^{-1} and frequency 1 Hz.

Table 4.3 Glass transition temperature and tanδ of acrylic rubber after immersed in biodiesel for 1008 hours by DMA technique

Acrylic rubber	Tg(°C)	tanδ
New	-10.4	1.162
Immersed in B100-P @ 50 °C	-21.0	0.969
Immersed in B100-P @ 100 °C	-22.8	0.894
Immersed in B100-C @ 50 °C	-21.2	0.981
Immersed in B100-C @ 100 °C	-23.8	0.924

The effect of biodiesel on value of tenδ and glass transition temperature are shown in Table 4.3. The tan δ is defined as the ratio of loss modulus to storage modulus. The glass transition temperature was taken as the temperature at which the loss factor tanδ reached a maximum. From Figures 4.61 -4.62, it can be seen that tanδ showed the maximum values around the transition region. It is apparent that the large energy loss peak associated with the large changes in the modulus. The high energy input was used for joint motion of parts of the main polymer chains in the transition region. The glass transition temperature and tanδ of acrylic rubber decreased when immersed in B100-P and B100-C and more decrease with increase temperature. It can be explained that acrylic rubber was dissolve due to swelling of rubber.

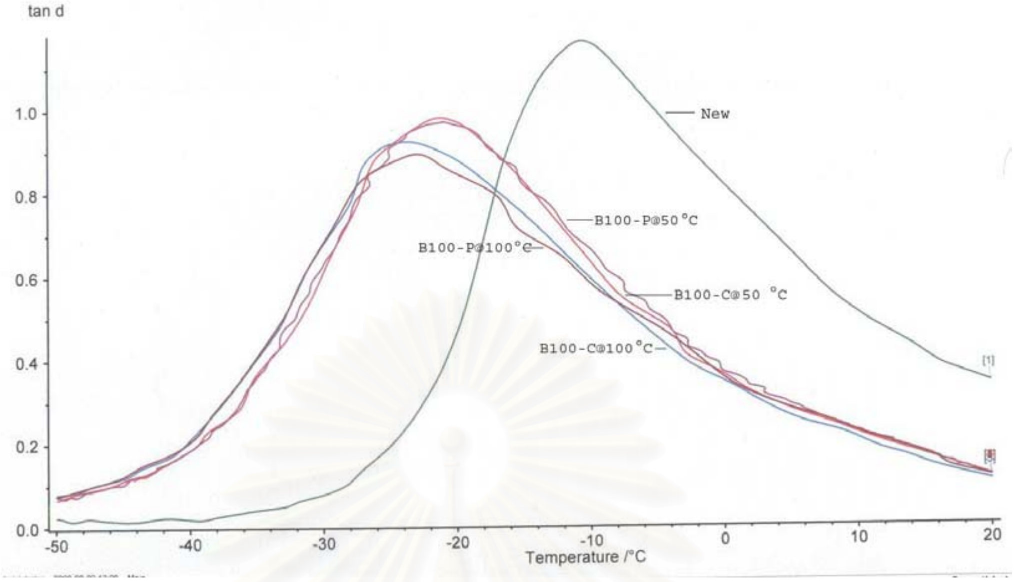

Figure 4.61 Loss Factor (tan δ) of the acrylic rubber after immersed in biodiesel

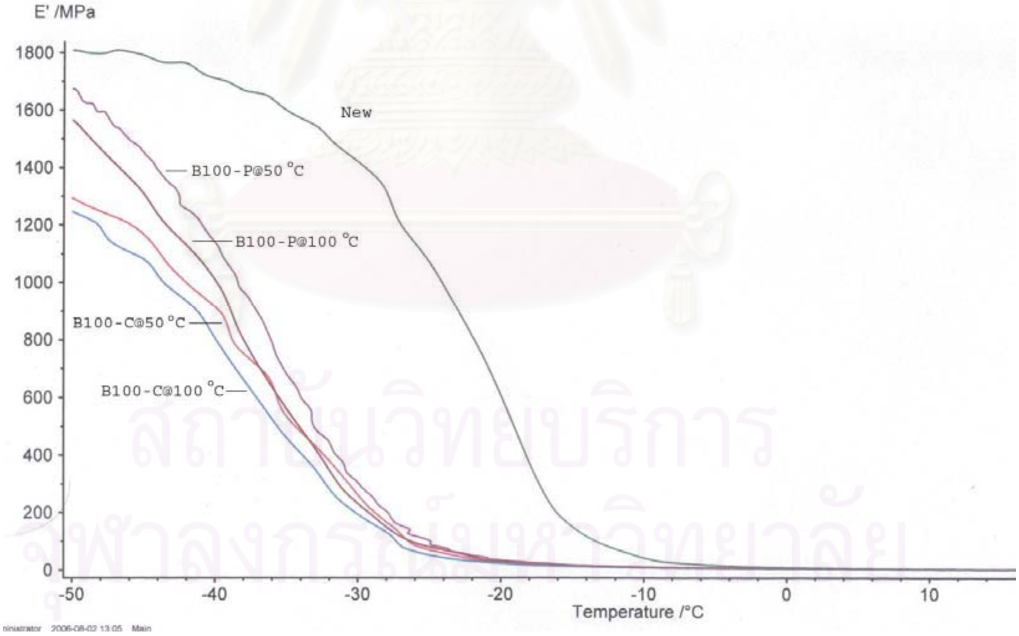

Figure 4.62 Storage modulus of the acrylic rubber after immersed in biodiesel.

In case of storage modulus (E’) on rubber were immersed in biodiesel with increased temperature. It decreased with increasing temperature. This is due to the relaxations arising from local motions of the polymer chain which is stiff around the transition region. The storage modulus decreased with acrylic rubber immersed in B100-C. The decrease in storage modulus can be explained that B100-C makes acrylic rubber increase in softness [28].

CHAPTER V

CONCLUSION AND SUGGESTION

5.1 Conclusion

In this research, the effect of biodiesel and biodiesel blends on engine elastomers properties was investigated. Elastomers studied are NBR, HNBR, NBR PVC, acrylic rubber, copolymer FKM and terpolymer FKM. The properties were measured according to European standard, EN 14214.

After immersed in diesel, biodiesel and biodisel blends at 50^{o}C, the mechanical properties of fluoroelastomer, copolymer FKM and terpolymer FKM showed slight change. Terpolymer FKM showed the least change of all elastomers. Properties of HNBR changed more than those of fluoroelastomer. NBR and NBR-PVC showed intermediate change. The elastomer which showed the highest change in its was the properties is acrylic rubber. The change increased with the increase in biodiesel content. Biodiesel increased the volume of the elastomers, that in turn affected to the hardness decrease. The elastomers were soften when immersed in the oil, so their tensile strength and elongation decreased. The result is similar to that described by Terry *et al.*[22] O-ring elastomers; NBR, HNBR and fluorocarbon polymer (medium and high fluorine content) that immersed in B5 and B20 of rapeseed methyl ester soy methyl ester and oxidized of soy methyl ester at temperature 60 ^{o}C for 1000 hours.

After immersed in the oil at 100^{o}C, propertie change of the elastomer were higher than at 50^{o}C. The higher change was found in acrylic rubber, NBR and NBR PVC after immersed in biodiesel. But in diesel and biodiesel blends the changes were slight. They were a little higher when immersion time was increased. The elastomer which shows the highest change was the acrylic rubber. For HNBR, the same result at 50^{o}C and 100^{o}C. When increasing time, volume and mass changes were increased in biodiesel. The elastomers which were very little affected are copolymer FKM and terpolymer FKM.

The elastomer which was very much affected was acrylic rubber. It was taken as a representative for dynamic mechanical analysis. It showed decrease in Tg and tanδ after immersed in biodiesel for 1008 hours. The acrylic rubber immersed in biodiesel produced from used cooking oil showed less value than that from refining palm oil.

5.2 Suggestion for the future work

Based on the above discussion and experimental results, the future work to improve the system should be focused on the study of the solubility parameter of biodiesel blends from different sources of biodiesel.

REFERENCES

[1]. Tickell, J. **From the Fryer to the Fuel Tank.** 3thed. New Orleans: Joshua Tickell Publications, 2003, pp. 11-14.

[2]. Phongsataya, U. Effect of palm oil methyl ester on polycyclic aromatic hydrocarbons emission of diesel engine. **Master's Thesis,** Program of Petrochemistry and Polymer Science, Faculty of Science, Chulalongkorn University, 2002, pp. 2

[3]. Kim, H.J., et al. Transesterification of vegetable oil to biodiesel using heterogeneous base catalyst. ***Catal. Today.*** **93-95** (2004): 315-320.

[4]. Jobe, J. **Biodiesel handling and use guidelines.**[Online]. Oak Ridge: National Biodiesel Board, 2004. Available from: http://www.biodiesel.org.

[5]. Bessee, G.B. and Fey, J.P. Compatibility of elastomers and metals in biodiesel fuel blends. ***SAE paper.*** **971690** (1997): 650-661.

[6]. Ranken, M.D.; Kill, R.C. and Baker, C. **Food Industries Manual.** London: Chapman & Hall, 1997, pp. 279.

[7]. deMan, J. M. **Principles of food chemistry.** 3thed. Maryland: Aspen Publishers, 1999, pp 65-70.

[8]. Schuchardt, U.; Sercheli, R. and Vargas, R.M. Transesterification of vegetable oils: a review, ***J. Braz. Chem. Soc.*** **9(1)** (1998): 199-210.

[9]. Graboski, M.S. and. McCormick, R.L. Combustion of fat and vegetable oil derived fuels in diesel engines. ***Prog. Energy Combust. Sci.*** **24** (1998): 125-164

[10]. Odian, G. **Principles of polymerization.** 4thed. New Jersey: A John Wiley & Sons, 2004, pp. 33-35.

[11]. McGraw, J.L. **Acrylonitrile-butadiene rubber.**[Online]. Texas: International Institute of Synthetic Rubber Producers. 2002. Available from: http://www.iisrp.com/WebPolymers/07NBR-18Feb2002.pdf.

[12]. McGraw, J.L. **Hydrogenated nitrile-butadiene rubber.**[Online]. Texas: International Institute of Synthetic Rubber Producers. 2001. Available from: http://www.iisrp.com/WebPolymers/03HNBR-11Dec2001.pdf

[13]. **Eriks sealing elements.**[Online]. 2002. Natherland. Available from: http:// o-ring.info/en/downloads.brochures/.

[14]. Harper, C.A. **Handbook of Materials for Product Design.** New York: McGraw-Hill, 2001, pp. 6.77-6.79.

[15]. McGraw, J.L. **Fluoroelastomer.**[Online]. Texas: International Institute of Synthetic Rubber Producers. 2002. Available from: http://www.iisrp.com/WebPolymers/06ModFluoroelastomersv1-4.pdf

[16]. Eisner, A.; Koos, R.E.; Bilyk, A.; Parker, W.E.; and Maerker, G. Rubber swell as a function of fatty acid ester chain length. ***J. Am. Chem. Soc.*** **49** (1972): 351-353.

[17]. Cusano, C.M.; Stafford, R.J.; and Lucas, L.M. Changes in elastomer swell with diesel fuel composition. ***SAE paper.*** 942017 (1994): 79-83.

[18]. Robertson, S.D et al. Effect of automotive gas oil composition on elastomer begaveiour. ***SAE paper.*** 942018 (1994): 1634-1653.

[19]. Kumnuantip, C. and Sombatsompop, N. Dynamic mechanical properties and swelling behaviour of NR/reclaimed rubber blends. ***Meter. Lett.*** **57** (2003) 3167-3174.

[20]. Hu, J.; Du, Z.; Tang, Z.; and Min, E. Study on the solvent power of a new green solvent: biodiesel. ***Ind. Eng. Chem. Res.*** **43** (2004): 7928-7931.

[21]. Nielsen, T.B.; and Hansen, C.M. Elastomer swelling and hanson solubility parameters. ***Polym. Test.*****24** (2005): 1054-1061.

[22]. Teery, B. Impact of biodiesel on fuel system component durability.[Technical report] Milton Keynes: The Associated octel company, 2005. Available from: http:// www.nrel.gov/vihiclesandfuels/npbf/pdf.39130.pdf.

[23]. Kader, M.K.; Bhowmick, A.K.; Thermal ageing, degradation and swelling of acrylate rubber, fluororubber and their blends containing polyfunctional acrylates. ***Polym. Degrad. Stab.*** (2003): 283-295.

[24]. Clamroth, R.; Tobisch, K.; Barczewski, H. and Wundrich, K. Precision of the results of standard clastomer ageing tests**.** ***Polym. Test.*****13** (1994):129-169.

[25]. Mathew, A.P.; Packirisamy, S.; Stephen, R.; and Thomas, S. Transport of aromatic solvents through natural rubber/polystyrene (NR/PS) interpenetrating polymer network membranes. ***J. Mem. Sci.*****201** (2002): 213-227.

[26]. Morrell, P.R.; Patel, M. and Skinner, A.R. Accelerated thermal ageing studies on nitrile rubber o-rings. ***Polym. Test.*****22** (2003): 651-656.

[27]. Perera, M.C.S.; Ishiaku, U.S. and Ishak, Z.A.M. Thermal degradation of PVC/NBR and PVC/ENR50 binary blends and PVC/ENR50/NBR ternary blends studied by DMA and solid state NMR. ***Polym. Degrad. Stab.*****68** (2000)393-402.

[28]. Fedors, R.F. Absorption of liquids by rubber vulcanizates. ***Polymer*****.20** (1979): 1087-1090.

APPENDICES

APPENDIX A

Table A1 Value of percent mass change at 50 °C

Elastomer	Fuel	22 hrs.		670 hrs.		1008 hrs.	
		Average change (%)	**S.D.**	**Average change (%)**	**S.D.**	**Average change (%)**	**S.D.**
NBR	Diesel	2.60	0.01	0.47	0.03	0.09	0.02
	B5-P	2.78	0.03	0.63	0.02	0.80	0.02
	B10-P	1.64	0.02	1.29	1.41	-0.33	0.05
	B100-P	11.19	0.07	7.11	0.04	7.40	0.03
	B5-C	2.99	0.02	0.92	0.05	0.64	0.03
	B10-C	1.48	0.00	-0.11	0.15	-0.47	0.03
	B100-C	10.91	0.05	6.95	0.08	7.41	0.03
HNBR	Diesel	2.00	0.01	5.85	0.01	5.84	0.01
	B5-P	1.97	0.06	5.81	0.00	5.99	0.01
	B10-P	4.89	0.05	6.76	0.06	6.57	0.01
	B100-P	2.55	0.01	5.87	0.01	6.13	0.06
	B5-C	2.14	0.03	5.82	0.02	6.38	0.02
	B10-C	4.78	0.18	6.51	0.06	6.89	0.03
	B100-C	2.81	0.05	6.01	0.04	6.16	0.02
NBR PVC	Diesel	2.15	0.03	-0.17	0.04	-0.69	0.05
	B5-P	2.36	0.02	0.00	0.04	0.15	0.20
	B10-P	2.96	0.12	0.96	0.20	0.16	0.10
	B100-P	12.60	0.07	9.32	0.07	9.30	0.27
	B5-C	2.38	0.01	0.47	0.06	0.02	0.02
	B10-C	2.82	0.01	0.66	0.02	-0.29	0.04
	B100-C	12.94	0.12	7.49	0.14	7.65	0.00

Table A1 Value of percent mass change at 50 °C (continue)

Elastomer	Fuel	22 hrs.		670 hrs.		1008 hrs.	
		Average change (%)	S.D.	Average change (%)	S.D.	Average change (%)	S.D.
Acrylic rubber	Diesel	2.72	0.07	4.08	0.02	3.89	0.02
	B5-P	2.36	0.02	4.44	0.02	4.49	0.04
	B10-P	5.85	0.07	6.77	0.14	5.86	0.08
	B100-P	13.07	0.07	22.05	0.03	22.34	0.08
	B5-C	2.97	0.01	4.49	0.04	4.65	0.05
	B10-C	5.55	0.10	5.75	0.06	5.48	0.00
	B100-C	12.90	0.03	22.66	0.01	22.93	0.17
Co FKM	Diesel	0.05	0.00	0.92	0.01	0.81	0.04
	B5-P	0.06	0.00	0.92	0.01	1.11	0.07
	B10-P	0.28	0.01	0.41	0.03	0.33	0.01
	B100-P	0.15	0.00	1.41	0.01	1.86	0.02
	B5-C	0.05	0.04	0.78	0.00	0.74	0.64
	B10-C	0.28	0.00	0.33	0.01	0.32	0.01
	B100-C	0.04	0.02	1.54	0.06	1.56	0.00
Ter FKM	Diesel	0.09	0.00	0.79	0.01	0.76	0.02
	B5-P	-1.07	0.93	0.88	0.07	1.06	0.11
	B10-P	0.73	0.00	1.22	0.06	1.19	0.01
	B100-P	-1.41	1.02	1.32	0.00	1.62	0.05
	B5-C	1.74	1.05	0.74	0.00	0.96	0.00
	B10-C	0.66	0.00	1.17	0.02	1.06	0.00
	B100-C	1.39	0.95	1.19	0.00	1.49	0.01

Table A2 Value of percent volume change at 50 ^{o}C.

Elastomer	**Fuel**	**22 hrs.**		**670 hrs.**		**1008 hrs.**	
		Average change (%)	**S.D.**	**Average change (%)**	**S.D.**	**Average change (%)**	**S.D.**
NBR	Diesel	3.99	0.00	1.63	0.01	1.28	0.06
	B5-P	4.21	0.11	2.02	0.03	2.01	0.19
	B10-P	2.68	0.14	2.36	1.61	0.47	0.14
	B100-P	15.78	0.08	10.79	0.02	11.06	0.01
	B5-C	4.33	0.04	2.45	0.05	2.00	0.15
	B10-C	2.63	0.02	-0.53	1.51	0.16	0.04
	B100-C	15.14	0.14	10.27	0.11	10.75	0.01
HNBR	Diesel	2.96	0.03	8.42	0.08	8.26	0.04
	B5-P	2.99	0.17	8.63	0.02	10.11	2.14
	B10-P	6.70	0.04	9.38	0.12	9.23	0.06
	B100-P	3.99	0.02	8.94	0.02	9.45	0.09
	B5-C	2.98	0.03	8.52	0.10	9.14	0.02
	B10-C	6.82	0.33	8.95	0.00	9.76	0.07
	B100-C	4.24	0.13	9.16	0.09	9.18	0.04
NBR PVC	Diesel	3.89	0.01	1.39	0.01	0.93	0.03
	B5-P	4.02	0.06	1.85	0.05	1.87	0.29
	B10-P	4.40	0.03	2.16	0.40	1.38	0.09
	B100-P	19.11	0.14	15.09	0.20	14.93	0.40
	B5-C	3.78	0.06	2.50	0.02	1.66	0.02
	B10-C	4.34	0.01	1.79	0.10	0.70	0.05
	B100-C	19.48	0.13	12.41	0.26	12.42	0.14

Table A2 Value of percent volume change at 50 ^{o}C.(continue)

Elastomer	Fuel	22 hrs.		670 hrs.		1008 hrs.	
		Average change (%)	**S.D.**	**Average change (%)**	**S.D.**	**Average change (%)**	**S.D.**
Acrylic rubber	Diesel	4.34	0.18	8.81	2.86	6.51	0.02
	B5-P	4.58	0.06	7.29	0.06	7.34	0.11
	B10-P	9.82	0.15	11.19	0.17	9.56	0.18
	B100-P	21.33	0.01	35.97	0.05	36.41	0.17
	B5-C	4.75	0.09	7.52	0.12	7.52	0.07
	B10-C	8.40	2.03	9.20	0.02	8.92	0.21
	B100-C	20.94	0.08	36.65	0.13	37.09	0.24
Co FKM	Diesel	0.01	0.03	2.12	0.04	2.14	0.02
	B5-P	0.06	0.01	2.31	0.07	2.63	0.12
	B10-P	1.02	0.01	1.33	0.14	1.42	0.01
	B100-P	0.37	0.03	2.99	0.00	3.93	0.02
	B5-C	0.06	0.04	2.05	0.00	2.03	0.97
	B10-C	1.06	0.01	1.40	0.08	1.39	0.05
	B100-C	0.30	0.10	3.44	0.02	3.26	0.09
Ter FKM	Diesel	-0.02	0.01	1.90	2.14	1.76	0.03
	B5-P	-0.89	0.96	1.97	0.07	1.77	0.60
	B10-P	1.68	0.04	2.62	0.08	2.51	0.05
	B100-P	-1.48	1.08	2.99	0.03	3.65	0.06
	B5-C	1.84	2.95	1.69	0.04	2.11	0.00
	B10-C	1.61	0.01	2.56	0.09	2.28	0.01
	B100-C	1.39	0.97	2.77	0.07	3.26	0.04

Table A3 Value of hardness change at 50 ^{o}C.

Elastomer	**Fuel**	**22 hrs.**		**670 hrs.**		**1008 hrs.**	
		Average change (%)	**S.D.**	**Average change (%)**	**S.D.**	**Average change (%)**	**S.D.**
NBR	Diesel	-0.37	0.21	6.17	0.93	7.43	0.51
	B5-P	-0.60	0.10	4.93	0.25	6.90	0.10
	B10-P	-2.83	0.45	1.10	0.79	-0.43	0.21
	B100-P	-5.57	0.06	-3.23	0.15	-2.43	0.45
	B5-C	-0.47	0.15	5.60	0.26	6.33	0.70
	B10-C	-1.77	0.49	1.63	0.15	0.50	0.10
	B100-C	-5.70	0.70	-3.13	0.31	-1.70	0.35
HNBR	Diesel	-1.80	0.10	-4.87	0.15	-4.80	0.30
	B5-P	-1.27	0.31	-5.37	0.90	-4.80	0.87
	B10-P	-4.70	0.50	-4.90	0.26	-5.60	0.20
	B100-P	-2.70	0.30	-6.13	0.25	-6.07	0.68
	B5-C	-1.33	0.32	-4.57	0.67	-5.13	0.40
	B10-C	-3.90	0.44	-4.40	0.56	-6.00	0.10
	B100-C	-2.63	0.12	-6.03	0.29	-5.97	0.21
NBR PVC	Diesel	-0.93	0.35	2.30	0.36	3.67	0.06
	B5-P	-2.13	0.50	2.37	0.51	2.20	0.46
	B10-P	-2.63	0.32	0.17	0.15	-0.20	0.35
	B100-P	-9.20	0.26	-6.77	0.49	-5.80	0.50
	B5-C	-1.73	0.15	1.80	0.17	3.03	0.23
	B10-C	-2.70	0.30	0.97	0.12	0.10	0.26
	B100-C	-9.03	0.32	-6.57	0.21	-5.87	0.29

Table A3 Value of hardness change at 50 ^oC.(continue)

Elastomer	Fuel	22 hrs.		670 hrs.		1008 hrs.	
		Average change (%)	S.D.	Average change (%)	S.D.	Average change (%)	S.D.
Acrylic rubber	Diesel	-2.27	0.67	-3.63	0.40	-2.33	0.15
	B5-P	-2.23	0.57	-4.10	0.17	-4.27	0.23
	B10-P	-5.80	0.40	-3.23	0.67	-4.07	0.12
	B100-P	-8.80	0.46	-15.30	0.36	-15.70	0.44
	B5-C	-2.30	0.70	-4.33	1.16	-4.43	0.67
	B10-C	-5.37	0.81	-4.57	0.45	-3.93	0.06
	B100-C	-9.33	0.45	-16.13	0.97	-15.60	0.78
Co FKM	Diesel	-0.77	0.50	-2.00	0.69	-2.43	0.68
	B5-P	-0.37	0.32	-2.87	0.40	-2.73	0.42
	B10-P	-1.77	0.68	-0.87	0.83	-2.93	0.15
	B100-P	-0.90	0.20	-5.33	0.21	-6.03	1.12
	B5-C	-1.07	0.32	-1.57	1.18	-4.03	0.42
	B10-C	-1.83	0.25	-0.40	0.70	-1.70	0.69
	B100-C	-0.23	0.55	-4.57	0.38	-4.43	0.80
Ter FKM	Diesel	-0.43	0.12	-2.30	0.69	-2.43	0.31
	B5-P	-0.73	0.47	-1.77	0.15	-2.27	0.15
	B10-P	-2.03	0.21	-1.73	0.40	-2.77	0.06
	B100-P	-0.47	0.25	-3.20	0.26	-3.93	0.15
	B5-C	-1.37	0.49	-1.87	0.21	-2.67	0.06
	B10-C	-1.83	0.15	-1.33	0.21	-2.80	0.20
	B100-C	-0.80	0.17	-3.07	0.40	-3.70	0.20

Table A4 Value of percent tensile change at 50 ^{o}C.

Elastomer	Fuel	22 hrs.		670 hrs.		1008 hrs.	
		Average change (%)	**S.D.**	**Average change (%)**	**S.D.**	**Average change (%)**	**S.D.**
NBR	Diesel	0.18	0.16	-6.55	1.09	-10.83	2.17
	B5-P	-1.90	2.17	-3.55	0.47	-14.96	2.33
	B10-P	-17.38	0.90	-19.82	0.21	-17.45	2.33
	B100-P	-28.13	1.71	-25.68	2.17	-29.11	2.69
	B5-C	-1.28	2.12	-4.61	2.17	-12.18	0.26
	B10-C	-4.47	2.21	-14.19	1.45	-26.26	0.31
	B100-C	-9.40	1.50	-19.86	0.05	-23.08	1.09
HNBR	Diesel	6.36	0.04	3.82	2.35	0.55	0.71
	B5-P	9.28	2.09	6.54	2.54	0.98	1.31
	B10-P	3.27	0.00	-3.09	1.83	-2.58	0.90
	B100-P	8.41	2.87	6.78	0.04	-1.40	0.78
	B5-C	3.93	2.27	1.24	0.11	1.00	0.97
	B10-C	2.06	0.00	0.87	1.68	-6.67	1.16
	B100-C	7.33	1.42	5.99	0.04	2.29	0.34
NBR PVC	Diesel	1.28	1.22	-6.10	0.12	-10.84	1.92
	B5-P	1.53	1.46	-5.94	1.87	2.33	2.68
	B10-P	-6.76	2.17	-9.14	0.75	-11.33	2.95
	B100-P	4.29	1.87	-5.94	1.28	-6.55	1.46
	B5-C	ND	ND	ND	ND	-17.85	0.76
	B10-C	-6.52	2.20	-16.11	2.09	-8.56	0.22
	B100-C	-3.92	1.57	-10.55	1.28	-10.39	1.98

Table A4 Value of percent tensile change at 50 ^{o}C.(continue)

Elastomer	**Fuel**	**22 hrs.**		**670 hrs.**		**1008 hrs.**	
		Average change (%)	**S.D.**	**Average change (%)**	**S.D.**	**Average change (%)**	**S.D.**
Acrylic rubber	Diesel	0.05	0.54	-7.44	2.99	-8.20	2.99
	B5-P	-1.25	1.46	-9.88	0.00	-11.62	1.38
	B10-P	-13.74	0.08	-23.62	1.46	-20.52	1.38
	B100-P	-21.39	0.00	-34.47	1.15	-31.16	1.54
	B5-C	-2.01	1.46	-16.56	1.00	-10.97	1.38
	B10-C	-18.89	2.00	-24.27	2.99	-21.88	1.46
	B100-C	-21.39	2.76	-33.71	2.99	-36.64	2.84
Co FKM	Diesel	-13.27	0.93	-12.62	1.32	-19.63	1.19
	B5-P	-12.06	1.32	-17.85	1.45	-20.19	1.45
	B10-P	-13.55	1.06	-15.98	2.64	-24.67	1.06
	B100-P	-9.16	0.13	-12.99	1.85	-27.20	1.85
	B5-C	-11.68	1.45	-16.64	2.78	-26.92	1.32
	B10-C	-14.58	1.06	-17.48	0.26	-23.46	1.98
	B100-C	-17.66	1.19	-18.88	0.13	-24.11	1.72
Ter FKM	Diesel	1.74	2.24	-21.03	2.35	-14.66	2.40
	B5-P	2.45	1.12	-18.02	1.12	-24.07	1.17
	B10-P	-6.13	1.17	-5.57	0.61	-19.64	0.39
	B100-P	0.67	2.29	-22.33	2.40	-26.80	2.12
	B5-C	2.85	0.11	-18.62	1.29	-17.39	2.35
	B10-C	-9.41	1.79	-16.25	2.18	-22.89	1.84
	B100-C	0.67	2.40	-13.72	2.29	-18.38	2.40

Table A5 Value of percent elongation change at 50 °C.

Elastomer	Fuel	22 hrs.		670 hrs.		1008 hrs.	
		Average change (%)	S.D.	Average change (%)	S.D.	Average change (%)	S.D.
NBR	Diesel	2.69	2.77	-33.50	3.46	-33.74	2.42
	B5-P	-2.20	2.07	-23.23	2.77	-35.45	2.77
	B10-P	-19.60	2.48	-20.63	2.29	-29.34	3.11
	B100-P	-17.11	3.80	-29.10	3.46	-35.21	2.42
	B5-C	3.18	2.77	-23.72	2.07	-30.56	4.15
	B10-C	-10.66	2.56	-19.34	2.11	-29.83	2.42
	B100-C	-11.98	2.07	-19.80	2.77	-32.27	1.73
HNBR	Diesel	3.87	1.49	-10.92	1.49	-13.03	2.49
	B5-P	4.93	0.00	-7.39	1.49	-13.03	1.49
	B10-P	4.93	1.00	-9.15	1.00	-16.20	1.00
	B100-P	11.62	1.49	-8.80	1.49	-14.79	1.00
	B5-C	2.11	1.00	-7.75	1.99	-13.38	2.99
	B10-C	8.45	1.00	-11.62	1.49	-16.90	1.99
	B100-C	10.92	1.49	-2.82	1.00	-3.87	2.49
NBR PVC	Diesel	1.87	1.32	-21.18	2.20	-25.86	0.88
	B5-P	0.93	1.76	-23.05	2.20	-23.05	3.08
	B10-P	1.90	1.92	-9.24	0.77	-7.79	0.88
	B100-P	2.18	0.88	-8.41	2.64	-10.28	2.64
	B5-C	4.36	3.97	-14.64	2.64	-19.63	2.64
	B10-C	5.61	3.08	-14.95	1.92	-17.76	1.76
	B100-C	2.18	0.88	-12.15	1.76	-17.45	2.20

Table A5 Value of percent elongation change at 50 ^{o}C.(continue)

Elastomer	Fuel	22 hrs.		670 hrs.		1008 hrs.	
		Average change (%)	S.D.	Average change (%)	S.D.	Average change (%)	S.D.
Acrylic rubber	Diesel	ND	ND	-8.02	2.00	-9.91	2.00
	B5-P	-0.47	3.34	-11.32	1.33	-10.85	2.00
	B10-P	-0.47	0.67	-5.19	2.00	-5.19	0.67
	B100-P	-16.04	1.33	-18.87	1.33	-26.89	0.67
	B5-C	-0.47	0.67	-13.21	1.33	-18.87	0.00
	B10-C	-0.94	0.00	-7.08	2.00	-9.43	1.33
	B100-C	-11.32	1.33	-24.06	3.34	-29.25	2.67
Co FKM	Diesel	0.40	1.15	-4.86	1.72	-14.98	2.29
	B5-P	-3.24	0.57	-2.02	1.15	-10.93	1.15
	B10-P	-9.31	1.15	-12.96	1.72	-11.74	2.29
	B100-P	-7.69	1.15	-10.93	1.15	-12.55	1.15
	B5-C	-8.50	2.29	-9.72	0.57	-15.79	2.29
	B10-C	-5.67	1.72	-10.12	2.29	-12.55	0.00
	B100-C	-6.48	1.72	-21.46	1.15	-15.79	1.15
Ter FKM	Diesel	-0.84	1.19	-7.56	2.38	-7.14	2.97
	B5-P	-4.62	1.78	-7.14	1.78	-4.20	2.38
	B10-P	-3.78	1.78	-3.36	2.38	-5.46	1.78
	B100-P	-2.52	2.38	-1.26	0.59	-0.84	1.19
	B5-C	-5.88	2.38	-8.82	2.97	-13.03	1.78
	B10-C	-4.62	1.78	-7.56	1.19	-8.40	2.38
	B100-C	-0.84	1.19	-0.42	0.59	-7.56	1.19

APPENDIX B

Table B1 Value of percent mass change at 100 ^{o}C.

Elastomer	Fuel	22 hrs.		670 hrs.		1008 hrs.	
		Average change (%)	S.D.	Average change (%)	S.D.	Average change (%)	S.D.
NBR	Diesel	1.61	0.08	0.13	0.03	-1.61	0.01
	B5-P	2.18	0.03	1.09	0.04	-1.45	0.05
	B10-P	3.32	0.10	2.24	0.04	-0.63	0.02
	B100-P	11.52	0.01	29.88	0.01	37.68	1.11
	B5-C	2.16	0.01	1.29	0.01	-1.32	0.06
	B10-C	2.16	1.90	2.30	0.09	-0.83	0.01
	B100-C	12.86	2.06	42.80	0.48	36.84	1.58
HNBR	Diesel	5.10	0.10	5.23	0.01	5.58	0.09
	B5-P	5.21	0.01	3.98	2.59	5.74	0.06
	B10-P	5.74	0.00	6.02	0.03	6.44	0.02
	B100-P	6.65	0.02	27.76	0.10	27.46	0.19
	B5-C	5.14	0.09	5.55	0.00	5.92	0.01
	B10-C	5.57	0.07	6.13	0.01	6.37	0.04
	B100-C	6.61	0.02	30.70	0.11	28.78	0.12
NBR PVC	Diesel	1.92	0.12	-0.62	0.06	-3.24	0.01
	B5-P	2.42	0.11	0.02	0.00	-2.58	0.01
	B10-P	3.79	0.04	1.45	0.04	-1.43	0.10
	B100-P	15.66	0.33	24.09	0.51	23.94	0.52
	B5-C	2.58	0.11	-2.78	0.01	-2.69	0.07
	B10-C	4.06	0.09	-1.93	0.02	-1.92	0.08
	B100-C	15.61	0.08	26.77	1.65	20.33	0.73

Table B1 Value of percent mass change at 100 ^{o}C.(continue)

Elastomer	**Fuel**	**22 hrs.**		**670 hrs.**		**1008 hrs.**	
		Average change (%)	**S.D.**	**Average change (%)**	**S.D.**	**Average change (%)**	**S.D.**
Acrylic rubber	Diesel	5.85	0.11	5.49	0.03	5.47	0.16
	B5-P	6.29	0.15	6.54	0.14	6.53	0.10
	B10-P	7.24	0.04	7.58	0.06	7.76	0.00
	B100-P	28.95	0.27	37.40	0.11	39.89	0.35
	B5-C	6.22	0.06	6.43	0.08	6.50	0.14
	B10-C	7.31	0.09	7.82	0.15	7.69	0.03
	B100-C	30.50	0.69	42.08	0.02	40.14	0.17
Co FKM	Diesel	1.12	0.06	1.21	0.01	-0.25	0.00
	B5-P	1.13	0.03	1.86	0.01	0.36	0.01
	B10-P	1.46	0.04	0.41	0.01	0.85	0.01
	B100-P	1.68	0.02	-0.48	0.03	0.42	0.12
	B5-C	0.99	0.02	0.23	0.02	0.11	0.01
	B10-C	1.16	0.05	0.47	0.01	0.59	0.02
	B100-C	1.76	0.01	2.32	0.01	2.59	0.03
Ter FKM	Diesel	1.28	0.05	1.29	0.05	1.76	0.01
	B5-P	1.09	0.01	1.64	0.03	1.75	0.02
	B10-P	1.13	0.03	1.95	0.04	1.99	0.08
	B100-P	1.73	0.02	2.87	0.01	2.93	0.00
	B5-C	1.06	0.02	1.69	0.03	1.80	0.02
	B10-C	1.16	0.00	1.85	0.03	1.88	0.00
	B100-C	1.76	0.02	2.65	0.04	3.10	0.01

Table B2 Value of volume change at 100 ^{o}C.

Elastomer	Fuel	22 hrs.		670 hrs.		1008 hrs.	
		Average change (%)	S.D.	Average change (%)	S.D.	Average change (%)	S.D.
NBR	Diesel	3.66	0.16	1.55	0.01	-1.26	0.76
	B5-P	4.44	0.07	2.64	0.14	-0.90	0.16
	B10-P	5.94	0.21	4.29	0.05	0.36	0.05
	B100-P	16.76	0.05	41.98	0.03	54.06	1.66
	B5-C	4.42	0.04	2.98	0.02	-0.68	0.03
	B10-C	4.76	1.81	4.32	0.23	0.10	0.02
	B100-C	16.31	4.69	60.87	0.58	53.20	2.28
HNBR	Diesel	7.66	0.08	7.75	0.08	8.29	0.10
	B5-P	7.89	0.04	6.21	3.48	8.50	0.26
	B10-P	8.54	0.04	9.04	0.02	9.58	0.03
	B100-P	10.31	0.09	39.44	0.33	39.35	0.12
	B5-C	7.72	0.06	8.43	0.07	8.82	0.10
	B10-C	8.48	0.15	9.11	0.05	9.67	0.14
	B100-C	10.25	0.01	43.76	0.11	41.16	0.12
NBR PVC	Diesel	5.08	0.09	1.32	0.11	-3.06	0.03
	B5-P	5.64	0.14	2.26	0.02	-2.60	0.94
	B10-P	7.62	0.08	4.63	0.19	-0.54	0.04
	B100-P	24.42	0.36	38.66	0.57	35.89	0.67
	B5-C	5.92	0.14	-2.11	0.03	-2.10	0.05
	B10-C	7.97	0.10	-0.99	0.06	-0.87	0.14
	B100-C	24.34	0.10	39.86	2.14	31.40	0.92

Table B2 Value of volume change at 100 ^{o}C.(continue)

Elastomer	Fuel	22 hrs.		670 hrs.		1008 hrs.	
		Average change (%)	S.D.	Average change (%)	S.D.	Average change (%)	S.D.
Acrylic rubber	Diesel	10.14	1.38	9.25	0.02	8.68	0.10
	B5-P	10.87	0.25	10.80	0.22	10.64	0.19
	B10-P	12.39	0.06	12.57	0.15	12.64	0.00
	B100-P	47.48	0.38	60.62	0.10	64.20	0.74
	B5-C	10.68	0.08	10.55	0.12	10.45	0.19
	B10-C	12.48	0.18	12.76	0.16	12.38	0.13
	B100-C	49.84	1.06	67.73	0.10	64.42	0.19
Co FKM	Diesel	2.82	0.18	2.96	0.00	0.85	0.07
	B5-P	2.89	0.01	4.41	0.00	1.93	0.03
	B10-P	3.60	0.02	2.21	0.01	2.90	0.15
	B100-P	4.12	0.06	1.63	0.07	3.60	0.09
	B5-C	2.60	0.02	1.75	0.01	1.53	0.24
	B10-C	3.00	0.14	2.18	0.01	2.72	0.02
	B100-C	4.23	0.02	7.25	0.04	8.14	0.18
Ter FKM	Diesel	3.02	0.08	3.18	0.33	3.57	0.01
	B5-P	2.57	0.08	3.80	0.07	3.33	0.04
	B10-P	2.70	0.10	3.76	0.15	3.85	0.12
	B100-P	3.94	0.08	5.55	0.01	5.42	0.01
	B5-C	2.55	0.01	3.53	0.11	3.48	0.08
	B10-C	2.69	0.09	3.79	0.16	3.53	0.12
	B100-C	4.04	0.13	5.10	0.08	5.98	0.00

Table B3 Value of hardness change at 100 ^{o}C.

Elastomer	**Fuel**	**22 hrs.**		**670 hrs.**		**1008 hrs.**	
		Average change (%)	**S.D.**	**Average change (%)**	**S.D.**	**Average change (%)**	**S.D.**
NBR	Diesel	3.83	0.74	8.43	0.31	11.20	0.46
	B5-P	2.07	0.25	6.83	0.38	7.73	1.27
	B10-P	0.30	0.61	3.63	0.59	5.70	0.70
	B100-P	-6.63	0.59	-13.07	0.50	-10.47	0.76
	B5-C	2.17	0.31	7.30	0.40	7.70	0.35
	B10-C	0.33	0.45	4.23	0.67	4.90	0.17
	B100-C	-6.47	0.55	-12.80	0.40	-13.60	0.46
HNBR	Diesel	-3.37	0.60	-5.30	0.95	-4.00	0.10
	B5-P	-4.70	0.60	-6.03	1.01	-4.70	0.10
	B10-P	-4.67	0.15	-7.03	0.81	-6.13	0.06
	B100-P	-8.00	0.78	-13.57	0.49	-12.87	0.23
	B5-C	-4.00	0.85	-5.20	0.30	-5.20	0.61
	B10-C	-5.13	1.21	-6.23	0.06	-6.90	0.26
	B100-C	-7.87	0.25	-13.97	0.59	-14.40	0.30
NBR PVC	Diesel	-2.63	0.61	6.67	0.55	6.50	0.53
	B5-P	-2.93	0.32	4.63	0.25	4.27	0.42
	B10-P	-4.37	0.55	1.13	0.15	2.30	0.44
	B100-P	-13.30	0.50	-19.97	0.12	-12.17	0.76
	B5-C	-2.83	0.49	2.63	0.15	4.40	0.26
	B10-C	-4.90	0.10	1.30	0.44	2.47	0.42
	B100-C	-13.43	0.38	-12.63	0.12	-11.70	0.26

Table B3 Value of hardness change at 100 ^{o}C.(continue)

Elastomer	**Fuel**	**22 hrs.**		**670 hrs.**		**1008 hrs.**	
		Average change (%)	**S.D.**	**Average change (%)**	**S.D.**	**Average change (%)**	**S.D.**
Acrylic rubber	Diesel	-6.37	0.38	-2.07	0.38	2.87	0.40
	B5-P	-6.70	1.11	-4.07	0.38	0.23	0.12
	B10-P	-7.53	0.35	-5.80	0.70	-3.00	0.52
	B100-P	-15.93	1.03	-19.47	0.57	-18.84	0.21
	B5-C	-6.50	0.17	-1.97	0.72	-0.70	0.62
	B10-C	-8.30	0.56	-4.07	0.70	-2.57	0.60
	B100-C	-16.77	1.21	-19.47	0.65	-19.30	0.20
Co FKM	Diesel	-1.50	0.78	-1.73	0.23	-0.80	1.18
	B5-P	-2.53	0.25	-1.97	0.15	-2.60	0.79
	B10-P	-3.47	1.53	-2.60	0.35	-2.97	0.06
	B100-P	-3.50	0.46	-3.33	0.50	-4.37	1.04
	B5-C	-2.33	0.67	-1.87	0.49	-2.00	0.66
	B10-C	-2.57	0.57	-2.63	0.45	-3.37	0.31
	B100-C	-3.63	0.12	-5.23	0.29	-5.37	0.40
Ter FKM	Diesel	-2.90	0.26	-2.27	0.55	-2.73	0.15
	B5-P	-3.00	0.30	-3.03	0.21	-3.27	0.15
	B10-P	-2.73	1.01	-3.03	0.25	-3.43	0.32
	B100-P	-4.03	0.40	-4.47	0.38	-4.80	0.44
	B5-C	-2.63	0.25	-2.47	0.15	-2.83	0.06
	B10-C	-3.03	0.25	-3.10	0.20	-3.07	0.67
	B100-C	-4.20	0.66	-5.37	0.15	-5.33	0.55

Table B4 Value of tensile change at 100 ^{o}C.

Elastomer	Fuel	22 hrs.		670 hrs.		1008 hrs.	
		Average change (%)	S.D.	Average change (%)	S.D.	Average change (%)	S.D.
NBR	Diesel	-7.97	2.48	-27.94	2.28	ND	ND
	B5-P	-13.75	2.17	-25.53	1.55	ND	ND
	B10-P	-22.28	0.05	-22.60	0.00	ND	ND
	B100-P	-52.74	2.07	-50.15	2.33	ND	ND
	B5-C	-18.29	2.38	-21.14	2.17	ND	ND
	B10-C	-15.14	2.17	-18.07	0.62	ND	ND
	B100-C	-50.26	2.17	-50.69	1.55	-46.09	1.86
HNBR	Diesel	16.88	0.75	11.23	0.45	4.80	0.37
	B5-P	14.50	1.86	14.19	1.49	5.43	0.22
	B10-P	12.03	1.34	11.71	0.67	4.17	1.86
	B100-P	2.53	0.22	5.96	0.75	1.11	1.34
	B5-C	10.44	0.60	13.45	0.75	4.27	1.72
	B10-C	11.71	0.67	12.08	0.37	5.17	0.60
	B100-C	7.23	0.75	1.00	1.49	1.85	1.72
NBR PVC	Diesel	-9.56	1.40	-5.77	1.28	ND	ND
	B5-P	-8.16	1.87	-5.11	1.28	ND	ND
	B10-P	-5.44	0.00	-3.30	0.23	ND	ND
	B100-P	-43.45	0.00	-51.53	1.28	ND	ND
	B5-C	-8.24	1.98	ND	ND	ND	ND
	B10-C	-16.49	1.28	ND	ND	ND	ND
	B100-C	-34.13	0.35	-35.61	1.40	ND	ND

Table B4 Value of tensile change at 100 °C.(continue)

Elastomer	Fuel	22 hrs.		670 hrs.		1008 hrs.	
		Average change (%)	S.D.	Average change (%)	S.D.	Average change (%)	S.D.
Acrylic rubber	Diesel	-16.61	1.54	-11.51	1.54	-24.10	1.23
	B5-P	-15.85	0.00	-17.59	1.69	-25.73	0.00
	B10-P	-19.98	2.00	-11.73	1.38	-16.83	1.23
	B100-P	-42.35	1.38	-52.88	1.23	-52.88	1.38
	B5-C	-16.72	1.23	-13.68	0.15	-22.15	0.00
	B10-C	-16.94	0.00	-18.89	1.38	-19.22	1.54
	B100-C	-40.28	0.77	-54.29	0.92	-51.14	1.07
Co FKM	Diesel	-27.94	0.26	-29.58	1.92	-25.09	1.52
	B5-P	-29.44	2.11	-26.03	0.86	-30.37	0.53
	B10-P	-28.64	1.26	-28.08	0.46	-23.64	2.25
	B100-P	-25.23	2.64	-36.59	0.33	-27.52	0.86
	B5-C	-27.52	0.86	-32.48	0.73	-24.11	1.98
	B10-C	-26.96	2.18	-28.36	0.33	-23.83	1.72
	B100-C	-5.61	0.66	-31.64	0.59	-35.51	0.66
Ter FKM	Diesel	-27.35	0.00	-20.71	0.11	-26.09	0.11
	B5-P	-18.06	1.73	-21.26	0.22	-25.69	1.12
	B10-P	-22.65	0.06	-20.47	1.12	-31.07	1.23
	B100-P	-20.24	0.00	-18.42	1.23	-22.29	1.12
	B5-C	-23.79	0.00	-23.16	2.12	-24.98	1.90
	B10-C	-30.43	2.01	-23.16	1.23	-27.75	1.01
	B100-C	-20.32	1.23	-19.76	0.56	-24.74	1.23

Table B5 Value of percent elongation change at 100 ^{o}C

Elastomer	Fuel	22 hrs.		670 hrs.		1008 hrs.	
		Average change (%)	S.D.	Average change (%)	S.D.	Average change (%)	S.D.
NBR	Diesel	-34.23	0.35	-44.25	0.69	-57.70	1.04
	B5-P	-35.70	1.04	-31.30	0.35	-53.55	1.38
	B10-P	-31.05	0.69	-38.14	1.73	-48.17	0.69
	B100-P	-47.68	0.69	-30.32	0.35	-54.03	0.69
	B5-C	-33.50	1.38	-28.85	1.73	-51.10	1.38
	B10-C	-28.12	0.69	-29.83	1.04	-44.25	1.38
	B100-C	-47.92	1.04	-38.39	0.69	-41.81	1.38
HNBR	Diesel	-7.04	2.99	-15.14	1.49	-23.94	1.99
	B5-P	-4.93	1.99	-8.45	2.99	-20.42	2.99
	B10-P	-8.10	1.49	-6.69	1.49	-17.25	2.49
	B100-P	-8.10	0.50	-3.87	1.49	-18.31	1.00
	B5-C	-10.92	1.49	-11.27	2.99	-26.06	2.49
	B10-C	-12.68	1.99	-4.58	2.49	-11.27	0.00
	B100-C	-4.23	1.00	-5.63	1.00	-11.97	0.00
NBR PVC	Diesel	-22.43	1.32	-43.61	1.32	-53.89	0.88
	B5-P	-23.99	0.88	-33.02	2.20	-49.53	0.88
	B10-P	-20.87	1.76	-41.12	0.44	-42.99	1.32
	B100-P	-35.83	0.88	-35.20	0.88	-43.93	0.00
	B5-C	-20.25	0.00	-33.02	0.44	-36.45	1.76
	B10-C	-20.87	1.76	-25.86	0.88	-22.43	1.32
	B100-C	-32.71	1.76	-33.02	0.44	-39.88	1.32

Table B5 Value of percent elongation change at 100 ^{o}C.(continue)

Elastomer	Fuel	22 hrs.		670 hrs.		1008 hrs.	
		Average change (%)	S.D.	Average change (%)	S.D.	Average change (%)	S.D.
Acrylic rubber	Diesel	-8.02	0.67	ND	ND	-16.51	0.67
	B5-P	-11.32	1.33	-21.23	2.00	-20.28	2.00
	B10-P	-26.89	0.67	-14.62	0.67	-22.64	1.33
	B100-P	-26.89	0.67	-31.13	1.33	-45.75	2.00
	B5-C	-13.21	1.33	-19.81	1.33	-18.40	0.67
	B10-C	ND	ND	-17.45	0.67	-23.58	2.67
	B100-C	-24.06	0.67	-38.21	0.67	-32.55	2.00
Co FKM	Diesel	-4.86	2.86	-13.77	0.57	-21.86	1.72
	B5-P	-12.96	1.72	-12.15	1.72	-17.81	2.86
	B10-P	-13.77	0.57	-17.81	2.86	-18.62	0.57
	B100-P	-13.36	0.00	-17.81	0.57	-19.43	1.72
	B5-C	-3.64	2.29	-12.96	1.72	-12.96	0.57
	B10-C	-16.60	1.15	-18.22	2.29	-17.81	1.72
	B100-C	-16.19	0.57	ND	ND	-22.27	0.00
Ter FKM	Diesel	-11.34	1.78	-6.30	1.78	ND	ND
	B5-P	-2.94	0.59	-1.68	1.19	-3.78	1.78
	B10-P	-3.36	2.38	-6.30	0.59	-1.26	0.59
	B100-P	-5.46	1.78	-4.62	1.78	-2.94	0.59
	B5-C	-2.10	0.59	-2.94	0.59	-7.56	2.38
	B10-C	-14.29	0.00	-3.78	1.78	-4.20	1.19
	B100-C	-6.30	1.78	-6.30	0.59	-3.36	2.38

VITAE

Mr. Suriya Porntangjitlikit was born on July 30, 1976 in Bangkok, Thailand. He received his Bachelor’s Degree of Science in Chemistry from Rajamangala University of Technology in 2000. He studied Master Degree in the Program of Petrochemistry and Polymer Science, Faculty of Science, Chulalongkorn University in 2003 and graduated in 2006.

His present address in 159/533 Siam Thoranee Soi, Kubon Road, Tha Raeng, Bang Khen, Bangkok, 10220, Thailand. Tel. 06-3794309.